

TABLE OF CONTENTS

	Page
LIST OF FIGURES	vi
LIST OF TABLES	viii
1.0 INTRODUCTION	1
1.1 Problem Statement	1
1.2 Research Objective and Scope	3
1.3 Research Methodology	5
1.4 Organization of the Dissertation	8
2.0 HURRICANE LOADING AND MODU CAPACITY MODELING	9
2.1 Introduction	9
2.2 Hurricane Models	12
2.2.1 Wind Field	12
2.2.2 Wave Field	13
2.2.3 Current Field	14
2.2.4 Surge of the Sea Surface	14
2.2.5 Expected Maximum Wave Heights	14
2.2.6 Shoaling Effect	15
2.2.7 Expected Maximum Wave Heights and Return Period	18
2.3 Hurricane Loads	20
2.3.1 Aerodynamic Loads	20
2.3.2 Hydrodynamic Loads	21
.1 Wave Theories	21
.2 Wave Directional Spreading	25
.3 Currents and Current Blockage	27
.4 Wave and Current Loads	28
2.3.3 A Simplified Load Model	30
.1 Wind Force	31
.2 Current Forces	31
.3 Wave Force	32
2.3.4 Verification of the Simplified Load Model	39
2.4 MODU Mooring Capacity	41

2.4.1	Overview of Mooring Analysis	41
2.4.2	Mooring Analysis in MODUSIM	46
2.4.3	Water Depth Factor	47
2.5	Summary	49
3.0	HURRICANE TRACK FORECASTING SIMULATION MODELS	51
3.1	Introduction to Hurricane Forecasting	51
3.2	Track Forecasting Models for Simulation	54
3.3	Track Forecast Error Statistical Model	55
3.4	Markov-Chain Simulation Model	66
3.4.1	Introduction to Markov Chains	67
3.4.2	State Probabilities	69
3.4.3	Hurricane Tracks Modeling in Gulf of Mexico	70
3.4.4	Steady State Probabilities	73
3.4.5	Hurricane Track Modeling for Texas-Mexico Coast	75
3.4.6	Examples of Markov Model Hurricane Tracks	76
3.5	Hurricane Strength Forecast Error Simulation Model	70
3.6	Summary	82
4.0	MONTE CARLO SIMULATION OF MODU COLLISION PROBABILITY	84
4.1	Introduction	84
4.2	Simulation Modeling	90
4.2.1	Hurricane Statistics	90
4.2.2	Modeling MODU Movement	93
4.2.3	MODU Moving Distance Modeling	94
.1	Case A: MODU Floating	94
.2	Case B: MODU Skipping	96
4.2.4	MODU Collision Modeling	96
4.2.5	Modeling of Holding after the Collision	98
4.3	Monte Carlo Simulation	100
4.3.1	Computer Simulation Approach	104
4.3.2	Variance Reduction Techniques	111
4.3.3	Sample size	112

4.4	Parametric and Case Studies	115
4.4.1	Introduction	115
4.4.2	Simulation and MODU's Parameters	116
4.4.3	Analysis of the Parametric Study Results	120
4.4.4	Case Studies	127
.1	Function #1	128
.2	Function #2	128
.3	Function #3	130
.4	Function #4	130
4.5	Simulations of the Movement of Bottom-Founded Platforms	134
4.5.1	Modeling Jack-up	134
4.5.2	Foundation Capacities	139
4.5.3	Failure Modes of Jack-up	140
4.5.4	Example of Martin 3 Jackup in Hurricane Andrew	144
5.0	SIMULATION MODEL FOR EVACUATION PROCEDURES	146
5.1	Introduction to Project Management	146
5.2	Background of Simulation Model	148
5.3	Development of the Simulation Model	152
5.4	Shutdown Criteria	155
5.5	Simulation Procedure	156
5.6	Case Studies	161
5.7	Possible Areas of Application	167
5.8	Summary	169
6.0	CONCLUSION AND RECOMMENDATION	170
6.1	Summary	170
6.2	Recommended Future Work	172
	REFERENCES	175

APPENDIX A	MODUSIM	
	MODU Movement Simulation Program	182
A1.	Introduction	184
A1.1	Introduction	184
A1.2	Application Range of MODUSIM	184
A1.3	Program Structure	185
A1.4	Installation	185
.1	Backup Disk	185
.2	System Requirements	185
.3	Installation	186
A2.	Input Data	187
A2.1	Introduction	187
A2.2	General MODU Information	189
A2.3	Mooring Capacity Information	192
A2.3	Simulation Setting Data	193
A2.4	Execute the Program	200
A2.5	General Jack-up Information	201
A3.	Output	203
APPENDIX B	EVACSIM	
	MODU Evacuation Procedures Simulation Program	208
B1.	Introduction	210
B1.1	Introduction	210
B1.2	Application Range of EVACSIM 1.0	210
B1.3	Program Structure	211
B1.4	Installation	211
.1	Backup Disk	211
.2	System Requirements	211
.3	Installation	212
B2.	Input Data	212
B2.1	Introduction	212
B2.2	Input Hurricane Forecasting Data	213
B2.3	Input Resource Environmental and Operational Down-Time Criteria	214

B3.	Simulation Procedure	215
B3.1	Deterministic Simulation	215
B3.2	Probabilistic Simulation	216
APPENDIX C	DISTRIBUTION FITTING AND GOODNESS-OF-FIT TEST	217
C.1	Estimating	217
C.2	Maximum Likelihood Estimators	218
C.3	The Levenberg-Marquardt Method	218
C.4	Goodness-of-Fit Tests	219
C.5	Confidence Levels and Critical Values	222

LIST OF FIGURES

Figure		Page
1.1	Interactive Development, Verification and Calibration of MODUSIM & EVACSIM	6
2.1	Alternative Approaches to Wave Loading Analysis	11
2.2	Shoaling Effect	17
2.3	Environmental Loading Return Period	19
2.4	Loading on MODU	20
2.5	Wave Train Definition Sketch	22
2.6	Regions of Applicability of Stream Function, Stokes V, and Linear Wave Theory	26
2.7	Simplified Load Model	30
2.8	Wave Force Components	33
2.9	Wave Drift Force and Motion for Semisubmersibles (Beam Seas and Bow Seas)	37
2.10	Wave Force on a Vertical Surface-Piercing Cylinder in Transitional Water ($d / gT^2 = 0.028$)	40
2.11	Mooring Configuration	41
2.12	Water Depth Factor vs. Water Depth	49
3.1	Determining the Track Forecast Error	56
3.2	Fit Results for Distance and Direction Forecasting Error	58
3.3	Example of Calculation of Probability Function in a Square	63
3.4	Forecast Mean Distance Error vs. Forecast Time Interval	65
3.5	Definition of Storm Track Transmission State	71
3.6	Probability Density Function of CTA in State 1,2,3	71
3.7	Examples of Track Forecast Generated by MCSM	76
3.8	Fit Results for Hurricane Strength Forecasting	80
4.1	Fit Results for Hurricane Parameters	91
4.2	Gulf Coastal Water Regions (Ward, et al., 1978)	92
4.3	Probability of Collision vs. Structure Numbers	97
4.4	Modeling of Holding	99
4.5	Monte-Carlo Simulation Reference	101
4.6	Monte-Carlo Simulation Procedure	102
4.7	Monte-Carlo Simulation Procedure	103
4.8	Environmental Force Configuration	108
4.9	Collision Probability vs. Sample Size	113
4.10	Storm Parameters for Hurricane Andrew	117
4.11	Reference Frame for Andrew	119
4.12	Changing MODU's Site	126

4.13	Probability of Failure vs. Forecast Time	129
4.14	Simulated Moving Route of Zane Barnes in Hurricane Andrew	131
4.15	Simulated Moving Route of Zapata Saratoga in Hurricane Andrew	132
4.16	Simulated Moving Route of Treasure 75 and Ocean Now Era in Hurricane Andrew	133
4.17	Jack-up: Single Degree of Freedom Model	136
4.18	Definition of Yield Moment	138
4.19	Example of Martin 3 Jack-up in Andrew	145
5.1	Probabilistic Simulation Procedure	154
5.2	Procedure of Determination Resource Workable Time Period	159
5.3	Deterministic Simulation Procedure	160
5.4	Modeling Whole Evacuation Operations	163
5.5	Example of Environmental Forecasting Input Data	162
5.6	Simulation Result for One Transportation Boat	164
5.7	Simulation Result for Two Transportation Boats	164
5.8	Probabilistic Simulation Result a	166
5.9	Probabilistic Simulation Result b	166
A1.1	Select 'Program Group' for MODUSIM Program	186
A1.2	Specify the Group Name and the Filename and Path	186
A2.1	MODUSIM is Popped Up	187
A2.2	Saved Simulation Result	188
A2.3	Input MODU General Information	189
A2.4	Input MODU Initial Location	190
A2.5	Input Target Circle Information	191
A2.6	Input Mooring System Information	192
A2.7	Set Up the Simulation	193
A2.8	Input Hurricane Parameters	194
A2.9	Environmental Simulation Settings	195
A2.10	Given Hurricane Track Information	196
A2.11	Input Calculation Coefficients	197
A2.12	Input Random Parameter Information	198
A2.13	Input Correlation Coefficients among Random Parameters	199
A2.14	Input Markov Model Setting	199
A2.15	@Risk Simulation Setting	200
A2.16	Jack-up Type Input Information	201
A2.17	General Jack-up Input Information	202
A2.18	Input Jackup Capacity Information	202
A2.19	Simulation Result	203
A2.20	Simulation Result for Target Circles	204
A2.21	Environmental Condition Simulation Result	205
A2.22	Type of Histogram	206
A2.23	Collision Happening Dialogue Box	207

LIST OF TABLES

Table	Page
3.1 Weighting Functions for Each Section	64
3.2 Observed Transitions in Gulf of Mexico (1950-1992)	72
3.3 P_{ij} Values	72
3.4 Observed Transitions in Gulf of Mexico (1950-1992)	75
3.5 P_{ij} Values	75
4.1 Hurricane Moment Statistics (110 Hurricanes Represented)	90
4.2 Correlation Coefficient Matrix	90
4.3 Hurricane Parameter Distributions	92
4.4 Estimated Collision Probability vs. Sample Size	114
4.5 Collision Probability in Free-Floating Condition	121
4.6 Collision Probability in Dragging Condition	122
4.7 Collision Probability vs. Mooring Capacity Simulation Results	123
4.8 Strategy Simulation Result in Free Floating Condition	124
4.9 Strategy Simulation Result in Dragging Condition	125
4.10 Simulation Results of Forecast Probability	129
4.11 General Dimensions of Average Jack-up Rig	135
4.12 Foundation Capacities of GOM	140

ACKNOWLEDGMENTS

This project was made possible by funding provided by the U.S. Minerals Management Service. Special appreciation is expressed to Dr. Charles Smith, Research Program Manager, Offshore Minerals Management Technology Assessment and Research Branch, Herndon, Virginia. Dr. Smith provided a number of key background references for the project and provided the overall direction for this work.

Appreciation is expressed to Dr. Malcom Sharples, Noble Denton and Associates, now with the American Bureau of Shipping, for his continue technical advice, information, and encouragement. Special thanks to Dr. Henry Chen, Ocean Systems Inc., Oakland, for his help in the evacuation part of the work.

This work was funded in part by a grant from the National Sea Grant College Program, National Oceanic and Atmospheric Administration, US Department of Commerce, under grant number NA36RG0537, project number R/OE28 through California Sea Grant College, and in part by the California State Resources Agency. The views expressed herein are those of the author and do not necessarily reflect the views of NOAA or any of its sub-agencies. The U.S. Government is authorized to reproduce and distribute for governmental purposes.

CHAPTER 1

INTRODUCTION

1.1 Problem Statement

Experience with Mobile Offshore Drilling Units (MODUs) in recent hurricanes in the Gulf of Mexico (GOM) has indicated the need to reassess where and how these units are sited.

In September 1992, hurricane Andrew swept through the eastern portion of the Gulf of Mexico (GOM). Five MODUs experienced damage and inflicted significant damage on surrounding facilities. The Zane Barnes, Zapata Saratoga, and Treasure 75 all moved very significant distances during hurricane Andrew. The storm snapped seven of the semi-submersible drilling unit Saratoga's eight anchor chains and drove the unit some 100 miles to the north, where it collided with several platforms. The Zane Barnes broke loose from its eight anchors, drifted northwest some 30 miles, colliding with several platforms and many pipelines. The anchors from the Treasure 75 reportedly collided with several platforms. The LOOP (Louisiana Offshore Oil Port) 36 inch diameter pipeline narrowly missed being snagged by the dragging anchors of one of these MODUs.

This is not the first hurricane to cause such damage. The destruction of the West Delta Block 134A platform by the semi-submersible drilling unit "Blue water I" during hurricane Betsy is one of the most notable of these earlier experiences. During the approach of hurricane Betsy, the Blue water I semi-submersible drilling unit broke from its mooring and was driven by the strong winds and currents some 25 miles to the southeast until it

collided with the industry's first platform installed in a water depth greater than 300 feet. Portions of the Blue Water drilling unit were found inside the destroyed platform.

This experience suggests that there are fundamental issues that need to be resolved regarding the policies and guidelines for manning, positioning and mooring semi-submersible drilling units in the GOM during the hurricane season. Special mooring areas and mooring systems need to be studied for MODU operation during hurricane season.

Also, as indicated by recent experience in Hurricane Andrew and Hurricane Juan, weather conditions can deteriorate rapidly. Timely decisions are critical to allow proper security and evacuation of MODUs. This is particularly crucial in areas with high storm intensity and low weather predictability and at a great distance from shore.

To limit the exposure of personnel and property, security and evacuation operations must be conducted within a reasonable time before storm conditions intensify to the point that evacuation would be hazardous. Developing frameworks for modeling these operation and evacuation systems for various weather conditions can assist in creating decision criteria for evacuations. Engineering analyses need to be performed to evaluate MODU security and evacuating alternatives, to develop general criteria and guidelines for evacuation planning. This work addresses the development of such a framework and evaluates various MODU securing alternatives using probabilistic risk analysis (PRA).

1.2 Research Objective and Scope

The fundamental issue addressed by this research is development of a rational and simplified method to evaluate the siting strategies and evacuation procedures for mobile offshore drilling units. The objective is to address this issue by developing and verifying such methods. There are two ways to approach such problems: 1) by analysis, and 2) by simulation. Simulation is normally employed when the problem is complex and there are few fundamental laws that can be used to predict the response of the system, and when the system components themselves are difficult to describe and represent.

An analytical method was developed by TRIDENT CONSULTANTS LTD (Trident Consultants Ltd., 1992) to solve a similar problem: estimate the probability of collision between a Floating Storage Unit (FSU) and surrounding platforms in the Gulf of Thailand (GOT). In that study, the probability that the FSU would collide with a platform was treated as the product of three other probabilities: the probability that the FSU would break its mooring, the probability that it would move in a given direction, and the probability that it would encounter a platform in its direction of travel. The detailed background of this analysis will be discussed in Chapter 4. This analysis is ideal for the problem in GOT, as the groups of platforms were all located within a 30 by 70 Nautical mile rectangle. Thus, it was relatively easy to calculate the three probabilities.

In the Gulf of Mexico there are much larger areas occupied by platforms. A MODU generally can have a long trip before it collides with platforms. Because hurricane centers

move with time, the associated wind and wave fields also change with time, and so the MODU's route will be variable. Also, there are different mooring system failure modes (e.g., mooring lines broken or anchors dragging), and different MODU moving modes (free floating or skipping). All these factors will have a great influence on the MODU's route and thus on the resulting collision probability. In this case, it is very difficult to calculate the three probabilities.

In this research, the problem is approached by direct computer simulations using probability models for the hurricane parameters and the MODU's approach to the site.

The first part of the report summarizes the development of an analytical model to evaluate MODU movements in response to the combined load effects of hurricane winds, waves and currents. In addition, a Monte-Carlo simulation process to evaluate the probability of collision between the MODU and surrounding large facilities is developed.

To evaluate MODU evacuation procedures in hurricanes, a computer simulation is clearly the best approach. McCarron (1971), Burke (1977), Hoffman (1978), Chen (1983), and Praught (1982) are examples that show industry's interests in decision-making using sophisticated computer simulation programs. The objective of the second part of the report is to summarize the models and procedures used to develop a computer simulation program, EVACSIM, to calculate the probability of safe evacuation, including the effects

of hurricane forecasting, evacuation start-times, available resources, and alternative evacuation procedures.

This report documents development and verification of computer models that can be used to simulate the MODU moving and colliding probabilities, and evacuation procedures during hurricanes.

1.3 Research Methodology

Figure 1.1 summarizes the approach used to develop, verify and implement the simulation models. Based on fundamentals of statistics, hurricane forecasting and modeling, fluid dynamics, mooring strength analysis, and Monte Carlo techniques, the first step of the research was to develop a basic simulation model MODUSIM, to evaluate the movement of MODUs in hurricanes. MODUSIM was then used to develop siting strategies for Mobile Offshore Drilling Units.

The simulation model incorporates models of hurricane winds, waves, currents, and tracks; storm wind, wave and current forces; mooring capacity characteristics, and finally, a model of movement characteristics that takes account free floating, intermittent grounding ('skipping'), collision 'holding', and anchor dragging characteristics. MODUSIM allows the user to specify hurricane characteristics in a probabilistic or deterministic manner. A Monte-Carlo simulation model is utilized to perform probabilistic calculations. The model includes a Markov model to describe the probabilities associated with changes

in the tracks of the hurricanes. The model incorporates variable hurricane parameters and their correlation, the storm spatial geometry, and shallow water shoaling effects. MODUSIM allows one to define the locations and sizes of 'critical facilities' near the MODU location, and then evaluate the probabilities of collisions between the MODU and the critical facilities. The organization and theoretical basis for MODUSIM will be detailed.

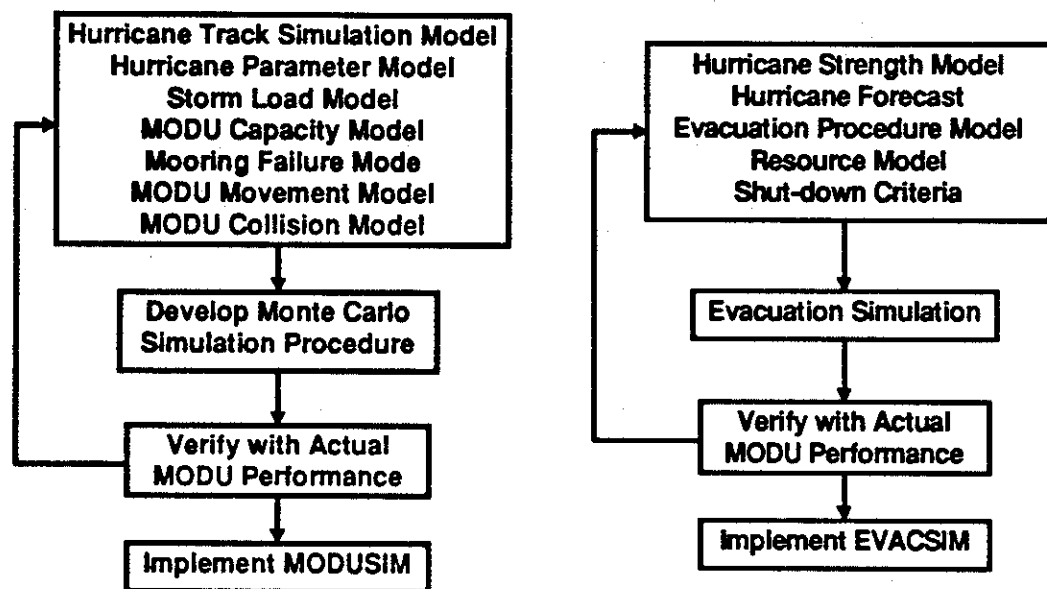


Figure 1.1 Interactive Development, Verification, and Calibration of MODUSIM & EVACSIM

Then, based on the project management and network simulation techniques, a computer simulation model EVACSIM was developed to help evaluate operational and evacuation systems for MODUs in hurricanes. Probabilistic risk analysis and Monte Carlo techniques

are used in the model to include the large uncertainties in hurricane forecasts and in the evacuation process.

To begin the evacuation simulation process, first, statistical analysis of the hurricane forecast was performed to calculate the forecast percent error based on the differences between forecasts and history. Then, the critical environmental shut-down conditions, for example, wave heights no higher than 40 ft, were used to determine the workable time period for different operations and resources based on the hurricane forecast. The entire evacuation sequence, including the time needed for operations and the relationship between operations, are modeled using network simulation techniques. The duration for safe completion of the evacuation was determined. Histograms of evacuation risks for different evacuation start times were obtained.

The platform security and evacuation operations are modeled in Microsoft Project 4.0. Microsoft Visual Basic is used to generate the input file of MS Project to determine the resources workable time. Because of the different resource workable times associated to different weather conditions, the evacuation duration and cost depend on the starting time. Results using different evacuation start times are compared. Probabilities are determined for evacuation and securing risks dependent upon the storm severity and the type of operational accident. Sensitivity of the overall failure probabilities to the weather conditions is examined.

1.4 Organization of the Report

Chapter 2 contains background about hurricane wind and wave field modeling and the development of a simplified storm loading calculation procedure. The modeling of MODU capacity is also discussed in this Chapter. Chapter 3 includes the development of two new hurricane track forecasting simulation models and a hurricane strength prediction simulation model, Track Forecast Error Statistical Model (TFESM), Markov-Chain Simulation Model (MCSM) and Strength Forecast Error Simulation Model (SFESM). Detailed Monte Carlo simulation process for MODU collision probability is discussed in Chapter 4. It includes background on Monte Carlo simulation techniques, hurricane modeling, mooring failure mode modeling, MODU moving mode modeling, parametric and verification studies. Lastly, the extension of MODUSIM to simulate movements of bottom founded platforms, ex., jack-up, is presented in this Chapter. Based on project network simulation techniques, a computer simulation model of MODU evacuation procedures (EVACSIM) is reported in Chapter 5. Risk analysis of evacuation procedure has been done based on simulation results. Chapter 6 contains a summary of the developments and findings of this research. Potential future research topics are also identified and discussed in this chapter.

Appendix A and B document the computer program MODUSIM and EVACSIM. Detailed program descriptions and user manuals are contained in these two appendixes. Appendix C contains the statistic background for distribution fitting, goodness-of-fit test performed in the research.

ACKNOWLEDGMENTS

This project was made possible by funding provided by the U.S. Minerals Management Service. Special appreciation is expressed to Dr. Charles Smith, Research Program Manager, Offshore Minerals Management Technology Assessment and Research Branch, Herndon, Virginia. Dr. Smith provided a number of key background references for the project and provided the overall direction for this work.

Appreciation is expressed to Dr. Malcom Sharples, Noble Denton and Associates, now with the American Bureau of Shipping, for his continue technical advice, information, and encouragement.

This work was funded in part by a grant from the National Sea Grant College Program, National Oceanic and Atmospheric Administration, US Department of Commerce, under grant number ####, project number #### through California Sea Grant College, and in part by the California State Resources Agency. The views expressed herein are those of the author and do not necessarily reflect the views of NOAA or any of its sub-agencies. The US Government is authorized to reproduce and distribute for governmental purposes.

CHAPTER 2

HURRICANE LOADING AND MODU CAPACITY MODELING

2.1 Introduction

One important step in the simulation process is to determine the environmental loads acting on MODUs. In general, these loads are due to wind, waves, currents which are generated by hurricanes.

Due to complexity and random nature of these loads, it is difficult, if not impossible, to develop theoretical models that accurately predict these loads and their effects on offshore structures. This is why offshore engineering research has traditionally used field measurements and laboratory experiments to calibrate existing loading models. The Conoco test Structure (Bea et al. 1986) and the Ocean test Structure (Haring et al. 1979) are two platforms highly instrumented for the purpose of measuring wind and wave forces on offshore structures.

Traditionally two different approaches have been utilized to predict the hydrodynamic loads on offshore installations: deterministic and stochastic (Bea et al., 1978). The deterministic approach itself can be pseudo-static or time-dependent. The pseudo-static deterministic approach uses the maximum wave kinematics which result in maximum loads. These loads are then used to perform static structural analyses. In the time dependent deterministic approach, loads are calculated as a function of time and used to

perform dynamic structural analysis. The stochastic approach treats the loading as a random process where the loading condition is described by spectral densities. Figure 2.1 summarizes these approaches and the major steps involved in each approach. The different methods are used to perform different types of analyses from static pushover for extreme conditions to fatigue analysis for nominal conditions.

To formulate current and wave forces on offshore platforms, two areas of fundamental research need to be addressed: a) fluid mechanics of steady and unsteady flows passing a body and b) fluid motion in a wave described by wave theories (Sarpkaya et al., 1981). For an overview of historical developments in the subject of hydrodynamic loads on offshore structures and a more detailed treatment of the subject, refer to Sarpkaya and Isaacson (1981).

The purpose of this research is to develop a simple procedure to determine the aerodynamic and hydrodynamic loads acting on a MODU. In the following sections, hurricane models are discussed first, then wind loads are formulated. The fluid mechanics background that is necessary to develop a simplified load calculation approach is also discussed. Finally, a simplified load model is introduced that uses an idealized structure and Stokes fifth order wave theory to predict the wave loads acting on MODUs. This load model is verified with results from more sophisticated current and wave load generating programs commonly used in industry.

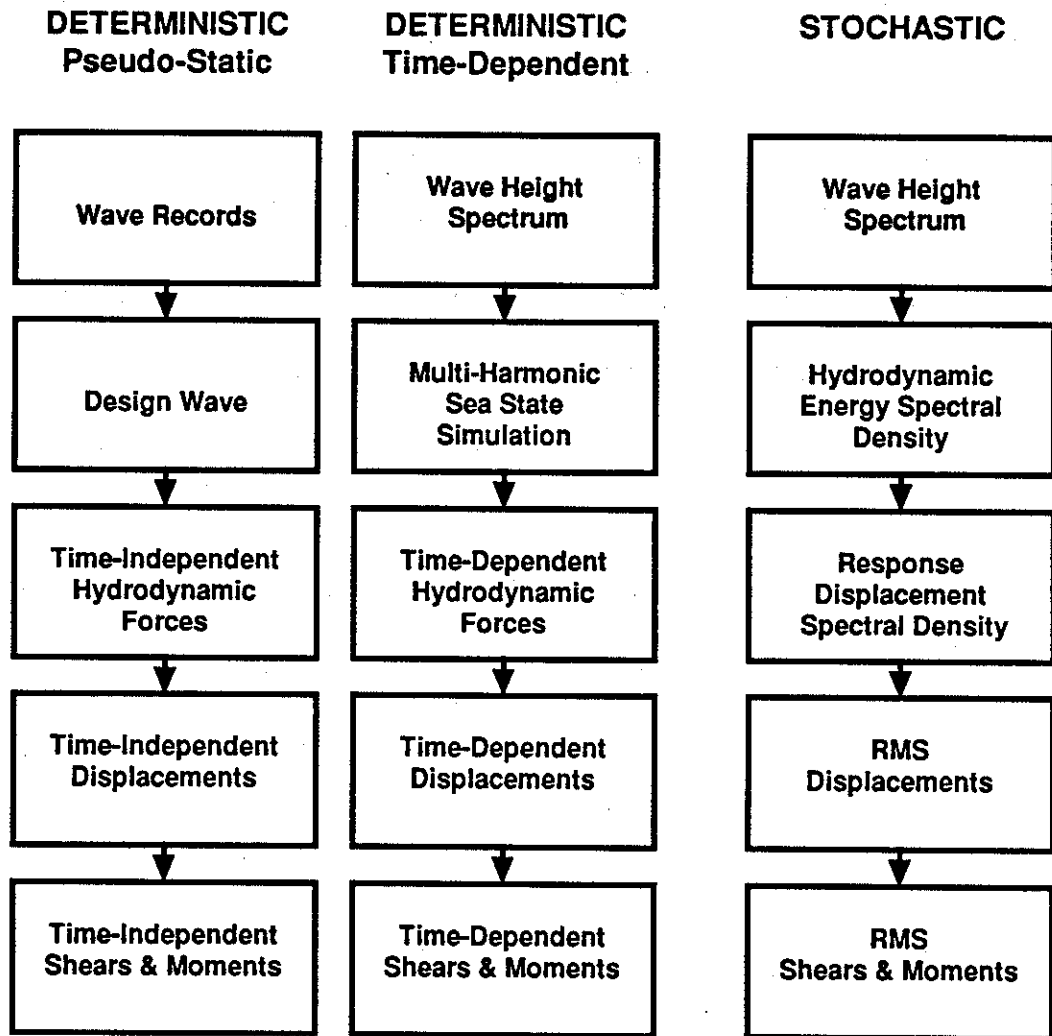


Figure 2.1: Alternative Approaches to Wave Loading Analysis (Bea and Lai, 1978)

2.2. Hurricane Models

The hurricane is assumed to travel along a straight line with a given translation speed and direction during each simulation time interval, e.g., 2 hours. The wind field is governed primarily by the three parameters: Pressure difference, radius of maximum wind speed and hurricane transition velocity, which are ΔP , R and V_t . Changes in the storm parameters after shelf edge crossing are not considered, i.e., the intensity of the hurricane is assumed to be stationary during passage over the continental shelf. The wind and wave field are based on parametric expressions derived from more sophisticated numerical models. These parametric models which were developed by Cooper (1988) give the wind velocity, significant wave height, and wave direction as functions of the hurricane parameters and the site position relative to the storm center. The current field is based on a one-dimensional numerical model which is a simplified version of the three-dimensional numerical model by Cooper. The models are briefly described in the following sections. Details can be found in Cooper (1988).

2.2.1 Wind Field

The wind speed (in m/s) and direction β (polar angle in degree) as functions of the position relative to the storm center in polar coordinates r and θ are given by:

$$W = W_m (r/R)^{\beta} \quad \text{for } r/R > 1 \quad (2.1)$$

$$W = 1.047 W_m [1 - \exp(-3.1r/R)] \quad \text{for } r/R < 1 \quad (2.2)$$

in which,

$$W_m = 0.885(5.6\sqrt{\Delta P} - 0.5Rf) + V_t \cos \theta \quad (2.3)$$

$$a = -0.38 + 0.08 \cos \theta \quad (2.4)$$

where, f = Coriolis parameter in rad/s, ΔP in mb, V_r in m/s, and R in m

$$\beta_{wind} = \theta + \alpha + 90^\circ \quad (2.5)$$

in which α is the deflection angle given by:

$$\alpha = 22 + 10 \cos \theta \quad (2.6)$$

2.2.2. Wave Field

The parametric model for significant wave height H_{sm} , in meter, at a given location can be expressed as a "25 percentile rule" (Bea, 1990) or:

$$H_m = 0.25 V_m \quad (2.7)$$

In which V_m is the local wind speed in m/s. The equation for the average wave direction ϕ (polar angle in degree) is:

$$\phi = \alpha + a(r/R)^b + \theta - 90^\circ \quad (2.8)$$

in which

$$a = 144 + 39 \cos \theta - 25 \sin \theta - 15 \cos 2\theta \quad (2.9)$$

$$b = -0.08 \quad (2.10)$$

The r.m.s. errors are of the order of 10 to 20 degrees.

The equation for peak period, T_p (s), is (Noble Denton, 1991):

$$T_p = a W^b \quad (2.11)$$

where,

$$a = 8.0 - 3.5 \cos \theta + 2.7 \sin \theta \quad (2.12)$$

$$b = 0.143 + 0.138 \cos \theta - 0.074 \sin \theta \quad (2.13)$$

2.2.3. Current Field

The following parametric model has been developed for the expected maximum storm current velocity (U_m , m/s, average velocity in upper 30-meter thick mixed layer), concurrent in time and direction with the occurrence of the expected maximum wave (Bea, 1990):

$$U_m = \bar{\epsilon} V_m \quad (2.14)$$

Where $\bar{\epsilon} \approx 0.02 - 0.03$, V_m is the 10m elevation, 10 minute average wind speed at the time that the cyclone crosses the site. The current direction is assumed the same as the wind and wave direction.

2.2.4. Surge of Sea Surface

The surge of the sea surface due to hurricane in deep water is determined as (Bea 1988):

$$\Delta h = 0.03 H_{max} \quad (2.15)$$

where, $H_{max} = f(\Delta p)$, is the maximum wave height due to the hurricane in deep water.

2.2.5. Expected Maximum Wave Heights, Given Significant Wave Heights

The expected maximum wave height, H_m , could be estimated from the short term wave height distribution based on 1000 waves (expressing a 3-hour duration of the maximum sea state intensity at the location) (Bea, 1990):

$$H_m = \zeta H_{\bar{m}} \sqrt{\frac{\ln N}{2}} \quad (2.16)$$

where $\zeta = 0.93$, $V_{\bar{c}} = 8\%$.

Thus, the expected maximum wave height could be estimated as:

$$H_m = 1.73 H_{\bar{m}} \quad (2.17)$$

2.2.6 Shoaling Effect

Storm waves tend to be attenuated by a variety of processes as they propagate across the relatively shallow depths of the Texas and Louisiana Continental Shelves. As a wave propagates from deep to shallow water, its height and length change. The transformed wave height, H , at shallow water depth relative to the original deep water wave height, H_o , can be computed from (Shore Protection Manual):

$$\frac{H}{H_o} = \left(\frac{V_o}{V}\right)^{\frac{1}{2}} \left(\frac{b_o}{b}\right)^{\frac{1}{2}} \quad (2.18)$$

Where V is the group velocity of the waves, b is the distance between pairs of adjacent wave rays, and the subscript o refers to deep water condition.

The term $\left(\frac{V_o}{V}\right)^{\frac{1}{2}}$ is also known as the shoaling coefficient, k . The shoaling coefficient is given according to linear wave theory by:

$$K's = \left(\frac{1}{\left(1 + \frac{2kh}{\sinh 2kh}\right) \tanh kh} \right)^{\frac{1}{2}} \quad (2.19)$$

Where h is the water depth and k is the wave number. Where, $L = \frac{gT^2}{2\pi} \tanh\left(\frac{2\pi d}{L}\right)$.

Eckart(1952) gives an approximate expression for Equation (2.19), which is correct to within about 5 percent. This expression is given by:

$$L = \frac{gT^2}{2\pi} \sqrt{\tanh\left(\frac{4\pi^2 d}{T^2 g}\right)} \quad (2.20)$$

$$T = 2.7 \sqrt{H_{max}} \quad (2.21)$$

K 's is then given explicitly as a function of wave length and water depth.

The term $\left(\frac{b_o}{b}\right)^{\frac{1}{2}}$ in the shoaling equation represents the relative spacing of adjacent wave rays and is also defined as the refraction coefficient, K_r . Physically, the relative spacing between wave rays represents the local wave energy density. It is generally assumed that the wave energy contained between wave orthogonal is conserved as the wave front progresses. Various graphical and numerical methods are available to compute wave refraction. In this study, the graphical procedure was adopted. However, most of the wave paths were near normal to the smoothed depth contours; thus, the wave refraction effects proved to be insignificant.

Based on data from Woodward-Clyde Consultants (1982), the shoaling effect of the current is modified as:

$$U = \left(2.5 - \frac{1.5}{250}d\right)U_o \quad (2.22)$$

where U_b is the current velocity at 250 ft depth of water (Figure 2.2).

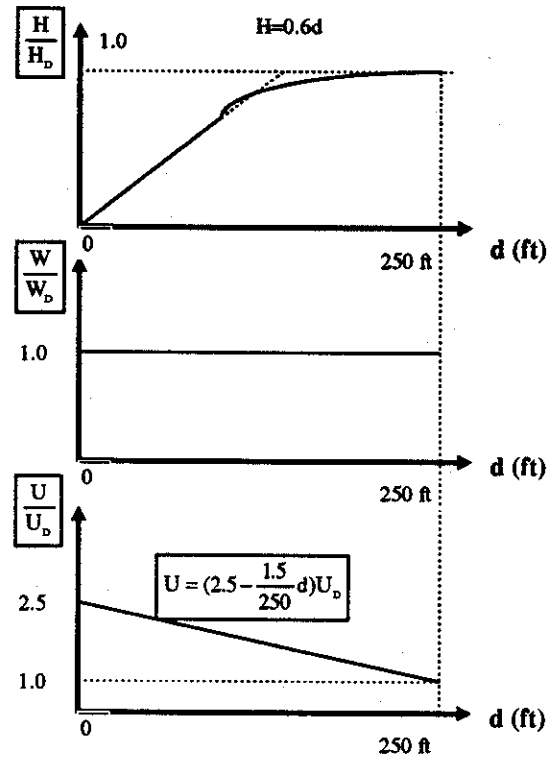


Figure 2.2 Shoaling Effect

The shoaling effect of the surge of the sea surface is defined as:

$$\Delta h' = \Delta h \cdot k \quad (2.23)$$

where k is the shoaling effect parameter:

$$K = (1 + \frac{3(300 - h)}{290}) \quad (2.24)$$

and, Δh is the surge in deep water (≥ 300 ft).

The wind velocity in shallow water is assumed the same as in deep water. (See Figure 2.2)

2.2.7. Expected Maximum Wave Heights and Return Period

The expected maximum deep water (300 ft) wave heights in Gulf of Mexico can be determined as (Bea, 1990):

$$H_m = C(\Delta P_m)^{\frac{1}{2}} \bar{\psi} \bar{\zeta} H_m \sqrt{\frac{\ln N}{2}} \quad (2.25)$$

where	$\bar{C} = 4.4$	$V_c = 6\%$
	$\bar{\psi} = 0.25$	$V_\psi = 10\%$
	$\bar{\zeta} = 0.93$	$V_\zeta = 8\%$
	$\bar{\Delta P} = 46.38$	$V_{\Delta P} = 68\%$

Assuming H_m can be characterized with a Lognormal distribution, we have,

$$\bar{H}_m = \bar{C}(\bar{\Delta P})^{\frac{1}{2}} \bar{\psi} \bar{\zeta} \sqrt{\frac{\ln N}{2}} \quad (2.26)$$

$$V_{H_m}^2 = V_c^2 + \left(\frac{1}{2} V_{\Delta P}\right)^2 + V_\psi^2 + V_\zeta^2 + \left(\frac{1}{2} V_{\frac{\ln N}{2}}\right)^2 \quad (2.27)$$

The average return period (ARP) was computed using Equation [2.28]:

$$ARP = \frac{1}{\lambda[1 - F(H_{e, \max})]} \quad (2.28)$$

where $F(H_{s,max})$ is the cumulative percentage of $H_{s,max}$ values equal to or less than a given value, and λ is the average number of important wave-generating hurricanes affecting this area each year.

With the same procedure, we can get the ARP of Maximum wind velocity and current velocity (Figure 2.3).

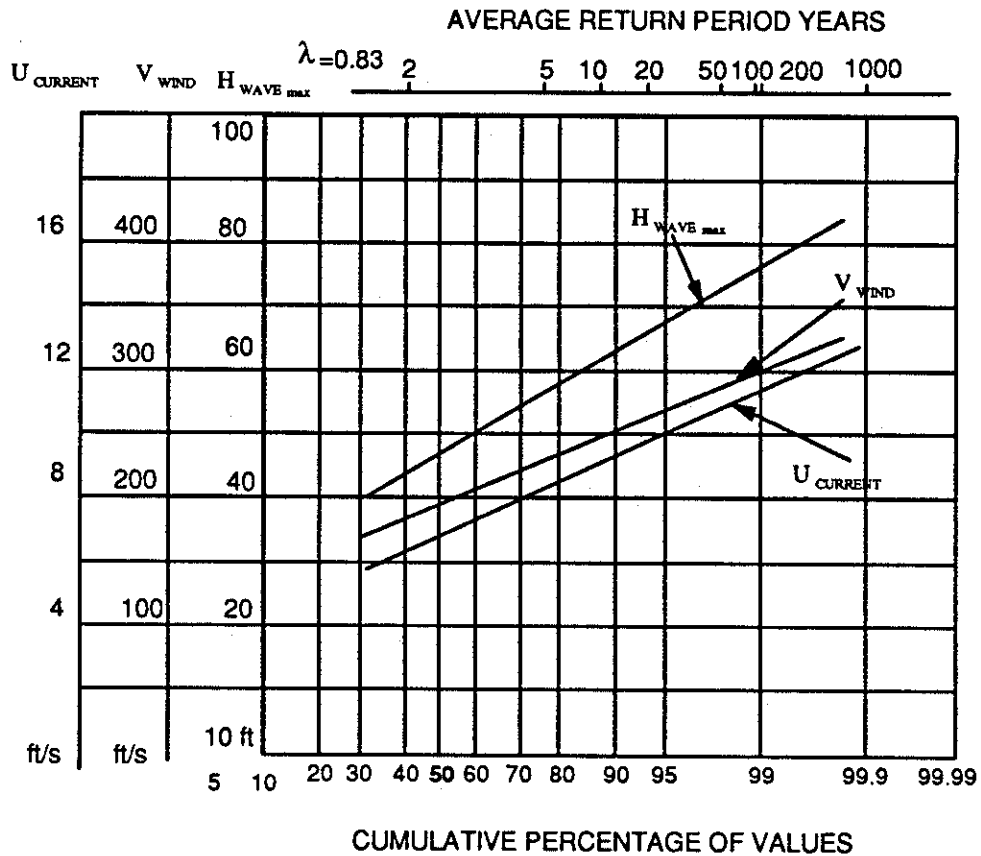


Figure 2.3 Environmental Loading Return Period

2.3 Hurricane Loads

There are three major hurricane loads on a MODU: wind load, hydrodynamic wave and current load (Figure 2.4).

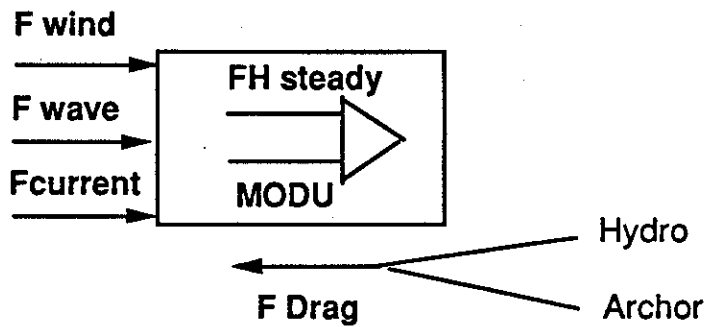


Figure 2.4 Loading on MODU

2.3.1 Aerodynamic Loads

Wind forces acting on the exposed portions of offshore platforms are in general not as significant as wave forces acting on these structures. However, their effect has to be included in the global structural movement analyses. Wind forces are generally composed of two components: a sustained (or steady) component averaged over a longer period of time (usually over one minute) and a gust (or fluctuating) component averaged over a shorter period of time (usually less than one minute). Sustained wind velocities are used to analyze the global platform behavior and gust velocities are used to analyze the local member behavior. In this research, the dynamic aspects of wind loading are neglected. Only sustained wind velocities are used to calculate the first order of the global platform movement.

Due to surface friction, the geostrophic wind velocity is reduced in the vicinity of ocean surface. API RP 2A (API, 1993) gives the following approximation to the wind profile,

$$u(1hr, z) = u(1hr, z_R) \left(z / z_R \right)^{0.125} \quad (2.29)$$

where z_R denotes a reference height usually taken as 10 meters.

2.3.2 Hydrodynamic Loads

To establish the hydrodynamic loads acting on an offshore platform, the following steps need to be taken:

- a) establish wave, current, and storm surge information based on site specific studies including recorded or hindcasted data,
- b) use an appropriate wave theory to describe the fluid motion and water particle kinematics,
- c) use a force transfer function to determine the loads acting on platform members. In the following sections, the last two steps, b and c, are described and discussed in detail.

2.3.2.1 Wave Theories

The problem of describing the wave motion has been dealt with for more than a century. Numerous text books have been devoted to development of various wave theories and describing their results (refer to Sarpkaya and Isaacson, 1981, for a comprehensive list of references). All of these wave theories are based on the following common assumptions: the waves are two-dimensional and propagate in horizontal direction in waters with

constant depth and a smooth bed. It is further assumed that the wave train profile does not change with time, no underlying current exists, and the water surface is tension-free (uncontaminated). Water itself is assumed to be incompressible, inviscid (ideal fluid), and irrotational. Figure 2.5 shows the definition sketch of a wave train with H , L , d , and η , denoting wave height and length, water depth and surface elevation respectively. The governing equations of wave motion can be found in any classical text book on fluid mechanics (e.g. Sarpkaya and Isaacson 1981) and are given below for the sake of completeness.

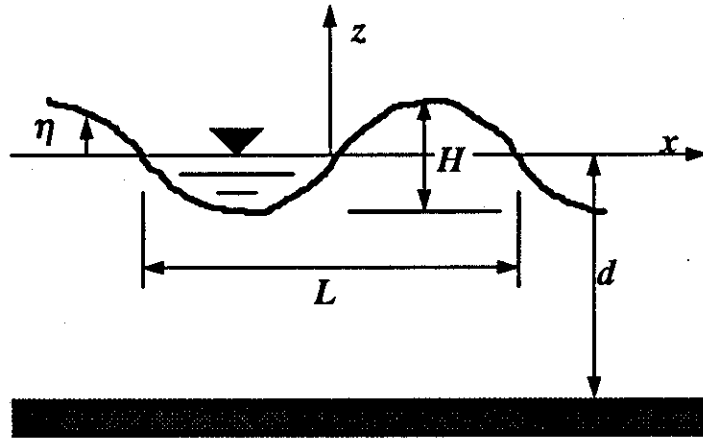


Figure 2.5: Wave Train Definition Sketch

Defining a scalar function $\phi=\phi(x,z,t)$ so that the fluid velocity vector can be given by the gradient of ϕ , it can be shown that based on the assumptions stated above, ϕ , the so-called velocity potential, satisfies the two-dimensional Laplace equation:

$$\nabla^2 \phi = \frac{\partial^2 \phi}{\partial x^2} + \frac{\partial^2 \phi}{\partial z^2} = 0 \quad (2.30)$$

and is subject to the following boundary conditions at water surface and seabed:

$$\frac{\partial \phi}{\partial z} = 0 \quad \text{at } z = -d \quad (2.31)$$

$$\frac{\partial \eta}{\partial t} + \frac{\partial \phi}{\partial x} \frac{\partial \eta}{\partial x} - \frac{\partial \phi}{\partial z} = 0 \quad \text{at } z = \eta \quad (2.32)$$

$$\frac{\partial \phi}{\partial t} + \frac{1}{2} \left[\left(\frac{\partial \phi}{\partial x} \right)^2 + \left(\frac{\partial \phi}{\partial z} \right)^2 \right] + g\eta = f(t) \quad \text{at } z = \eta \quad (2.33)$$

$$\phi(x, z, t) = \phi(x - ct, z) \quad (2.34)$$

The boundary condition at the seabed states that the velocity vector has no component in vertical direction (Equation 2.31). The kinematics boundary condition at the water surface states that the velocity component normal to the water surface is equal to the velocity of water surface in that same direction (Equation 2.32). The dynamic boundary condition at the water surface states that the pressure along the surface is constant (equal to atmospheric pressure) (Equation 2.33). Equation (2.34) is based on the assumption of periodicity of the wave train where $c=L/T$ denotes the wave celerity.

Given the wave height, period and the water depth, the question is what shape does the wave take and how to describe the water particles motion (displacements, velocities, and accelerations) throughout the flow. In solving the governing Laplace Equation (2.30) subject to boundary conditions explained in Equations (2.31-2.34), the following problems are encountered: the boundary conditions at the water surface are nonlinear and specified at a surface elevation η , which is itself unknown. The various wave theories developed in

the past have tried to solve these problems with reasonable approximations. These include linear or Airy wave theory (also known as small amplitude wave theory), Stokes finite amplitude wave theories, Dean's stream function theory, and nonlinear shallow wave theories (such as Cnoidal wave theory). The question of suitability of a given wave theory for a particular application is a difficult one. One selection criteria is the amount of effort needed to produce the desired results. The more advanced the theory is, the more sophisticated the tools need to be to perform the analyses. Theoretical charts have been developed that show the ranges of best fit to the free surface boundary conditions for different wave theories (e.g., Figure 2.6). Experimental comparisons of different wave theories have not resulted in clear trends regarding the applicability of any particular wave theory (Sarpkaya and Isaacson, 1981). For the sake of simplicity and within the framework of a simulation analysis, only Airy small amplitude and Stokes finite amplitude wave theories are considered in this research.

The linear wave theory provides a first approximation of the wave motion. It is derived based on the assumption of relatively small wave heights, it is $H \ll L, d$. The boundary conditions are satisfied at $z=0$. Airy wave theory is very attractive to use for many engineering applications. It is simple and does not require computer analysis. There are approximations to linear wave theory for shallow water, intermediate depth and deep water ranges (see e.g. Sarpkaya and Isaacson, 1981). A practical approximation to Airy wave theory is the "depth-stretched" linear wave theory. In this approach, the water

surface is “stretched” to the wave crest elevation. The water particle kinematics are estimated according to the Airy small amplitude wave theory.

Based on a perturbation method, Stokes finite amplitude wave theories attempt to solve Equation (2.30) subjected to boundary conditions explained in Equations (2.31-2.34) more closely. However, like many other wave theories, convergence conditions put numerical limitations on wave heights in certain water depths. Worked by Skjelbreia and Hendrickson (1960) and Fenton (1985) on a fifth-order Stokes wave theory has found widespread interest and usage in engineering applications. Their formulations do not require extensive computer programming effort and is used in this research to develop a simplified load model.

2.3.2.2 Wave Directional Spreading

Real storm conditions include waves from multiple directions. Directional spreading of the waves reduces the loads acting on marine structures which are computed based on a two dimensional, long crested, regular wave grid propagating in a single horizontal direction. This load reduction is mainly due to change in water particle kinematics. Wave components from different directions can partially cancel each other. The effects of wave directionality have been investigated by many authors (e.g. Dean, 1977).

The detailed treatment of the subject is not within the scope of this work. In engineering practice, wave directional spreading effects are captured by a single wave kinematics modification factor. The actual water particle velocity is estimated by multiplying the

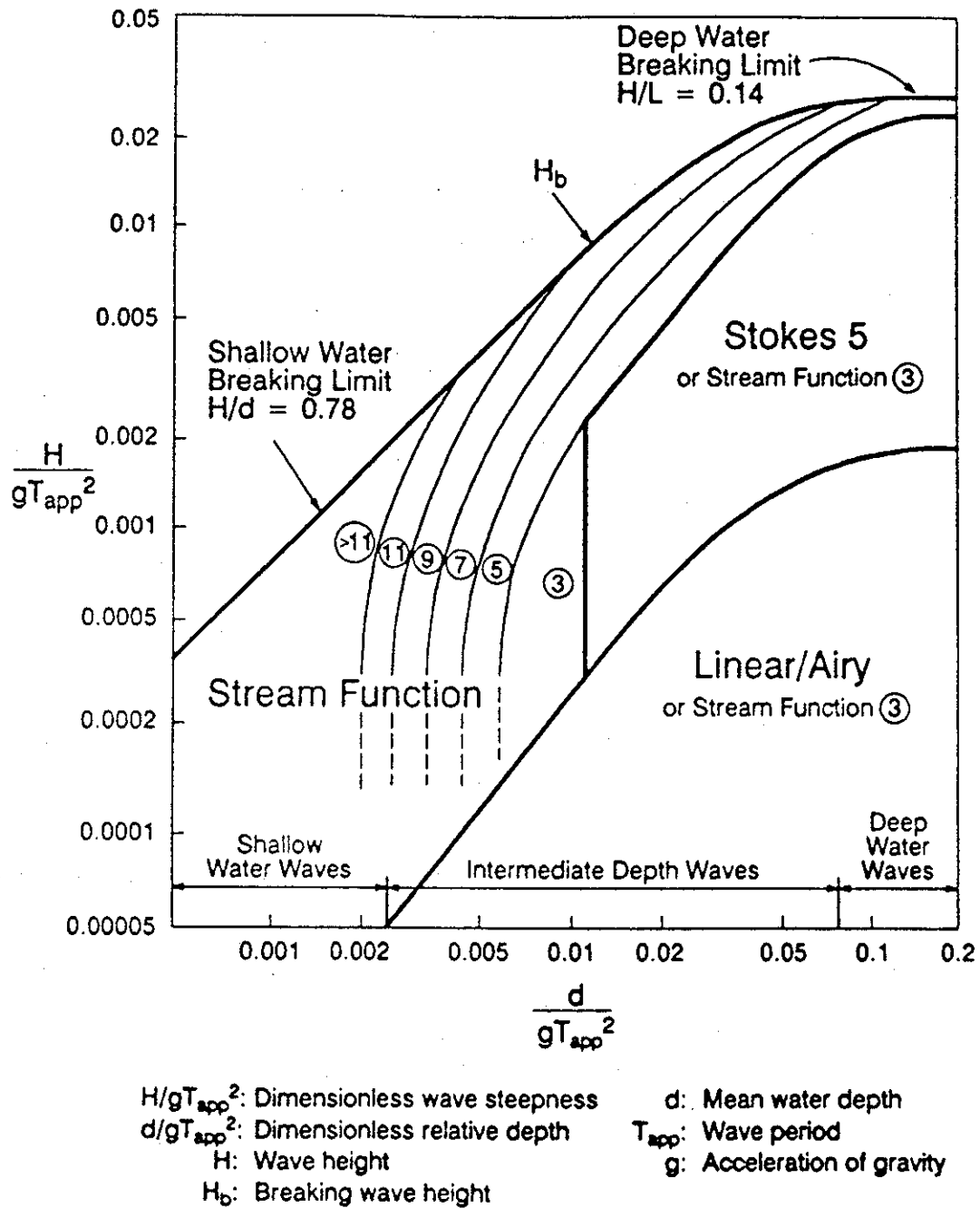


Figure 2.6: Regions of Applicability of Stream Function, Stokes V, and Linear Wave Theory (API, 1993a)

velocities based on a two-dimensional wave theory with a wave kinematics modification factor. Measurements indicate a range of 0.85 to 1.0 for highly directional seas during tropical storms to extra-tropical storm conditions (API, 1993).

2.3.2.3 Currents and Current Blockage

Currents can be a major contributor to total hydrodynamic forces acting on an offshore platform. In general, currents are generated in three ways: there are tidal, circulation, and storm generated currents. Tidal currents can be important in shallow waters of continental shelves (coastal regions and inlets). The Gulf Stream in the Atlantic Ocean and the Loop Current in the Gulf of Mexico are examples for large-scale circulation currents. Winds and pressure gradients during storms are the source of storm generated currents. These currents can be roughly estimated to have surface speeds of 1-3% of the one hour sustained wind speed during storms (API, 1993). The profile of storm generated currents is largely unknown and the subject of research. Here, in the MODU simulation model, three different types of current profile can be chosen. They are uniform, triangular and second order.

In determining the water particle kinematics due to currents, it should be recognized that, due to existence of the structure, the current is disturbed and its speed in the vicinity of the platform differs from that in the free field. Based on experimental test data, approximate current blockage factors for typical MODUs are given in API RP 2A (API, 1993). The actual current velocity in the vicinity of the structure is obtained by multiplying the free field current speed with the current blockage factor.

2.3.2.4 Wave and Current Loads

Morison, Johnson, O'Brien and Schaff (1950) proposed the following formulation for the force acting on a section of a pile due to wave motion:

$$F = F_i + F_d = C_m \rho V \frac{du}{dt} + \frac{1}{2} C_d \rho A u |u| \quad (2.35)$$

This formulation is widely known as Morison equation. According to Morison et al. (1950), this force is composed of two components: an inertia component related to the acceleration of an ideal fluid around the body, F_i , and a drag component related to the steady flow of a real fluid around the body, F_d . C_m is the so-called inertia coefficient, ρ is the mass density of fluid, V is the volume of the body and du/dt is the fluid acceleration. C_d is the so-called drag coefficient, A denotes the projected area of the body normal to the flow direction, and u is the incident flow velocity relative to pile.

Vortex shedding, drag and lift forces are all phenomena observed in real (viscous) fluids due to wake formation when the fluid passes a body. These phenomena do not exist in an ideal (inviscid) fluid. They have been the subject of comprehensive research for many decades and are now well understood and described for simple, idealized cases. In such cases, numerical computations are able to simulate these phenomena with reasonable degrees of accuracy. However, these programs are not yet efficient enough to be used by engineers and designers to calculate the forces on “real” marine structures.

Although extremely simple, the Morison's equation has been used for many years by researchers and engineers to calculate the wave forces on “slender” marine structures. An

important assumption implicit in the Morison equation is that the incident flow remains undisturbed in the vicinity of the body. This condition is satisfied when the body is small relative to the wave length. If the body is large relative to the wave length, the incident flow will not remain uniform and will be refracted due to presence of the body. In this case the refraction problem needs to be solved. For detailed treatment of the subject refer to Sarpkaya and Isaacson (1981). The refraction problem is not considered in this research since the platform dimensions are much smaller than the wave length in the extreme storm conditions.

The drag and inertia coefficients in Morison equation have empirical nature and depend on many factors including flow characteristics, shape and roughness of the body and its proximity to sea floor or free surface. One important flow parameter reflecting its uniformity is Keulegan-Carpenter (KC) number which is defined as:

$$KC = \frac{UT}{D} \quad (2.36)$$

where U and T are the velocity amplitude and period of the oscillatory flow and D is the diameter of the cylinder. Reynolds number, Re, is another important parameter that characterizes the flow regime reflecting its turbulence and is defined as:

$$Re = \frac{UD}{\nu} \quad (2.37)$$

where ν denotes the fluid viscosity. Past field tests have indicated a large scatter in the values of drag and inertia coefficients when they are plotted against either the Reynolds number or the Keulegan-Carpenter number. This scatter is largely attributable to the

irregular nature of the ocean waves. Typical values for Reynolds and Keulegan-Carpenter numbers in extreme conditions are $Re > 10^6$ and $KC > 30$. For these ranges and based on experimental and field test data, mean drag and inertia coefficients are established for cylinders with smooth and rough surface (e.g. API, 1993).

2.3.3 A Simplified Load Model

Based on the background developed in the previous sections, a simplified load calculation model is developed and discussed in the following. Wind, current and wave forces are considered (Figure 2.7).

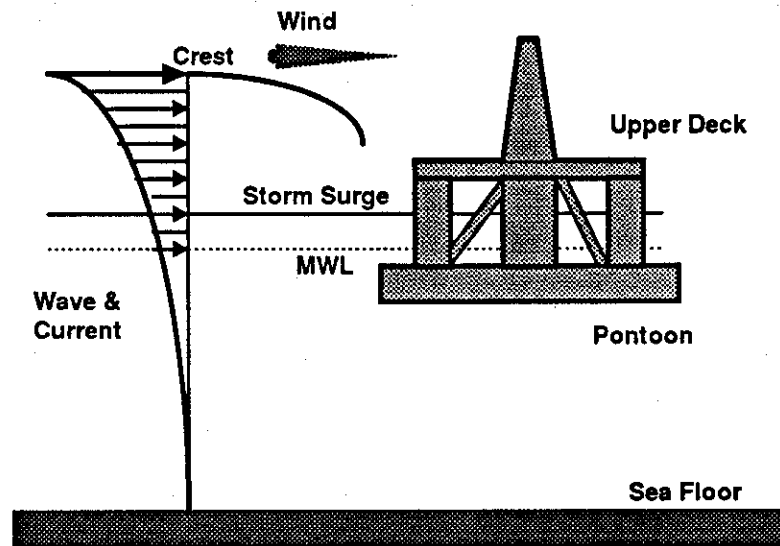


Figure 2.7: The Simplified Load Model

2.3.3.1 Wind Force

Given the wind velocity, the wind force acting on a moored floating MODU can be determined using Equation (2.38):

$$F_w = C_w \sum (C_s A) V_w^2 \quad (2.38)$$

where:

F_w = wind force, lb. (N)

C_w = 0.0034 lb / (ft² • kt²) (0.615 N sec² / m⁴)

C_s = shape coefficient

A = vertical projected area of each surface exposed to the wind, ft² (m²)

V_w = local wind speed, knots (m/sec)

The projected area exposed to the wind should include all columns, deck members, deck houses, trusses, crane booms, derrick substructure and drilling derrick as well as that portion of the hull above the water line.

2.3.3.2 Current Forces

Current forces are normally treated as steady state forces in a mooring analysis. Current force acting on semisubmersible hulls can be calculated as:

$$F_c = C_c (C_d A_c + C_d A_r) U^2 \quad (2.39)$$

where:

F_c = current force, lb(N)

C_u = current force coefficient for semisubmersible hulls

$$= 2.85 \text{ lb} / (\text{ft}^2 \cdot \text{kt}^2) (515.62 \text{ Nsec}^2 / \text{m}^4)$$

C_d = drag coefficient (dimensionless)

= 0.6 for circular members; 1.0 for members having flat surfaces.

A_c = summation of total projected areas of all cylindrical members below the waterline. $\text{ft}^2 (\text{m}^2)$

A_f = summation of projected areas of all members having flat surfaces below the waterline. $\text{ft}^2 (\text{m}^2)$

2.3.3.3 Wave Force

Interactions between ocean waves and a floating vessel results in forces acting on the vessel, which can be conveniently split into three categories (Figure 2.8):

- (1) First-order forces that oscillate at the wave frequencies. They induce first-order motions which are also known as high frequency or wave frequency motions.
- (2) Second order forces with frequencies below wave frequencies. They induce second order motions which are also known as low frequency motions.
- (3) Steady component of the second order forces which is known as mean wave drift force.

- Wave Frequency MODU Motions

The motions of the MODU at the frequency of the waves is an important contribution to the total mooring system loads, particularly in shallow water. These wave frequency

motions can be obtained from regular or random wave model test data, or computer analysis using either time or frequency domain techniques. The method used in this work is based on the widely used Morison Equation (Eq. 2.35).

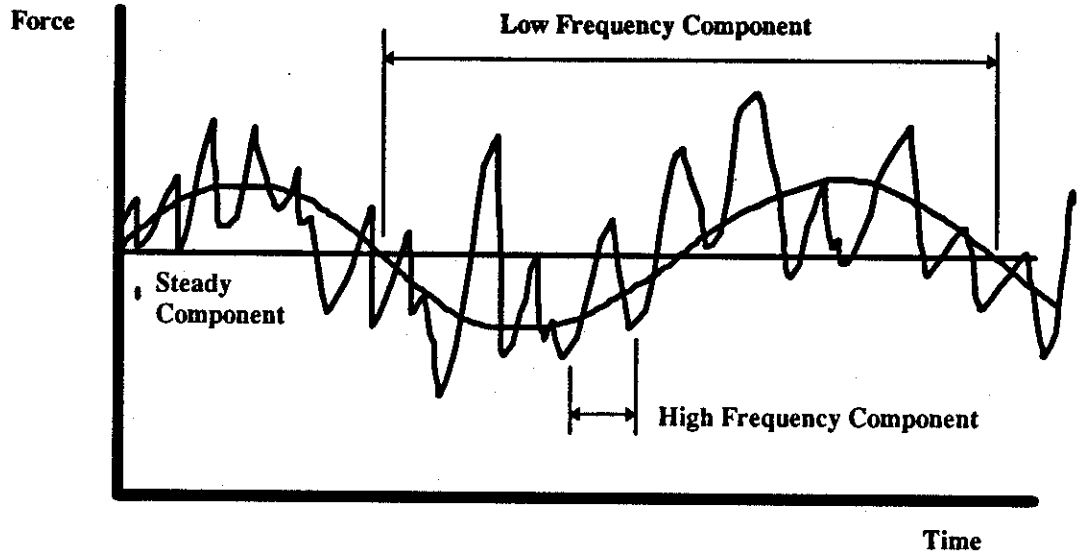


Figure 2.8 Wave Force Components

The total hydrodynamic force per unit length, F , is comprised of a drag force, F_d , and an inertia force, F_i :

$$F = F_d + F_i \quad (2.40)$$

where,

$$F_d = C_d (\rho / 2) (D) u |u| \quad (2.41)$$

$$F_d = K_d u |u|$$

and, $F_i = C_m (\rho \pi D^2 / 4) a \quad (2.42)$

$$F_i = K_m (a)$$

The total lateral force can be calculated by integrating the local forces over the entire structure. Due to 90 degree phase angle difference between the maximum drag and inertia force components and the relatively large dimensions of a typical MODU type platform, the wave force is inertia force dominant. That means that at the time the inertia forces acting on the platform reach a maximum value the drag forces are relatively small and hence are neglected in this work.

All of the structure elements are modeled as equivalent vertical cylinders (Mortazavi, Bea, 1995). Appurtenances (conductors, boat landings, risers) are modeled in a similar manner. For wave crest elevations that reach the lower decks, the horizontal hydrodynamic force acting on the lower decks are computed based on the projected area of the portions of the structure that would be able to withstand the high pressures.

Airy wave theory and Stokes 5th theory are used to calculate wave kinematics:

a. Airy Wave Theory

For uni-directional (long-crested) waves, water particle horizontal velocities, u_w and accelerations, a_w are

$$u_w = (\pi H / T) e^{\pi z} \cos(\theta) \quad (2.43)$$

and,
$$a_w = (2\pi^2 H / T^2) e^{\pi z} \sin(\theta) \quad (2.44)$$

where k is the wave number ($k = 2\pi / L$), z is the vertical coordinate which is zero at the still water level and positive upward, and θ is the wave phase angle ($\theta = kx - \omega t$, ω is the wave circular frequency, $\omega = 2\pi / T$, x is the horizontal coordinate measured from the wave crest, and t is the time coordinate).

b. Stokes' 5th Theory

For Stokes theory, using equations given by Skjelbreia and Hendrickson (1961) and Fenton (1985), a computer program was developed to determine the wave kinematics (Preston, 1994). Given the wave height H , period T and water depth d , the vertical profile of maximum horizontal velocities and accelerations beneath the wave crest are estimated as:

$$\frac{U}{C} = K_{\alpha} \sum_{n=1}^5 n \Phi_n \cosh(nks) \quad (2.45)$$

$$\frac{a_v}{\omega c} = K_{\alpha} \sum_{n=1}^5 n^2 \Phi_n \cosh(nks) \quad (2.46)$$

where K_{α} is a coefficient that recognizes the effects of directional spreading and wave irregularity on the Stokes wave theory based velocities. k is the wave number and s is the vertical coordinate counting positive upward from the sea floor. c is the wave celerity and given as:

$$\frac{c^2}{gd} = \frac{\tanh(kd)}{kd} [1 + \lambda^2 C_1 + \lambda^4 C_2] \quad (2.47)$$

The crest elevation η is estimated as:

$$k\eta = \sum_{n=1}^{\infty} \eta_n C_n \quad (2.48)$$

Φ_n and η_n are given functions of λ and kd . C_n are known functions of kd only, given by Skjelbreia and Hendrickson (1961). The wave number k is obtained by implicitly solving equation given by Fenton (1985):

$$\frac{2\pi}{T(gk)^{0.5}} - C_0 - \left(\frac{kH}{2}\right)^2 C_2 - \left(\frac{kH}{2}\right)^4 C_4 = 0 \quad (2.49)$$

The parameter λ is then calculated using the equation given by Skjelbreia and hendrickson(1961):

$$\frac{2\pi d}{gT^2} = \frac{d}{L} \tanh(kd) [1 + \lambda^2 C_1 + \lambda^4 C_2] \quad (2.50)$$

- Mean Wave Drift Force

The mean wave drift force is induced by the steady component of the second order wave forces. The determination of mean drift force requires motions analysis computer programs or model tests. Design curves for estimating mean wave drift forces for semisubmersibles are provided in API (1991, 1994) (Figure 2.9). The curves are applicable to typical MODU type vessels.

- Low Frequency Vessel Motions

Low frequency motions are induced by the low frequency component of the second order wave forces which in general are quite small compared to the first order forces. Sometimes the second order forces are amplified through resonance into motions which can become very large and neglecting low frequency motions can provide non-

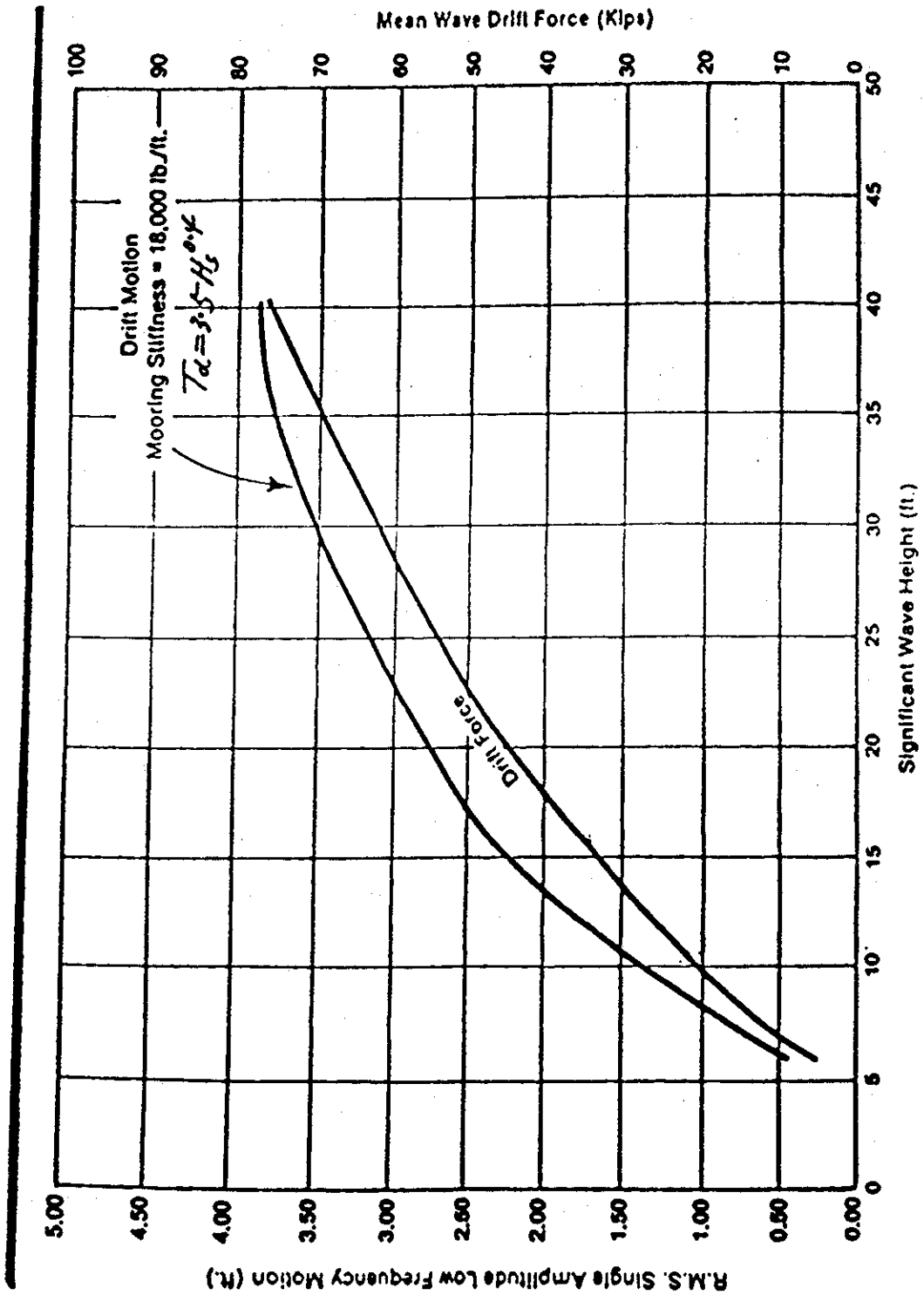


Figure 2.9a Wave Drift Force and Motion for Semisubmersibles (Beam Seas)

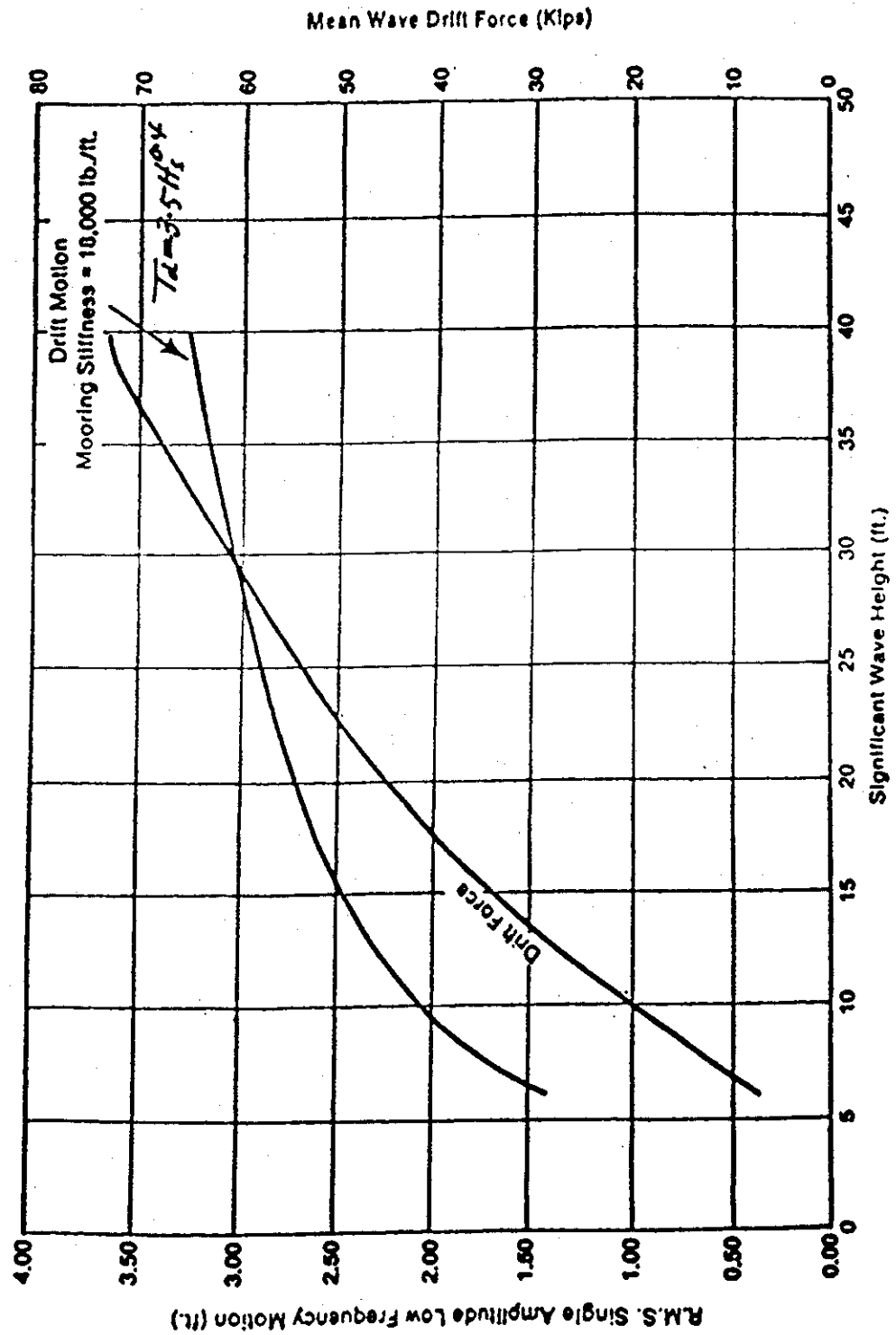


Figure 2.9b Wave Drift Force and Motion for Semisubmersibles (Bow Seas)

conservative answers. But due to the difficulty in predicting the magnitude of resulting low frequency tensions, their effect is neglected.

2.3.4 Verification of the Simplified Load Model

The procedure used to estimate the wave forces acting on MODUs has been verified and calibrated against results from more sophisticated computer programs. In an initial verification effort, the computer output for one design wave cases on single surface piercing cylindrical piles were used. These data were produced during an analytical wave force study conducted by Exxon and Shell Research Companies and documented by Bea (1973). In this study, the maximum wave force acting on a 20 ft diameter surface piercing cylinder was estimated where nondimensional water depths d/gT^2 is 0.028. Based on the simplified procedure developed in the previous sections of this chapter, the maximum wave force acting the same cylinder is also estimated using Stokes fifth-order and depth stretched linear wave theories. A inertia coefficient of $C_m=1.5$ is used. The results are also compared to those gained by using Dean's Charts that are developed based on ninth-order stream function theory (Dean, 1973). The results are summarized in Figure 2.10.

From Figure 2.10 it can be found that, Stokes V results in an estimate of base shear which is in good agreement with results reported in Exxon-Shell wave force study, which is about 1900 kips. Dean's Charts result, which is about 1600 kips, slightly underpredict the total force. Surprising is the result gained by using depth-stretched linear wave theory, which gives a base shear that is almost 40% less than that given by Stokes V.

Field measurements in intermediate water depths indicate that depth-stretched Airy theory provides an acceptable fit to the actual wave kinematics. With this in mind, the results plotted in Figures 2.10 indicate that wave force predictions based on finite amplitude wave theories (Stokes V or stream function) might be conservatively biased. The variabilities of the force coefficients given by Bea (1990) were used to estimate the uncertainties associated with the wave force, which were $B = 0.66$ and $V_s = 0.47$. These estimates are consistent with the simplified analytical models employed to calculate the loadings. Based on the results of this initial verification case study, Stokes fifth-order theory was used in this research.

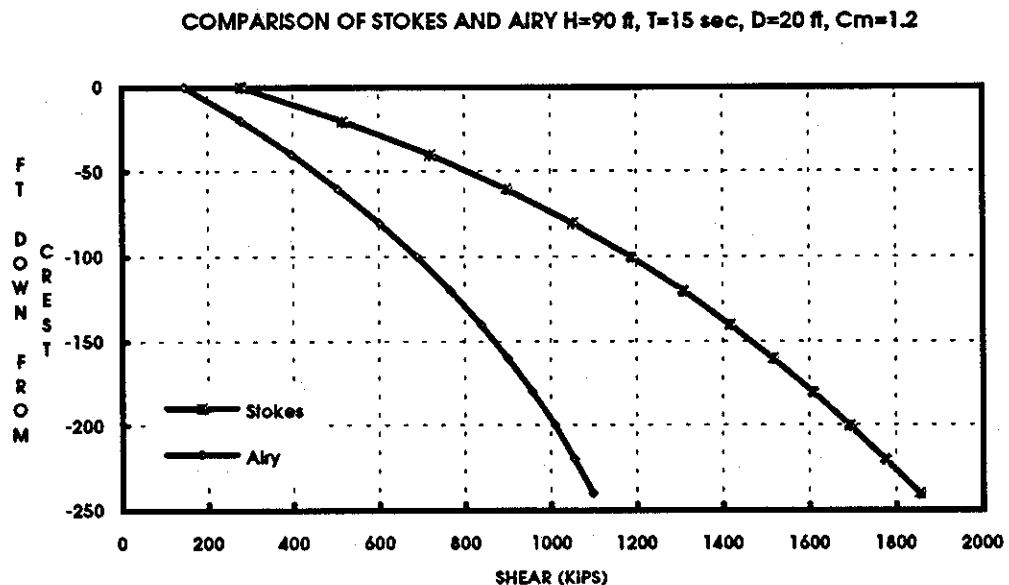


Figure 2.10: Wave Force on a Vertical Surface Piercing Cylinder in Transitional Water ($d / gT^2 = 0.028$)

2.4 MODU Mooring Capacity

2.4.1 Overview of Mooring Analysis

Generally, the mooring system of a semi-submersible is as shown in Figure 2.11.

Permanent mooring systems should be designed for two primary considerations: system overloading and fatigue. For MODU moorings, only analysis for extreme response is required.

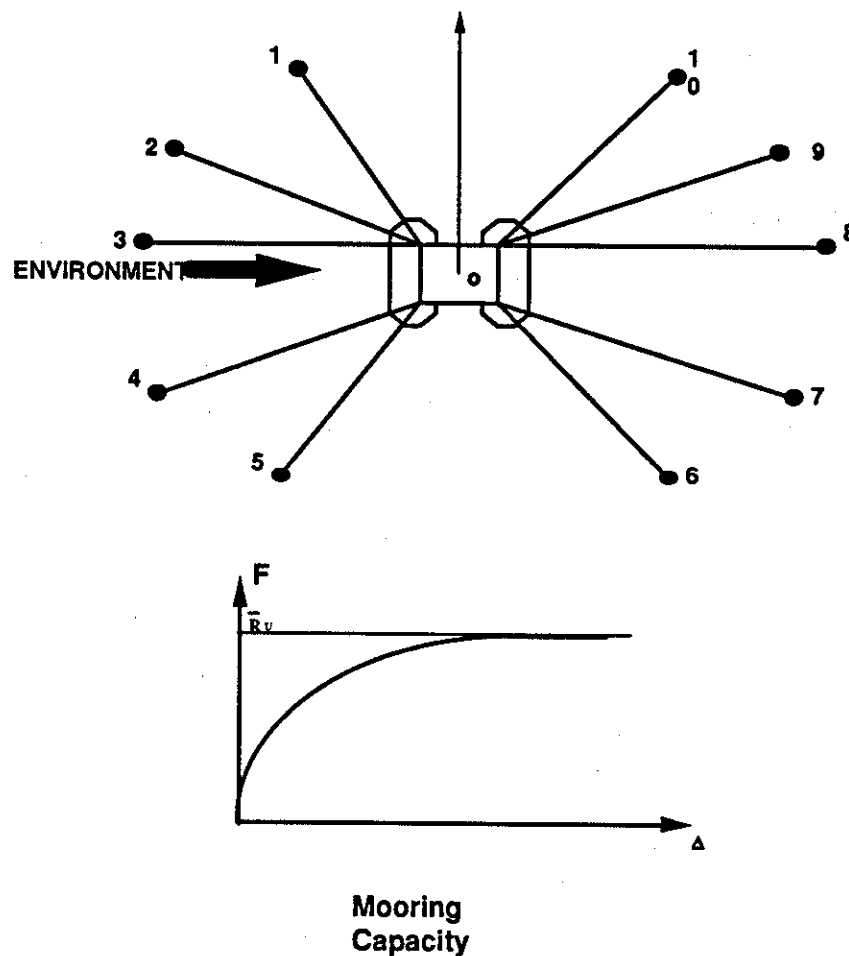


Figure 2.11 Mooring Configuration

Extreme responses normally govern the design of the MODU mooring. They include MODU offset, mooring line tension, anchor load, and suspended line length. The environmental effects can be divided into three categories:

- Steady state forces including current force, mean wind and mean wave drift forces;
- Low frequency MODU motions due to wind and waves;
- Wave frequency MODU motions.

The responses of a mooring system to mean forces are predicted by static catenary equations. Generally speaking, the responses to low frequency motions can also be predicted by the same method because of the long periods of these motions. The responses to wave frequency MODU motions are usually predicted by one of the following two methods:

(1) Quasi-Static Analysis

In this approach, the dynamic wave loads are taken into account by statically offsetting the MODU by an appropriately defined wave included motion. MODU moored motions and dynamic effects associated with mass, damping and fluid acceleration are neglected. Research in mooring line dynamics has shown that the reliability of the mooring designs based on this method can vary widely depending on the MODU type, water depth and line configuration. Therefore, the quasi-static method is not recommended for the final design

of a permanent mooring. However, because of its simplicity, this method can be used for temporary moorings and preliminary studies of permanent moorings with higher factors of safety.

(2) Dynamic Analysis

Dynamic analysis accounts for the time-varying effects due to mass, damping, and fluid acceleration. In this approach, the time-varying fairlead motions are calculated from the MODU's surge, sway, heave, pitch, roll and yaw motions. Generally it is sufficient to account for only the vertical and horizontal fairlead motions in the plane of the mooring line. Dynamic models are used to predict mooring line responses to the fairlead motions. Several dynamic analysis techniques are available. The distinguishing feature among various dynamic analysis techniques is the degree to which non-linearity are treated. There are four primary nonlinear effects which can have an important influence on mooring line behavior:

- Nonlinear Stretching Behavior of the Line
- Changes in Geometry
- Fluid Loading
- Bottom effects

Two methods, frequency domain and time domain analyses, are commonly used for predicting dynamic mooring loads. In the time domain method, all of the nonlinear effects

can be modeled. The elastic stretch is mathematically modeled, the full Merinos equation is included, the position of the mooring line is updated at each time step and the bottom interaction is included using a frictional model. The general analysis implies the recalculation of each mass term, damping term, stiffness term, and load at each time step. Hence, the computation can become complex and time consuming.

The frequency domain method, on the other hand, is always linear because the principle of linear superposition is used. Hence, all nonlinearities must be eliminated, either by direct linearization or by an iterative linearization.

The procedure outlined below is recommended for the analysis of extreme response using a quasi-static or dynamic approach. The calculated response in accordance with this procedure should satisfy the design criteria.

The analysis is normally performed with the following computer programs:

1) Hydrodynamic Motion Analysis programs

These programs are used to determine wave frequency and low frequency vessel motions.

2) Static Mooring Analysis program

This program is used to analyze mooring line response to steady state environmental forces and low frequency motions.

3) Dynamic Mooring Analysis program

This program is used to analyze mooring line response to wave frequency motions.

The recommended analysis procedure is described below (API, 1994):

- a) Determine wind and current velocities, and significant wave heights and periods, for both the maximum design, and operating conditions in accordance with guidelines.
- b) Determine the mooring pattern, characteristics of chain and wire rope to be deployed, and initial tension.
- c) Determine the steady state environmental forces acting on the hull.
- d) Determine the vessel's mean offset due to the steady state environmental forces using the static mooring analysis program.
- e) Determine the low frequency motions. Since calculation of low frequency motions requires the knowledge of the mooring stiffness, the mooring stiffness at the mean offset should be determined first using a static mooring analysis computer program.
- f) Determine the significant and maximum single amplitude wave frequency vessel motions using a hydrodynamic motion analysis program.
- g) Determine the vessel's maximum offset, suspended line length, quasi-static tension, and anchor load.
- h) Determine the maximum line tension and anchor load. A frequency domain or time domain dynamic mooring analysis program should be used.
- i) Compare the maximum vessel offset and suspended line length from step g and maximum line tension and anchor load from step g or h. If the criteria are not met, modify the mooring design and repeat the analysis.

The recommended analysis procedure is described below (API, 1994):

- a) Determine wind and current velocities, and significant wave heights and periods, for both the maximum design, and operating conditions in accordance with guidelines.
- b) Determine the mooring pattern, characteristics of chain and wire rope to be deployed, and initial tension.
- c) Determine the steady state environmental forces acting on the hull.
- d) Determine the vessel's mean offset due to the steady state environmental forces using the static mooring analysis program.
- e) Determine the low frequency motions. Since calculation of low frequency motions requires the knowledge of the mooring stiffness, the mooring stiffness at the mean offset should be determined first using a static mooring analysis computer program.
- f) Determine the significant and maximum single amplitude wave frequency vessel motions using a hydrodynamic motion analysis program.
- g) Determine the vessel's maximum offset, suspended line length, quasi-static tension, and anchor load.
- h) Determine the maximum line tension and anchor load. A frequency domain or time domain dynamic mooring analysis program should be used.
- i) Compare the maximum vessel offset and suspended line length from step g and maximum line tension and anchor load from step g or h. If the criteria are not met, modify the mooring design and repeat the analysis.

2.4.2 Mooring Analysis in MODUSIM

Due to the complexity of the mooring analysis procedures, it is difficult, if not impossible, to perform detailed mooring analysis procedures in each simulation step. That would be both time consuming and unnecessary. A simplified mooring capacity model is developed for the simulation purpose.

In MODUSIM, it is assumed that the total expected lateral capacity of the mooring system is \overline{R}_t (Figure 2.11). There are two modes of mooring system failure:

- 1) all the mooring lines are broken and the MODU is in the free floating condition;
- 2) the horizontal hurricane load is larger than the total anchor holding force and some of the mooring lines are not broken so that the MODU is in a dragging condition. Thus:

\overline{R}_{a1} , failure mode one (free floating), and

\overline{R}_{a2} , failure mode two (anchors dragging).

These failure modes are determined by the MODUSIM user. The effects of different mooring line models are not considered. Users can modify \overline{R}_t to include such effects.

For more detailed mooring analysis in MODUSIM, users can use the following simplified formulation which is derived from regression analysis to determine the maximum line tension of the MODU in different environmental conditions:

1. Determine mean environmental force;
2. Determine mean offset;

$$\text{Mean.Offset} = A * F_{\text{mean}} + B \quad (2.51)$$

3. Determine dynamic offset;

$$\text{Dyn. Offset} = C * H_s^2 + D * H_s + E \quad (2.52)$$

Where H_s is the significant wave height.

4. Determine total offset;

$$\text{Total. Offset} = \text{Mean. Offset} + \text{Dyn. Offset} \quad (2.53)$$

5. Determine maximum line tension.

$$\text{Tension} = F * \text{Tot. Offset}^2 + G * \text{Tot. Offset} + H \quad (2.54)$$

Parameters A, B, C, D, E, F, G, H are determined from regression analysis by users.

If information on the parameters are not available, it is recommended to use the assumption that if the environmental force is larger than the mooring capacity, the mooring system will fail.

2.4.3 Water Depth Factor

The algorithm discussed above is specific for one rig type at a given water depth and mooring system. The maximum line tension calculated from the processes presented above is a function of vessel type, mooring system, mean offset wave height and water depth. Changes in any of these make the constants in the algorithm change. The influence of these different variables can cause havoc when trying to create a simple algorithm. For example, a given dynamic offset may increase tensions significantly in shallow water and have no impact in deep water. With a large mean offset, a small dynamic offset can cause a large increase in tensions. The variables are highly non-linear and difficult to predict.

When determining a safe location to stack a MODU, one of the important criteria is adequate water depth. To have the best possible chance for survival in a hurricane, this may be interpreted as choosing a location with the optimal water depth for the mooring system. Research results from Noble Denton Inc. shows that as a rig is moved into shallow water, the capacity of the mooring system decreases (Noble Denton, 1991). This reflects an increase in mooring system stiffness as water depth decreases, and for a stiffer system, a given vessel offset will produce larger tensions.

A possible simple way to solve this problem is to introduce a "water depth correction factor" to modify the calculated forces. The forces are calculated as before and then multiplied by a "water depth correction factor". The resulting force could then be used to determine the approximate total tension. Based on the mooring system performance curves from Noble Denton (Noble Denton, 1994), a regression analysis was performed and the water depth correction factor (WDF) was defined as (Figure 2.12):

$$\text{WDF} = 0.056 * \left(\frac{\text{water depth}}{250}\right)^2 - 0.45 * \left(\frac{\text{water depth}}{250}\right) + 1.89 \quad (2.55)$$

where the unit of water depth is feet.

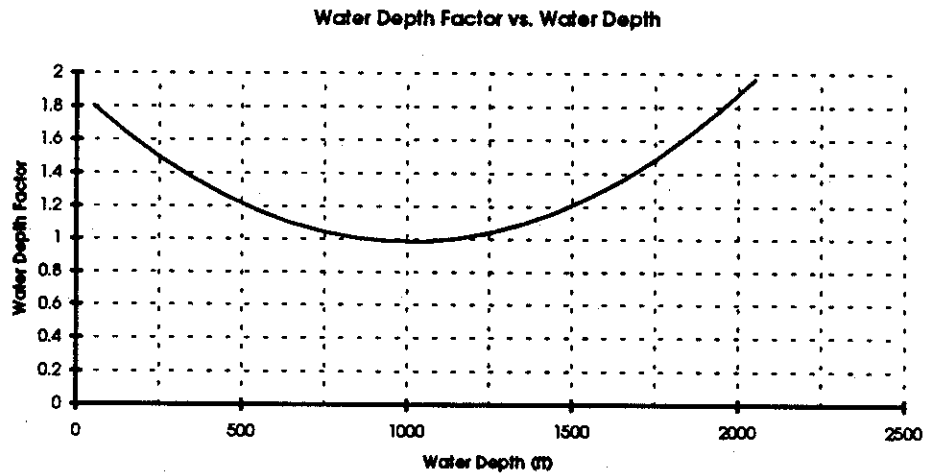


Figure 2.12 Water Depth Factor vs. Water Depth

2.5 Summary

A simulation procedure to characterize hurricane generated wind, current and wave fields with the consideration of shoaling effects was developed based on Cooper (1988). A simplified environmental loading model was developed that is able to develop estimates of total lateral wind, wave and current loadings acting on MODUs. Based on sustained wind velocity at a reference height, wind forces are estimated according to API RP 2A (API, 1993a). The wave loading prediction model utilizes Stokes fifth-order wave theory. The current velocity profile is added to the wave velocity profile. Wave directional spreading and current blockage are taken into account. The hydrodynamic forces acting on a simplified model of the structure is estimated using the Morison's equation.

The simplified load prediction procedure was verified with results reported in a wave force study performed by Exxon and Shell Research Companies (Bea, 1973). Good agreement

has been achieved for wave loading on a surface piercing cylinder in transitional water depth conditions using Stokes V theory.

Based on API (1994), a simplified MODU mooring capacity model was developed. The model takes account two mooring system failure modes: free floating and anchors dragging. A “water depth factor” was proposed to modify the calculated forces for different water depths.

CHAPTER 3

HURRICANE TRACK FORECASTING SIMULATION MODELS

3.1 Introduction to Hurricane Forecasting

The goal of hurricane forecasting is to predict accurately the temporal evolution of the areas of significant surface winds and heavy precipitation. The precipitation issue will not be considered here. The ideal hurricane wind-area prediction would accurately specify at any time the horizontal distributions of wind areas expected to contain damaging winds & cause high seas, perhaps in categories of minor, major and severe. From a user's perspective, the primary concern is the accuracy of forecast times of these wind speeds for a particular location. Forecasters usually think in terms of hurricane track, intensity, and size.

The track, intensity, and size components of a hurricane forecast are dynamically interdependent. For example, even if the intensity and size of a hurricane were to be precisely forecast, a relatively small cross-track forecast error might lead to an extreme overestimate of surface winds for a location near the forecast track. Conversely, an accurate intensity and track forecast accompanied by a size forecast that fails to account for substantial growth of the extent of gale-force winds will lead to a large underestimate in wind speed at a location forecast. Since this research deals with structures that are located on the continental shelf of the Gulf of Mexico, with water depth up to 600 ft, and the changes in the storm parameters after shelf-edge crossing are usually very small until

they reach land, the size and intensity of the hurricane are assumed to be stationary during passage over the continental shelf. The important factor remaining is the hurricane track forecast.

One of the simplest track prediction schemes is to assume persistence of recent motion. The physical basis for this assumption is that a tropical cyclone is normally a small vortex embedded in a large-scale flow. The recent motion of the storm is a result of the interaction of the vortex and the large-scale flow. If the vortex, large-scale flow and the interaction processes do not change, the future motion should resemble the past motion. Persistence is a reasonable, first-order approximation for prediction short-term motion.

The simplest prediction of the future track is to assume that the present storm will move with the average direction and speed of all past storms near that location. This is another important hurricane track prediction scheme, climatology. To make a track prediction, the climatological velocity vectors at the appropriate locations are multiplied by the time interval and the resulting displacements are added to the present latitude and longitude. The pure climatology forecast is more effective at longer forecast intervals.

A combination of persistence plus climatology is expected to provide an improvement over the separate techniques. A typical combination is half persistence and climatology. An alternative is a blend that weights persistence higher early in the forecast and

climatology higher later. This empirical blending presumably takes advantage of the best characteristics of each scheme.

Statistical track forecasting models derive their variance reducing potential from one or more of four sources of predictive information: climatology, persistence, environmental data and numerically forecast environmental data. A statistical combination of CLImatology and PERsistence (CLIPER), developed for the Atlantic region by Neumann (1972), has been extended to other basins (Leftwich and Neumann, 1977; Xu and Neumann, 1985). A similar persistence and climatology technique for the Western North Pacific is used by the Shanghai Typhoon Institute (Z. Wu, 1985, IWTC). Predictors such as the present latitude and longitude, the components of the recent motion of the storm and the intensity are used. Least-squares fitting of the basic predictors and various polynomial combinations are used in CLIPER to derive regression equations for future latitudinal/longitudinal displacements in 12-hour increments. Thus, this technique makes use of the "climatology" of past tropical cyclone tracks and the persistence components of the present storm to generate a forecast.

Several forecast centers also use the probabilities to describe uncertainties in the spatial and temporal occurrence of tropical cyclones. The most common uses of forecast probability in relation to the occurrence of severe cyclonic effects such as the distribution of hurricane-force winds, the height of sea waves and the elevation of storm surges, are:

- a. to extend the useable length of forecasts despite their increasing uncertainty as the forecast period increases;
- b. to provide a quantitative assessment of the threat posed by a cyclone approaching possible landfall;
- c. to compare the relative threat to different places at the same time, or at different times as a threat develops;
- d. to cause a consistent response to the same or similar set of circumstances; and
- e. as a tool in risk analysis, both in respect to long-term protective measures, and for contemporary warning purposes.

For a comprehensive overview of the types of probabilities presently available, the reader is referred to Jarrel and Brand (1983).

3.2 Track Forecasting Models for Simulation

In previous simulation studies (Wen, 1988), the hurricane was assumed to be a storm traveling along a straight line with a given translation speed and direction. In fact, hurricane tracks are generally curved. Based on a statistical analysis of hurricane route histories, one can characterize the parameters that influence changes of hurricane direction, and estimate their probability distributions.

All the models discussed above are suitable for forecasting the track of a typical incoming hurricane. For a model to be suitable for Monte Carlo simulation, it must be complete

enough to include all the available hurricane information but still simple enough to run quickly if many simulations are needed. All the methodologies existing or discussed above are complicated and time consuming, and not suitable for simulation. As a result, two hurricane track forecasting model are developed especially for Monte Carlo simulation purposes:

- 1) The Track Forecast Error Statistical Model generates hurricane track forecast based on the 72 hour real-time hurricane forecast from hurricane forecast centers, and statistical analysis of historical hurricane track forecast error from the same hurricane forecast center. This model is especially useful to generate hurricane track forecast to perform simulations for a special incoming hurricane with 72 hour hurricane forecast.
- 2) The Markov-Chain Simulation Model generates hurricane track forecasts based on the Markov transition probability matrix, developed from hurricane track history statistics. This model is especially useful to generate hurricane track forecasts to perform simulations of long-term period, for example, one year, while the real time forecast data are not available during the period. This model is used in this study to calculate MODUs annual collision probabilities.

3.3 Track Forecast Error Statistical Model

Hurricane track actual and forecast data are obtained from the Joint Typhoon Warning Center (JTWC). For each past hurricane, the forecast track and actual track are compared

and forecast errors are calculated. Forecast errors are decomposed into along-track errors (ahead & behind) and cross-track errors (left & right). The errors are also decomposed into orientation and distance errors. As in Figure 3.1, the forecast distance error is defined as the distance between the forecast track point and the actual track point, and forecast orientation error is defined as the angle between the forecast track direction and the straight line passing through the forecast track point and actual track point. For a typical 72 hour hurricane track forecast, the data are given at 6 hour time intervals. The histogram of forecast errors are calculated on different forecast time interval data (6, 12, 24, 36, 48, and 72 hour intervals).

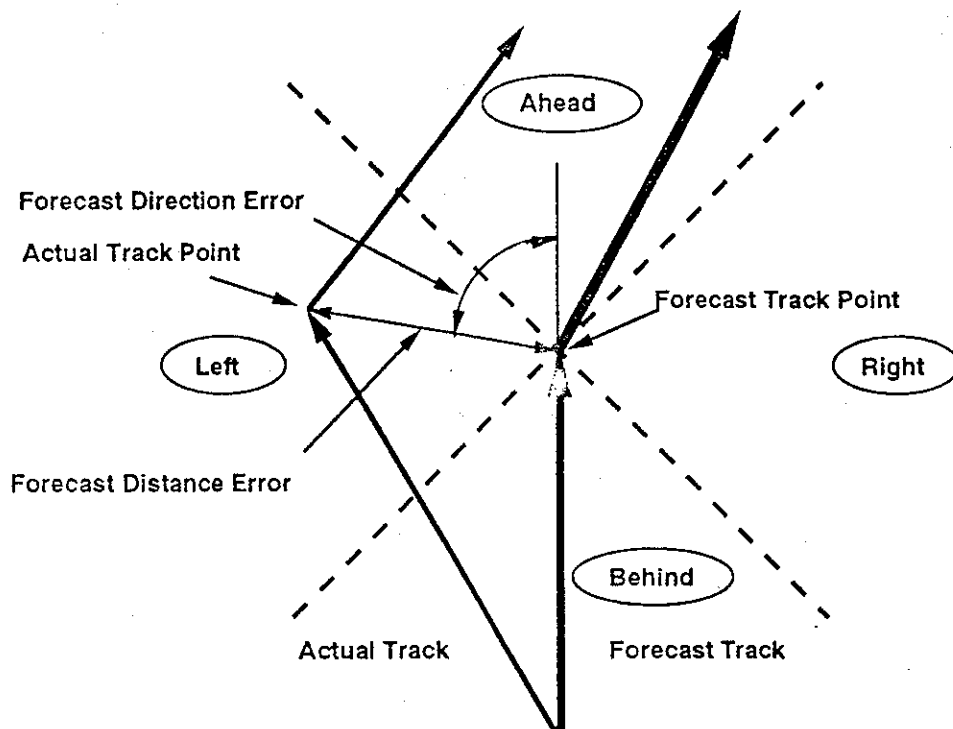
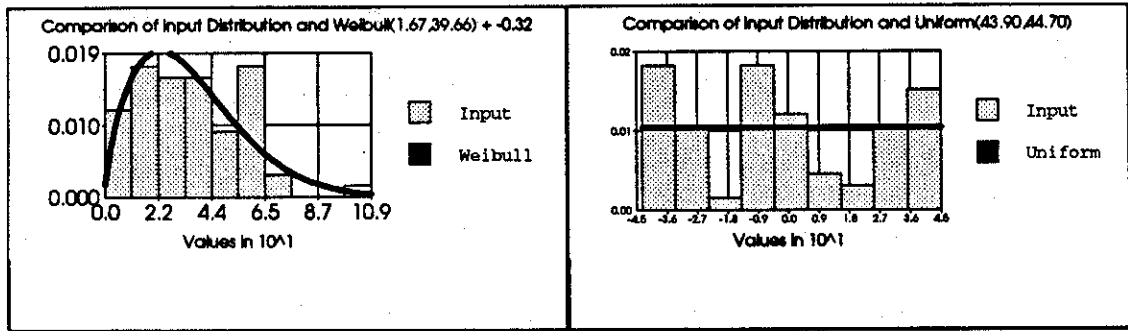


Figure 3.1 Determining the Track Forecast Error

Comparison between forecast error data in different sections and best-fitting Weibull and Uniform distributions are presented in Figure 3.2. Goodness-of-Fit tests (Chi-Square Test) were also performed for each fitted distributions (Refer to Appendix C for detailed procedures about these tests). It was found that, from the statistical point of view, adequacy of the fit varied considerably. For fit results of distance error, some of the fit results are good, e.g., for distance error of 36 hours and right error section, the significance level for the hypothesis that the fitted distribution gave the data is 4%. But most of the fit results have a large significance level and can not pass the goodness-of-fit test with significance level 5%, e.g., distance error of 24 hour right section.

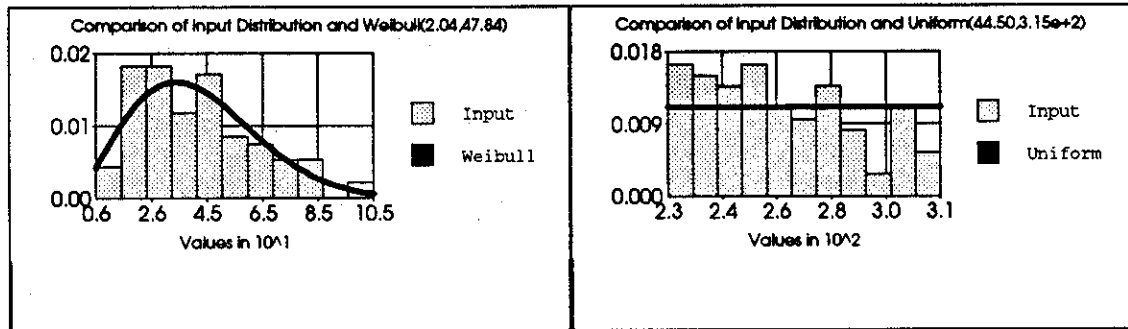
Direction errors were analyzed similarly, to obtain distributions that characterize the input data adequately for the purpose of this engineering application.

Among the 8 distribution families fitted to the distance error data, a Weibull distribution was found to fit best. The best fitting distribution for direction error among these fittings is a uniform distribution. Also, it was found that the correlation between the orientation error and the distance error was insignificant.



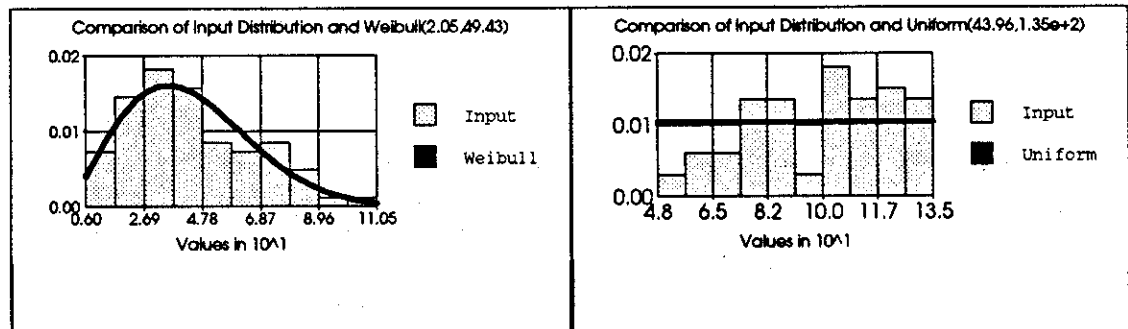
Distance_Ahead_12 hour

Direction_Ahead_12 hour



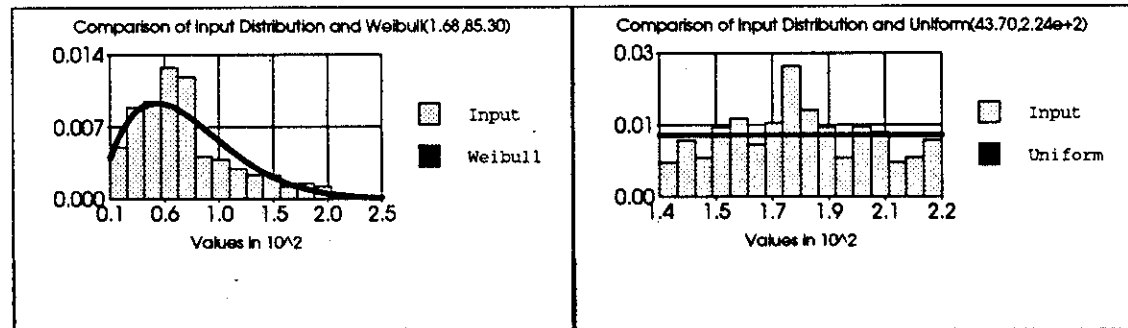
Distance_Left_12 hour

Direction_Left_12 hour



Distance_Right_12 hour

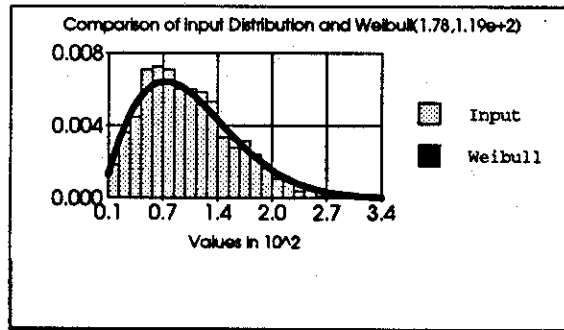
Direction_Right_12 hour



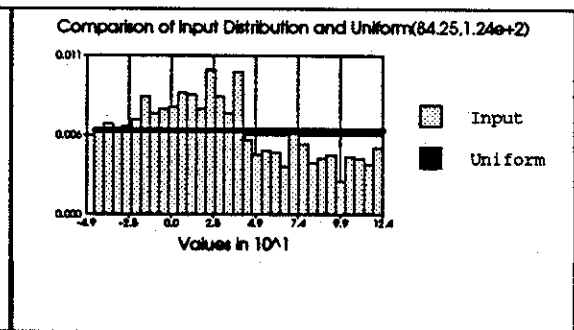
Distance_Behind_12 hour

Direction_Behind_12 hour

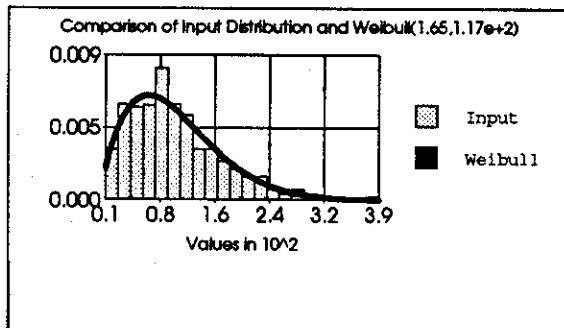
Figure 3.2 Fit Results for Distance and Direction Forecasting Error



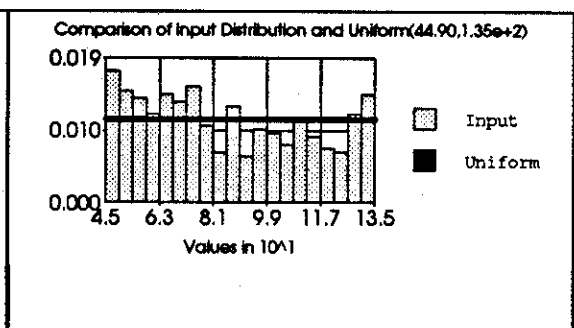
Distance_Ahead_24 hour



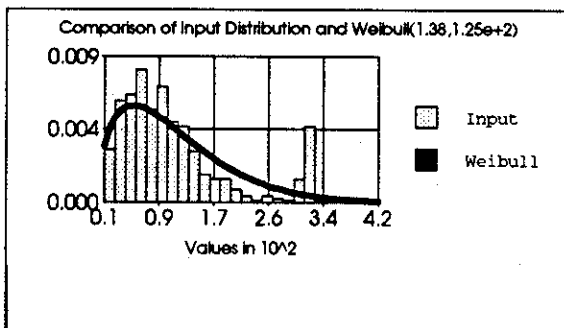
Direction_Ahead_24 hour



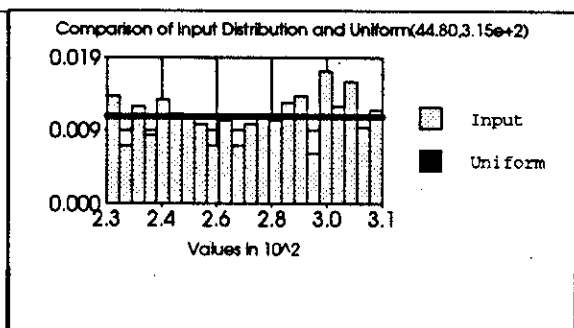
Distance_Left_24 hour



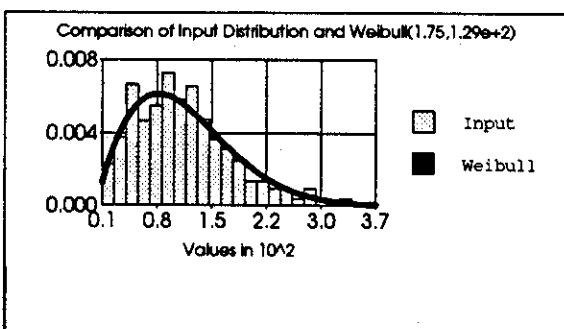
Direction_Left_24 hour



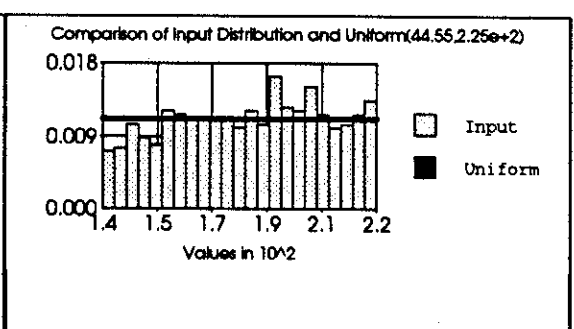
Distance_Right_24 hour



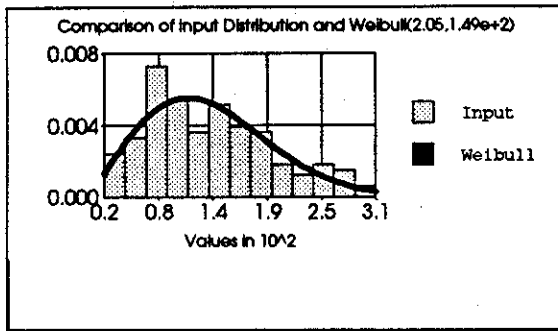
Direction_Right_24 hour



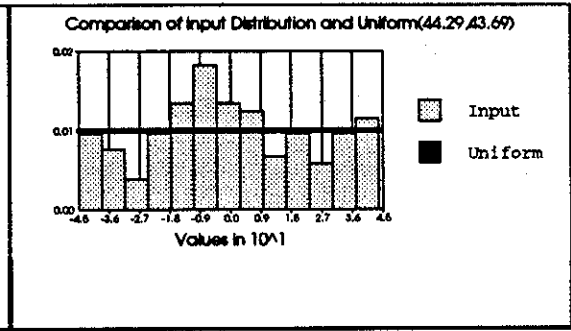
Distance_Behind_24 hour



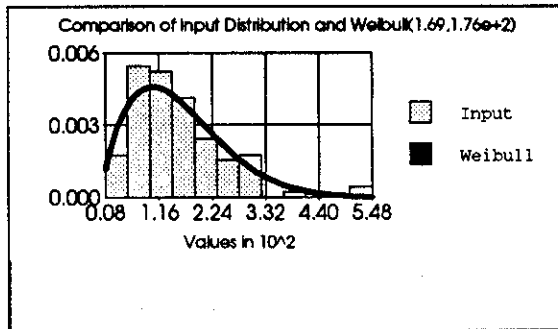
Direction_Behind_24 hour



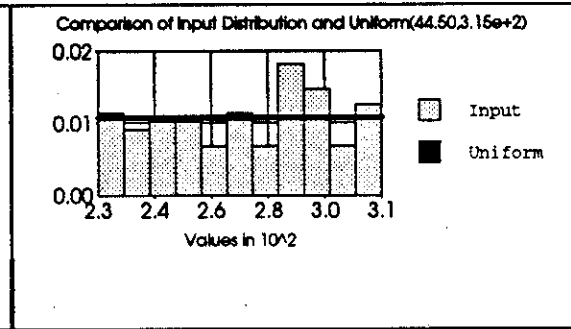
Distance_Ahead_36 hour



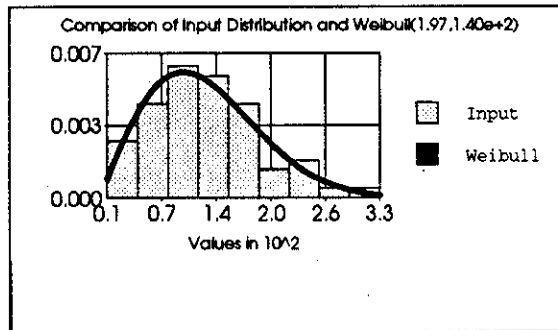
Direction_Ahead_36 hour



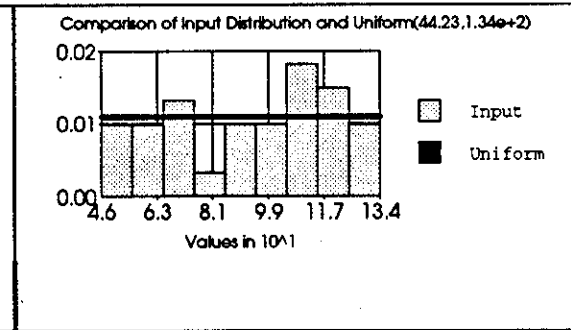
Distance_Left_36 hour



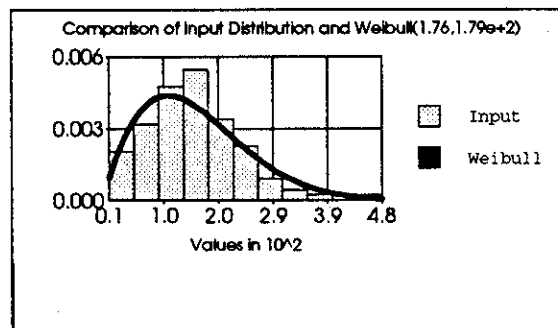
Direction_Left_36 hour



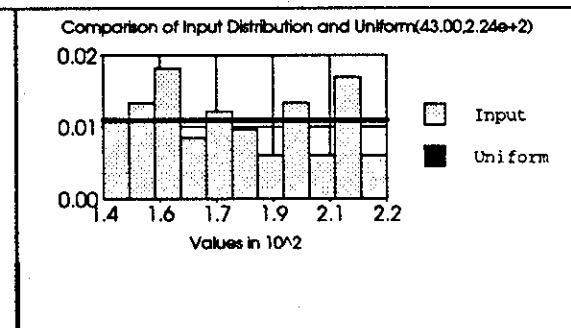
Distance_Right_36 hour



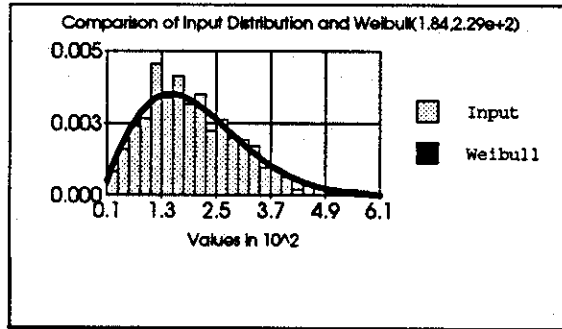
Direction_Right_36 hour



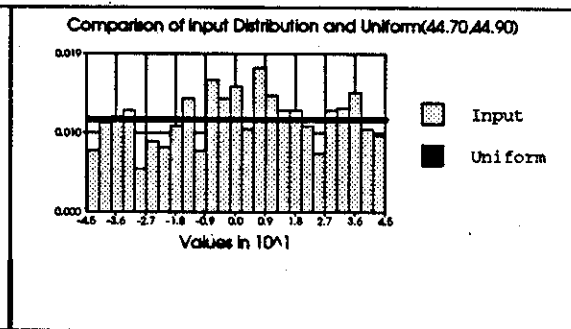
Distance_Behind_36 hour



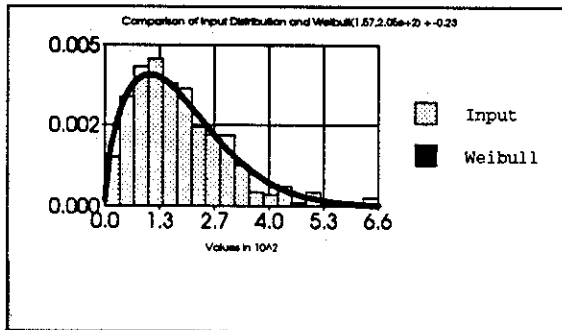
Direction_Behind_36 hour



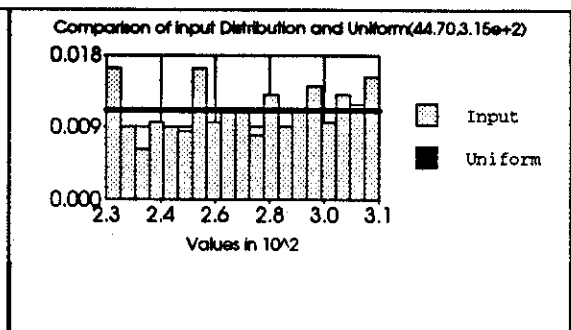
Distance_Ahead_48 hour



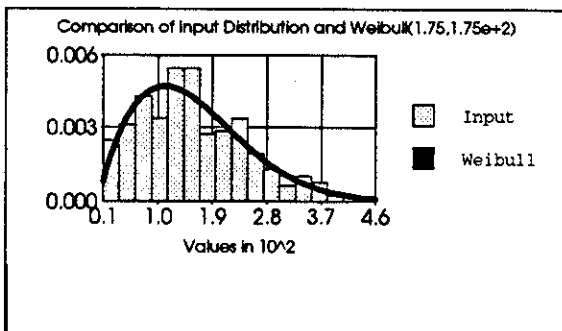
Direction_Ahead_48 hour



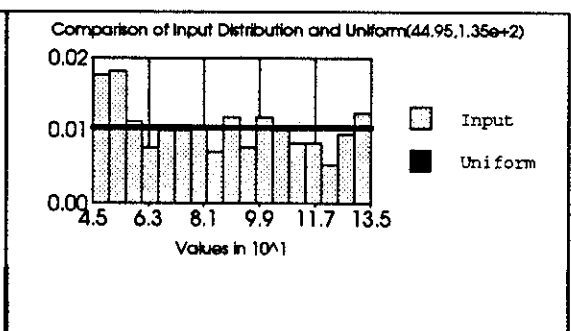
Distance_Left_48 hour



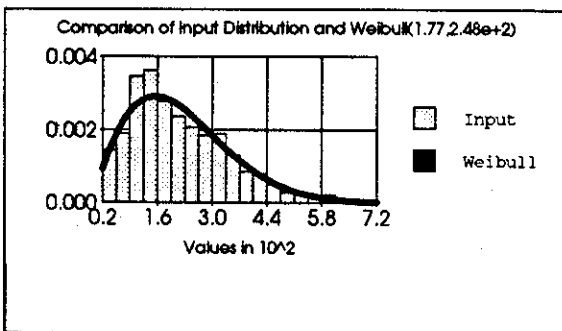
Direction_Left_48 hour



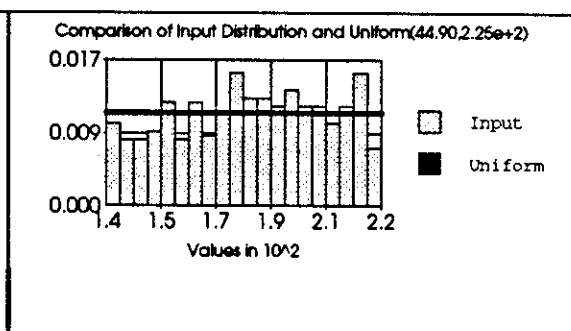
Distance_Right_48 hour



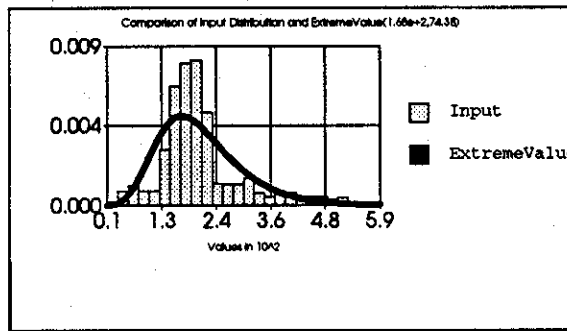
Direction_Right_48 hour



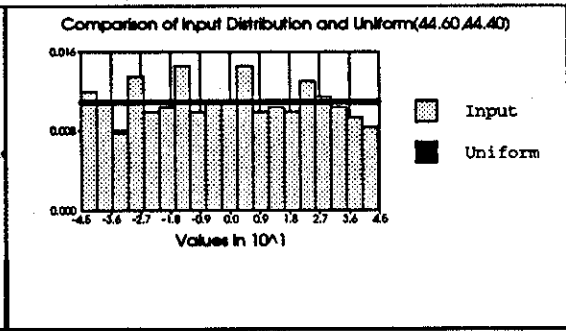
Distance_Behind_48 hour



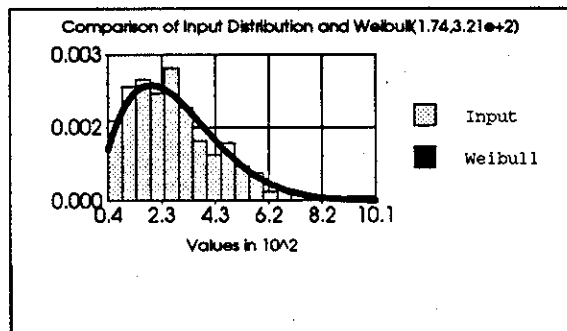
Direction_Behind_48 hour



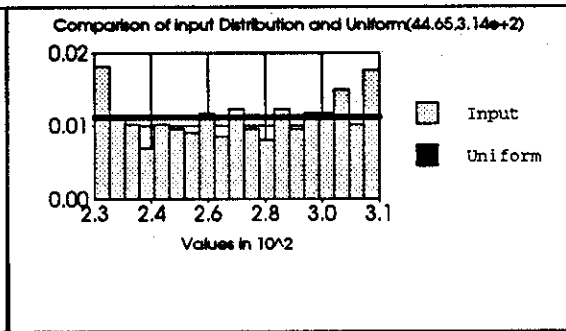
Distance_Ahead_72 hour



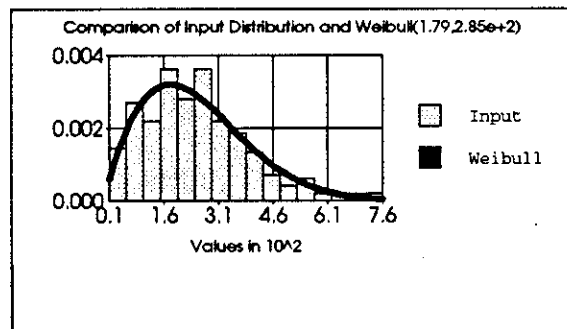
Direction_Ahead_72 hour



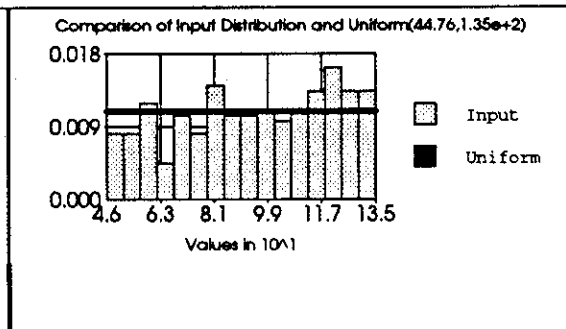
Distance_Left_72 hour



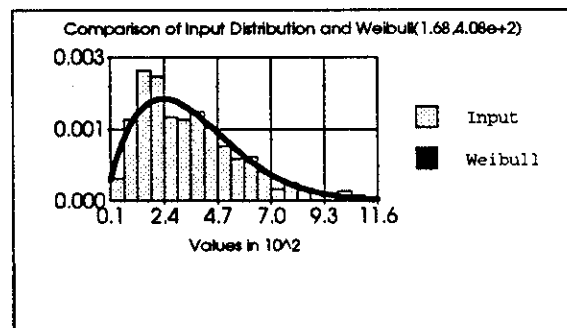
Direction_Left_72 hour



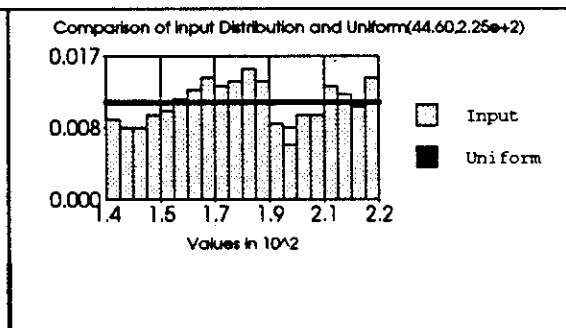
Distance_Right_72 hour



Direction_Right_72 hour



Distance_Behind_72 hour



Direction_Behind_72 hour

To perform simulations, a circular region of radius from 100-500 nm is divided into small sections of equal angular & radius extent. The angular interval is 30° ; the radial interval is 30 nm (Figure 3.3). For example, for 24 hours interval forecast, the chance that the forecast distance error beyond a circle of radius 300 nm is negligible. Within the circular region, the chance that the storm center is in each small section at the end of the forecast interval can be estimated. The sum of all such probabilities must be 1.

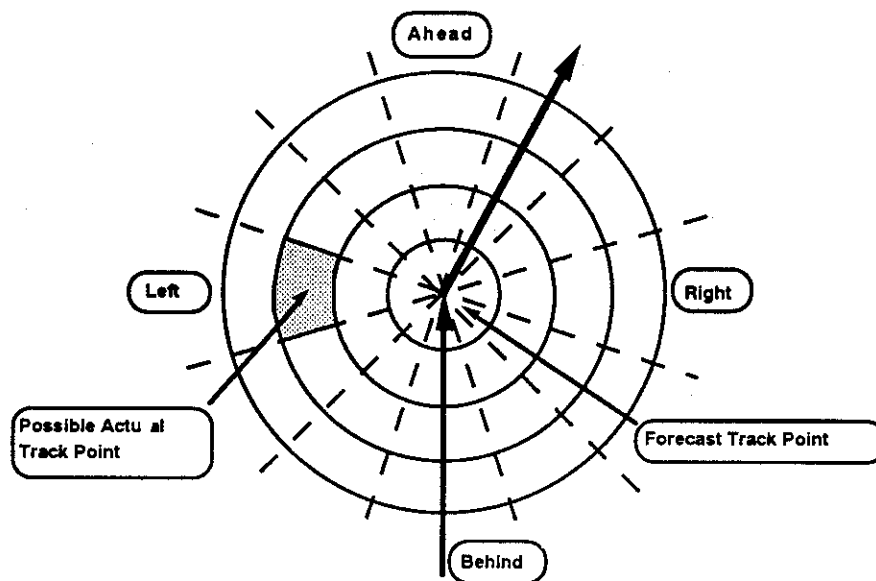


Figure 3.3 Example of Calculation of Probability Function in a Square

The procedure for estimating the probability function of the shaded square in Figure 3.3 for a 48 hour forecast point is as follows:

$$P = P_{\text{Section}} \cdot P_{\text{Dir}} \cdot P_{\text{Weibull}} (30 < \text{Error} < 60) \quad (3.1)$$

Where P_{Section} is the weighting function for each angular section (Table 3.1). For 48 hour forecast and the Left section here, $P_{\text{Section}} = 0.2$. P_{Dir} is the weighting function for direction error, here $P_{\text{Dir}} = 1/3$ because the direction errors are uniform distributed and the shaded area has 30° angular extend, $1/3$ of the Left section. $P_{\text{Weibull}}(30 < \text{Error} < 60)$ is the probability of forecast error larger than 30 nm and less than 60 nm which we have taken to be Weibull distributed with parameters estimated from historical data. So, we have:

$$P_{\text{Shade}} = P_{\text{Section}} \cdot P_{\text{Dir}} \cdot P_{\text{Weibull}}(30 < \text{Error} < 60) = 0.2 \cdot \frac{1}{3} \cdot 0.105 = 0.007$$

Table 3.1 Weighting Functions for Each Section

Interval	Ahead	Left	Right	Behind
12	0.21	0.31	0.24	0.24
24	0.32	0.23	0.19	0.26
36	0.34	0.26	0.15	0.25
48	0.40	0.20	0.16	0.24
72	0.27	0.27	0.16	0.30

The probability that the actual track point is in each different small section can be estimated by the same procedure, and hurricane tracks can be simulated by generating pseudo-random tracks, according to that estimated probability distributions.

Figure 3.4 is the plot of forecast mean distance error vs. forecast time interval. The mean error of 12 hours forecasts is about 50 nm with standard deviation 25 nm, while for 72 hours forecasts, the mean is almost 300 nm with standard derivation almost 200 nm. It is found that the mean hurricane track forecast error increases approximately linearly with

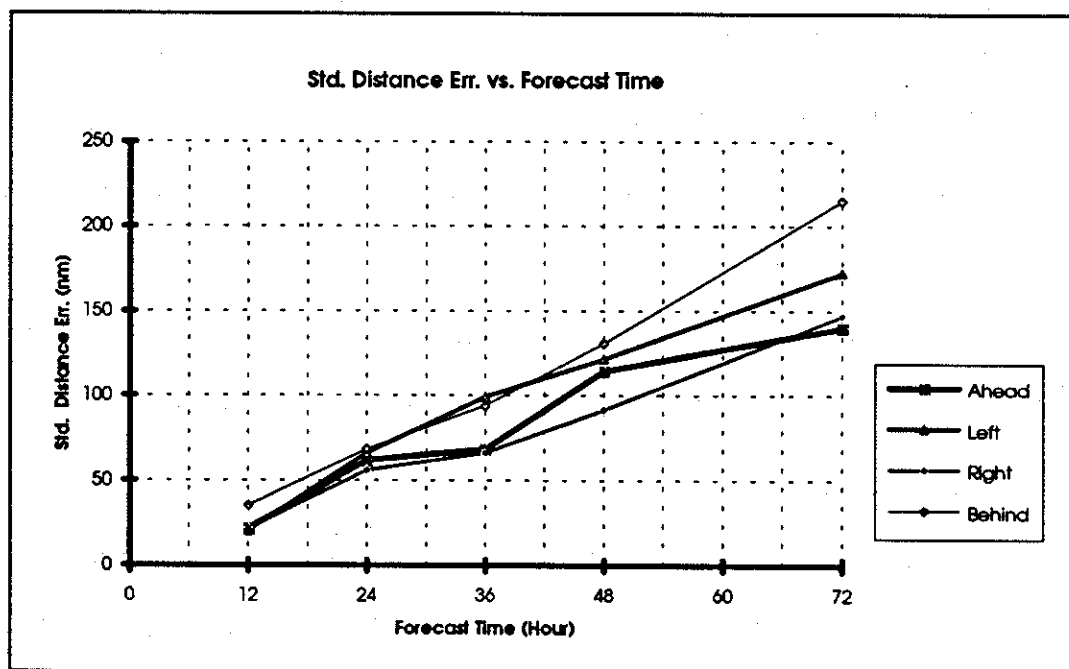
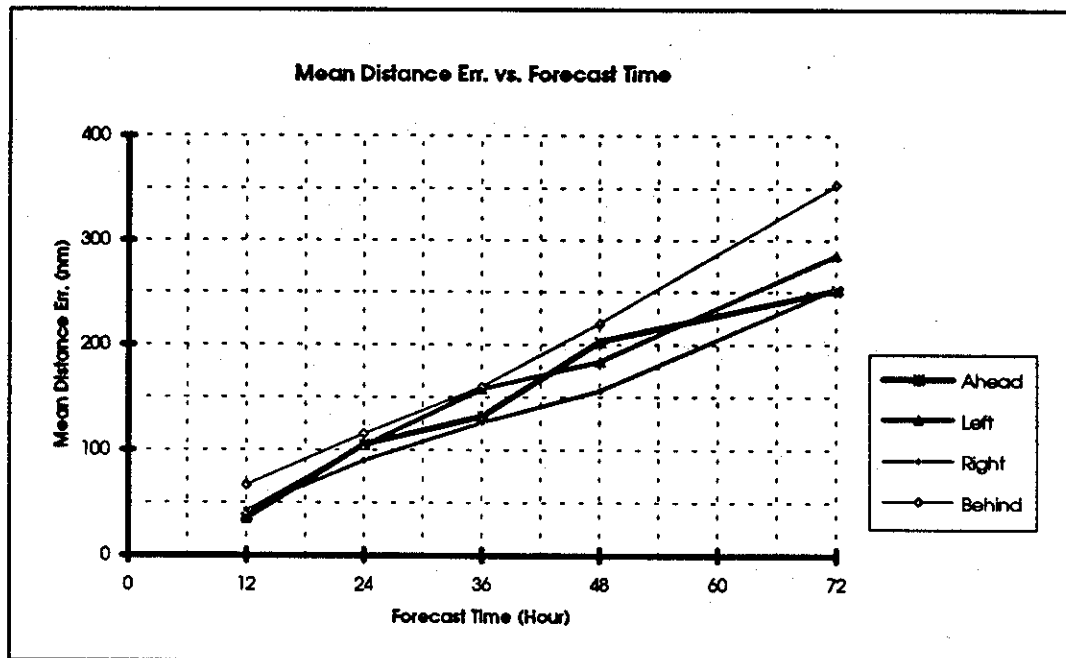


Figure 3.4 Forecast Mean Distance Error vs. Forecast Time Interval

forecast time interval. So does its standard deviation. It is the long "tail" of large forecast errors that place the users of hurricane forecasting at risk. There are large uncertainties associated with hurricane track forecasting and reliability is a very important concept. Simulations are a useful tool to approach the problem.

The same approach can be used to analyze the strength forecast error if changes of hurricane strength need to be included in the simulation.

3.4 Markov-Chain Simulation Model

Sometimes, the simulation is not restricted to one special hurricane and what we are interested is a long-term period probability. For example, to calculate the annual collision probability of MODU with large surrounding facilities, the hurricane is generated according to Poisson distribution in a one year period and there is no real time hurricane forecast data available. The Markov-Chain simulation model is effective for this purpose.

Based on the data from the MMS (MMS, 1993), the transition probability matrix to describe the probabilities of changes in the storm track directions for Gulf of Mexico hurricanes have been developed. As it was discussed in Section 3.1, the most important hurricane track forecast techniques are persistence and climatology. The Markov model is a combination of these techniques. It is a blend that weights persistence higher early in the forecast and climatology higher later. This empirical blending presumably takes advantage

of the best characteristics of each scheme. The next section provides an introduction to Markov processes.

3.4.1 Introduction to Markov Chains

The state of a system invariably changes with respect to some parameter, for example, time or space. The transition from one state to another as a function of the parameter, or its corresponding transition probability, may generally depend on the prior states. However, if the transition probability depends only on the current state, the process of change may be modeled with the Markov process. If the state space is a countable or finite set, the process is called a Markov Chain.

Consider a system with m possible states, namely $1, 2, \dots, m$, and changes in state can occur only at discretized values of the parameter; for example, at times t_1, t_2, \dots, t_n . Let X_{n+1} denote the state of the system at t_{n+1} . In general, the probability of a future state of the system may depend on its entire history; that is, its conditional probability is:

$$P(X_{n+1} = i | X_0 = x_0, X_1 = x_1, \dots, X_n = x_n) \quad (3.2)$$

where $|X_0 = x_0, X_1 = x_1, \dots, X_n = x_n$ represent all previous states of the system. If the future state is governed solely by the present state of the system, that is, the conditional probability, Eq.(3.2) is:

$$P(X_{n+1} = i | X_0 = x_0, X_1 = x_1, \dots, X_n = x_n) = P(X_{n+1} = i | X_n = x_n) \quad (3.3)$$

then the process is a Markov chain. For a discrete parameter Markov chain, the transitional probability from state i at time t_m to state j at time t_n may be denoted by:

$$p_{ij}(m,n) = p(X_n = j | X_m = i); \quad n > m \quad (3.4)$$

The Markov chain is homogeneous if $p_{ij}(m,n)$ depends only on the difference $t_n - t_m$; in this case, we define:

$$p_{ij}(k) = p(X_t = j | X_s = i) = p(X_{t+s} = j | X_t = i) \quad s \geq 0 \quad (3.5)$$

as the k -step transition probability function. Physically, this represents the conditional probability that a homogeneous Markov chain will go from state i to state j after k times stages. This probability can be determined from the one-step transition probabilities, namely $p_{ij}(1)$ or simply p_{ij} , between all pairs of states in the system. These transition probabilities can be summarized in a matrix for a system with m states, called the transition probability matrix:

$$P = \begin{bmatrix} P_{1,1} & P_{1,2} & \cdots & P_{1,m} \\ P_{2,1} & P_{2,2} & \cdots & P_{2,m} \\ \vdots & \vdots & \ddots & \vdots \\ P_{m,1} & P_{m,2} & \cdots & P_{m,m} \end{bmatrix} \quad (3.6)$$

As the states of a system are mutually exclusive and collectively exhaustive after each transition, the probabilities in each row add up to 1.0. For a homogeneous discrete Markov chain, the probabilities of the initial states are the only other information needed to define the model behavior at any future time.

3.4.2 State Probabilities

The probabilities of the respective initial states of a system may be denoted by a row matrix:

$$P(0) = [p_1(0), p_2(0), \dots, p_n(0)] \quad (3.7)$$

where $p_i(0)$ is the probability that the system is initially at state i . In the special case for which the initial state of the system is known, for example, at state i , then $p_i(0) = 1.0$ and all other elements in the row matrix $P(0)$ are zero. After one transition, the probability that the system is in state j is given by the theorem of total probability as:

$$P_j(1) = P(X_1 = j) = \sum_i P(X_0 = i)P(X_1 = j|X_0 = i) \quad (3.8)$$

Hence,
$$P_j(1) = \sum_i P_i(0)P_{i,j} \quad (3.9)$$

In matrix notation, the single state probabilities become,

$$P(1) = P(0)P \quad (3.10)$$

which is also a row matrix.

Similarly, the probability that the system is in state j after two transitions is given by:

$$P_j(2) = \sum_i P(X_1 = k)P(X_2 = j|X_1 = k) = \sum_i P_i(1)P_{i,j} \quad (3.11)$$

or in matrix notation,

$$P(2) = P(1)P = P(0)PP = P(0)P^2 \quad (3.12)$$

Therefore, by induction, it can be shown that the n-stage state probability matrix is given by:

$$P(n) = P(n-1)P = P(n-2)PP = \dots = P(0)P^n \quad (3.13)$$

3.4.3 Hurricane Tracks Modeling in Gulf of Mexico (GOM)

For application to hurricane tracks, the states are defined as different directions of storm tracks. And the transition step size is two hours. As shown in Figure 3.5, and based on the statistical analysis of storm track histories, the plane 0 to 180 degrees is divided into 3 blocks. Then there are 3 possible states (1,2,3) and the transition probability matrix **P** is 3×3 :

1--direction 0-75 degrees

2--direction 75-100 degrees

3--direction 100-180 degrees

And from the statistical analysis of storm track histories, we also assume that, within each state of direction, the moving direction has a probabilistic distribution. It is a uniform distribution in state 1 and triangular distribution in state 2 and 3. The distribution functions are shown in Figure 3.6.

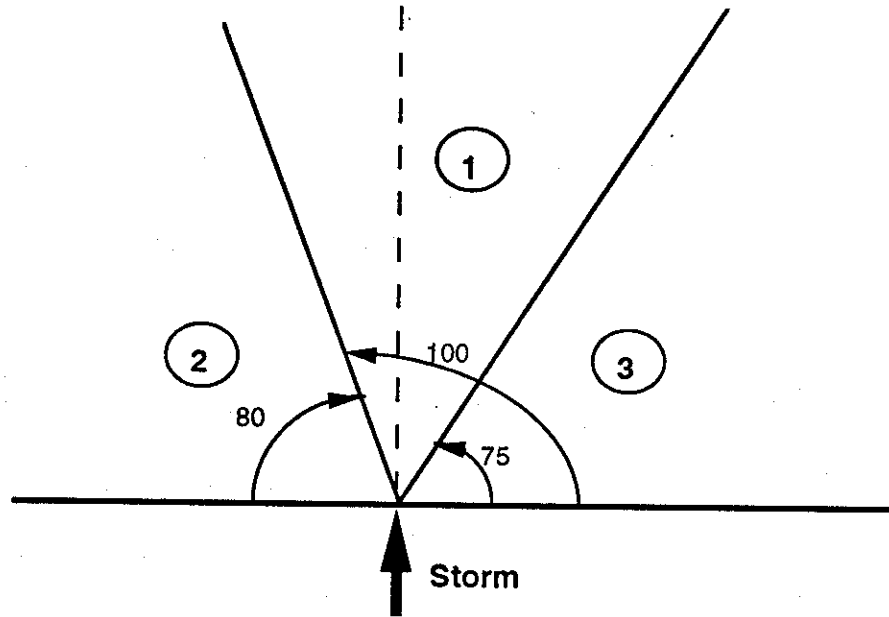


Figure 3.5 Definition of Storm Track Transmission State

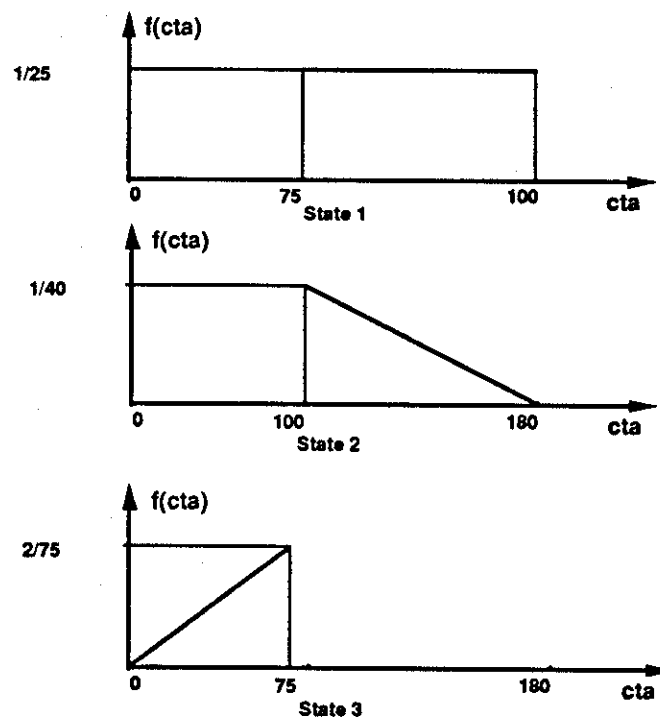


Figure 3.6 Probability Density Function of CTA in State 1,2,3

The transition probabilities are estimated by calculating the times of storm track direction changes from one state to the other based on the database of hurricane track history from MMS (MMS, 1993). The Table 3.2 shows the observed transitions in Gulf of Mexico (Florida to Texas) from 1950 to 1992.

Table 3.2 Observed Transitions in Gulf of Mexico (1950 - 1992)

From\To	1	2	3	Total
1	99	12	25	136
2	10	2	4	16
3	14	4	15	33

The $P_{i,j}$ values are estimated from Table 3.2 using the formula:

$$P_{i,j} = \frac{a_{i,j}}{\sum_j a_{i,j}} \quad (3.14)$$

Table 3.3. $P_{i,j}$ Values

From\To	1	2	3
1	0.73	0.09	0.18
2	0.63	0.12	0.25
3	0.43	0.12	0.45

The resulting transition probability matrix is:

$$P = \begin{bmatrix} 0.73 & 0.09 & 0.18 \\ 0.63 & 0.12 & 0.25 \\ 0.43 & 0.12 & 0.45 \end{bmatrix} \quad (3.15)$$

3.4.4 Steady State Probabilities

We note that the state probabilities starting with two different initial states approach one another as the number of transition stages increases. In fact, the state probabilities will converge to a set of steady-state probabilities p^* , which are independent of the initial states. Therefore, at steady-state condition,

$$P(n+1) = P(n) = P^* \quad (3.16)$$

$$\text{Hence,} \quad P(n+1) = P(n)P \quad (3.17)$$

$$P^* = P^*P \quad (3.18)$$

For a Markov chain with m states, this matrix equation represents a set of simultaneous equations as follows:

$$[p_1^* \cdots p_m^*] = [p_1^* \cdots p_m^*] \begin{bmatrix} p_{1,1} & \cdots & p_{1,m} \\ \vdots & & \vdots \\ p_{m,1} & \cdots & p_{m,m} \end{bmatrix} \quad (3.19)$$

We can find that Eq.(3.19) contains one degree of freedom. The required constraint to obtain P^* is:

$$p_1^* + p_2^* + \cdots + p_m^* = 1.0 \quad (3.20)$$

Given a particular state matrix P_1 , the probabilities of being in the various possible states after n transitions are found from:

$$P_{n+1} = P_1 \cdot P^n \quad (3.21)$$

Using the hurricane route input as $P_1 = [1 \ 0 \ 0]$, after every two hours, the probability matrix is :

$$P_2 = [0.73 \ 0.09 \ 0.18]$$

$$P_3 = [0.667 \ 0.098 \ 0.235]$$

$$P_4 = [0.649 \ 0.099 \ 0.250]$$

$$P_5 = [0.643 \ 0.101 \ 0.256]$$

And the P^* matrix is calculated as:

$$P^* = [0.643 \ 0.101 \ 0.256] \quad (3.22)$$

This implies that the hurricane track has about a 64.3% probability to change to state 1, about a 10.1% to state 2 and about a 25.6% to state 3. Also, it can be seen that the future transition probability are not strongly dependent upon the present state matrix. After only four transitions, the state probability matrix coverages to the steady-state probability matrix.

3.4.5 Hurricane Track Modeling for Texas-Mexico Coast

The hurricane route history statistics for Texas-Mexico coastline is calculated based on MMS hurricane forecast database (MMS, 1993). The results are presented as follows:

Table 3.4 Observed Transitions in Texas-Mexico Coast

From\To	1	2	3	Total
1	725	74	135	934
2	55	22	21	98
3	120	19	93	232

Table 3.5 P_{ij} Values

From\To	1	2	3
1	0.78	0.08	0.14
2	0.56	0.22	0.22
3	0.52	0.08	0.40

The transition probability matrix is:

$$P = \begin{bmatrix} 0.78 & 0.08 & 0.14 \\ 0.56 & 0.22 & 0.22 \\ 0.52 & 0.08 & 0.40 \end{bmatrix} \quad (3.23)$$

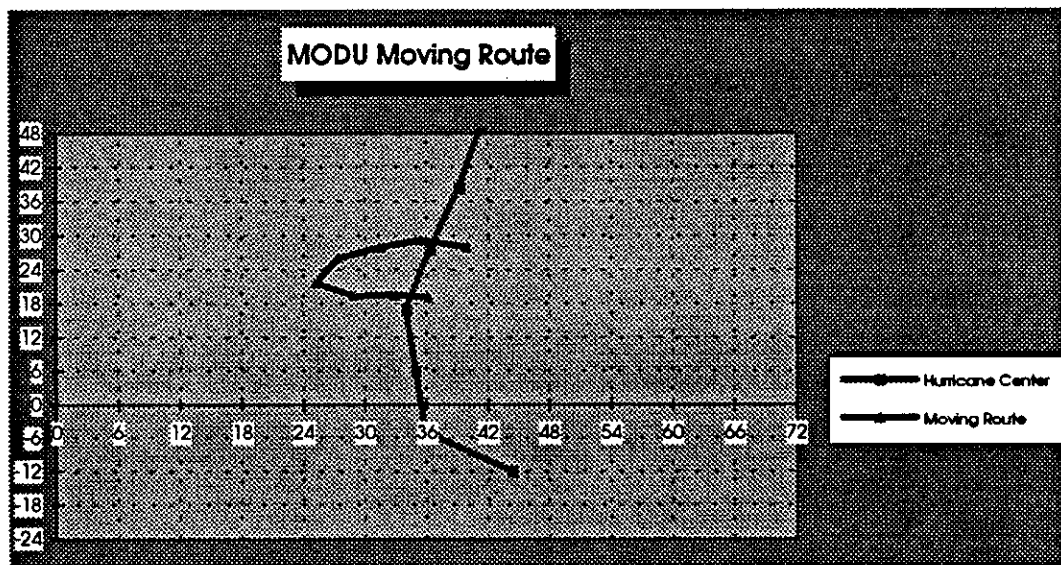
The steady-state P^* matrix is calculated as:

$$P^* = [0.708 \quad 0.093 \quad 0.199] \quad (3.24)$$

Comparing the transition matrix of GOM (Table 3.3) with that of the Texas-Mexico coast (Table 3.5), it is seen that the two matrixes are close to each other. It is also seen that storms tends to move clockwise in the GOM and more straight in the Texas-Mexico coast.

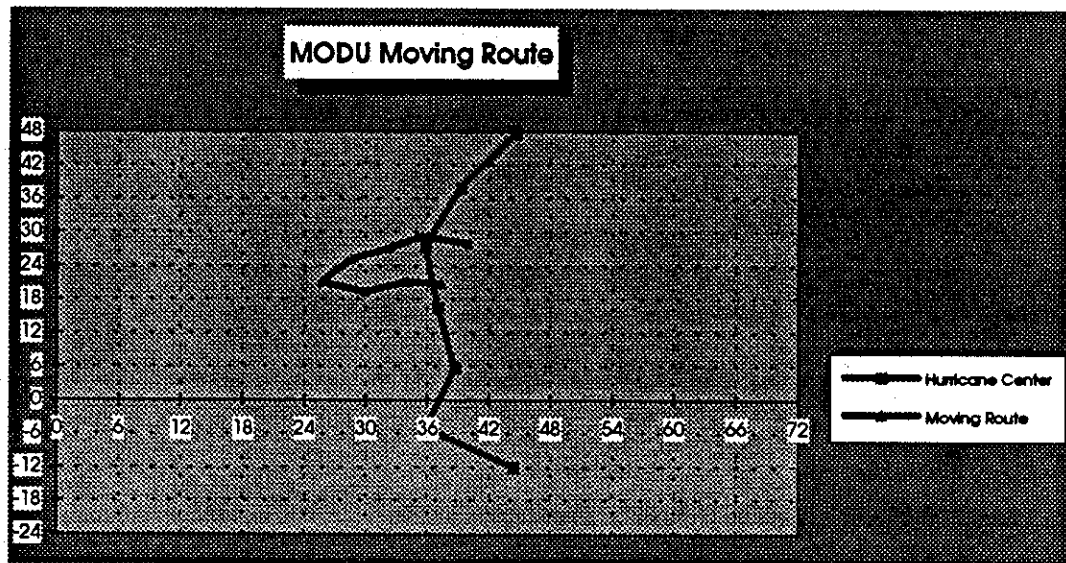
3.4.6 Examples of Markov Model Hurricane Tracks

In Figure 3.7, there are five hurricane track examples generated by MODUSIM based on Markov-Chain model. Study of a wide range of hurricane characteristics indicates that the simulated tracks are representative of real hurricane tracks..

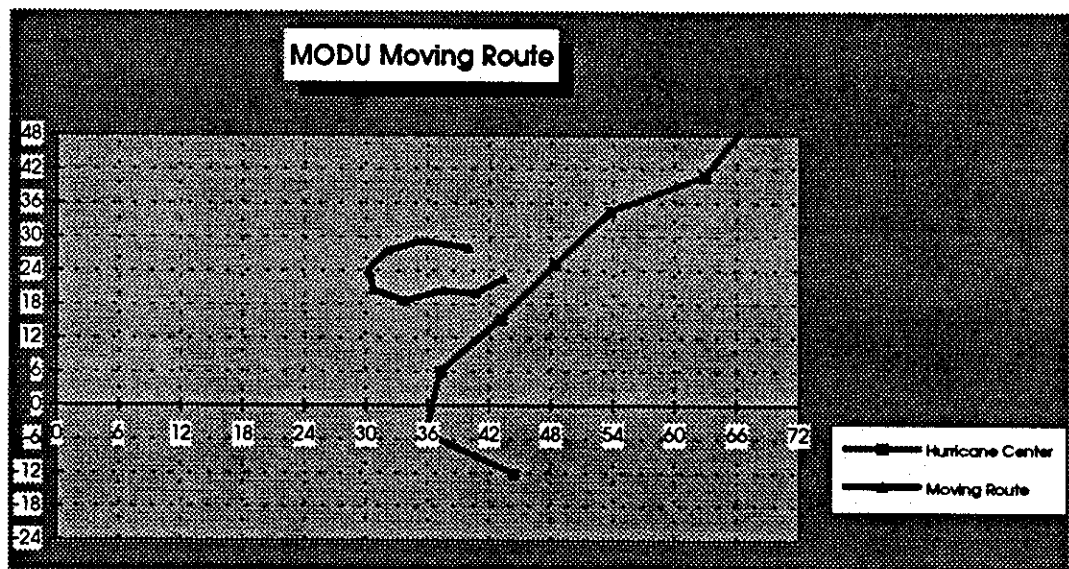


Example 1

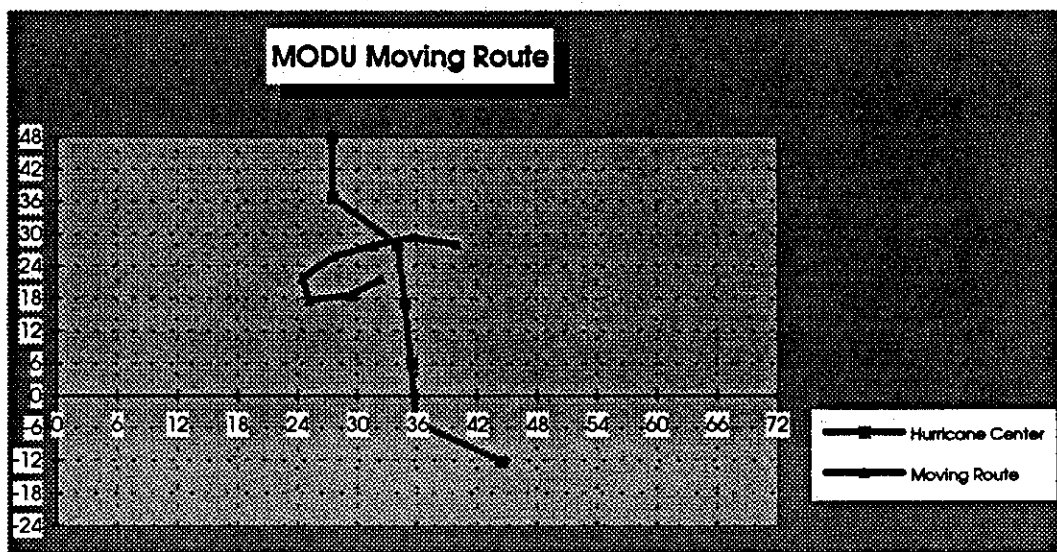
Figure 3.7 Examples of Track Forecast Generated by MCSM



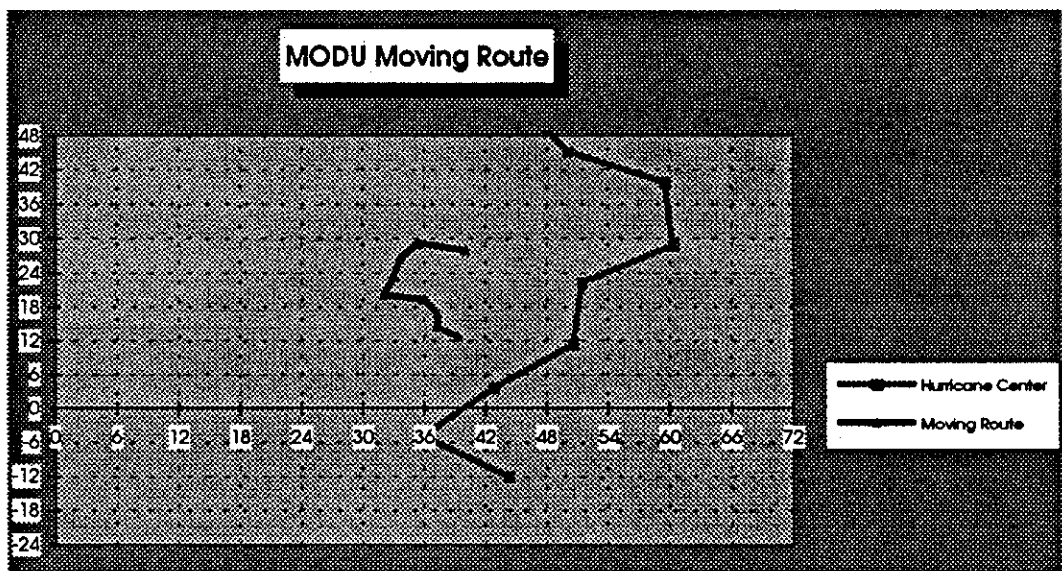
Example 2



Example 3



Example 4



Example 5

3.5 Hurricane Strength Forecast Error Simulation Model

The most important input parameters for EVACSIM are the forecast wind strength & wave height data at the site. Statistical analysis is needed to simulate the hurricane strength forecasts.

Since the forecasting strength error is roughly proportional to the actual hurricane strength, the statistical analysis of the forecast strength error is based on the relative percent error, which is defined as:

$$\text{err}\% = \frac{\text{Forecast} - \text{True}}{\text{True}} \times 100\% \quad (3.25)$$

The fit results of error percent on different forecast time intervals are presented in Figure 3.8. Again, goodness-of-fit tests were performed. The goodness-of-fit test results were similar to those of track results. The results show that the normal distribution fits the data best (0.1 significance level) among distribution families used (See Appendix C for other distribution families).

To simulate hurricane strength using 72 hours real time forecast data as the most probable value, simulation data are generated as:

$$\text{Simulation.data} = \frac{\text{Forecast}}{1 - X} \quad (3.26)$$

where X is has a normal distribution with parameters as given in Figure 3.8.

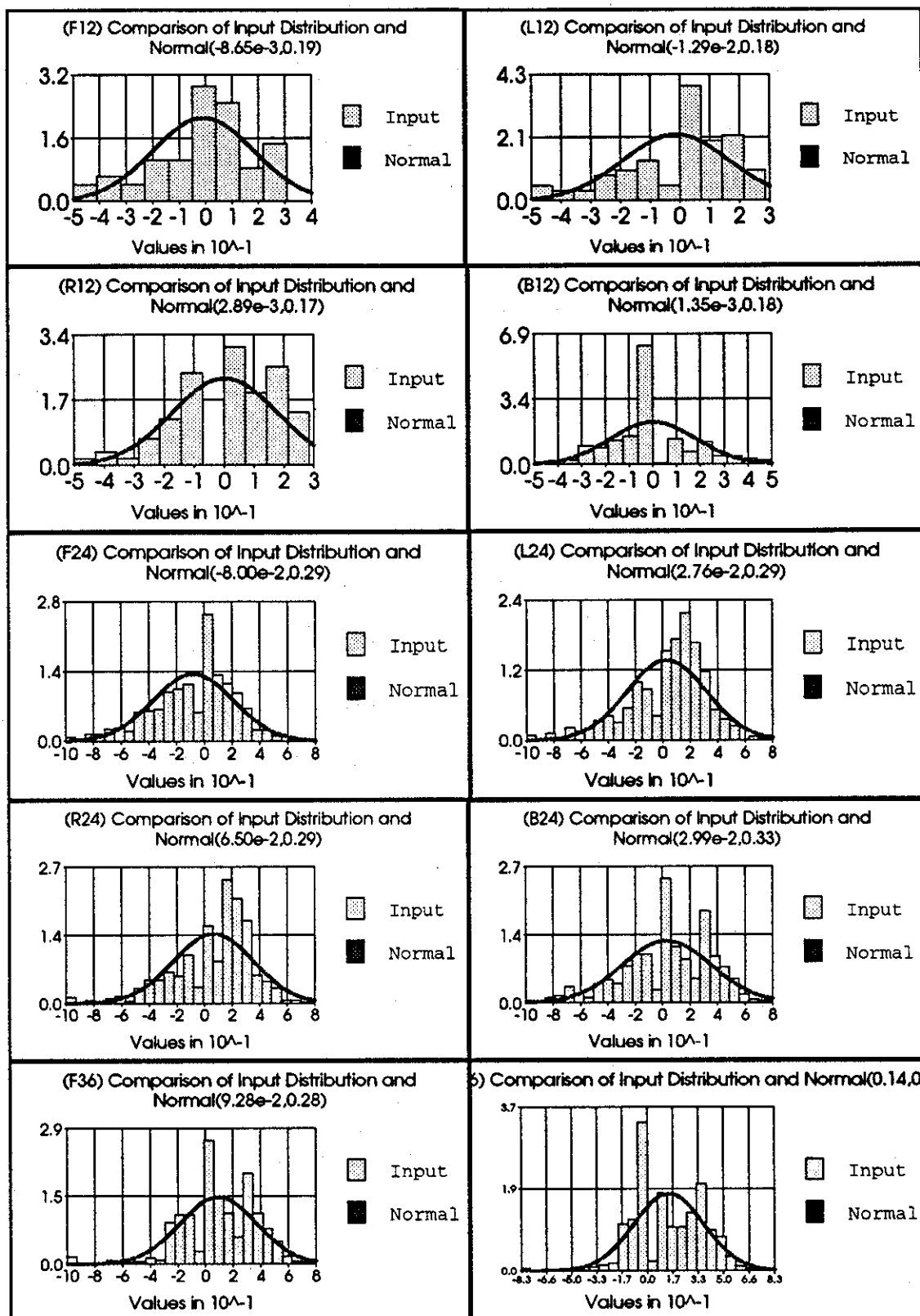
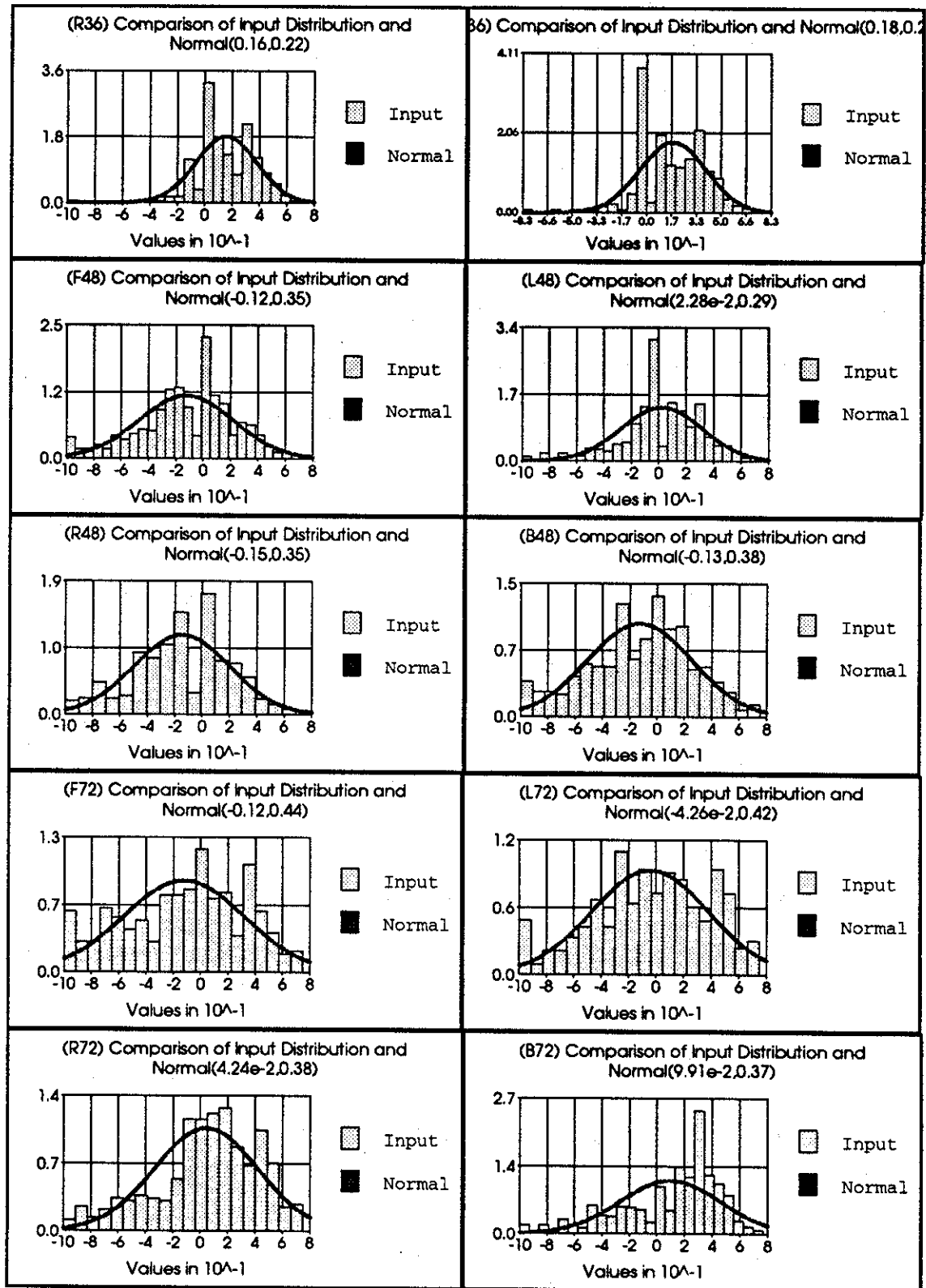


Figure 3.8 Fit Test Results for Hurricane Strength Forecasting



There is high correlation among forecasts 5 hours apart. Based on analysis of the forecast data, the 6 hours correlation coefficient is found to be 0.8.

3.6 Summary

Historical hurricane track forecast data show that there are large uncertainties associated with hurricane track forecasting. Simulation is a suitable way to include the reliability in hurricane track forecasts. An analytical approach would be very difficult, if not impossible, for such a complicated system.

Existing track forecast models are not suitable for simulation processes since they are all complicated and time consuming. Based on a statistical analysis of hurricane track forecast history data, two track forecast simulation models, track forecast error statistical model (TFESM) and Markov-chain simulation model (MCSM), have been developed.

TFESM generates hurricane track forecasts based on the 72 hour real time hurricane forecasts from hurricane forecast centers, and statistical analysis of historical hurricane track forecast errors from the same hurricane forecast centers. This model is especially useful to generate hurricane track forecasts to perform simulations for a special incoming hurricane. MCSM generates hurricane track forecasts based on the Markov transition probability matrix, which is estimated from hurricane track history statistics. The Markov model is a combination of the most important hurricane track forecast techniques, persistence and climatology. It is a blend that weights persistence higher early in the

forecast and climatology higher later. This model is especially useful to generate hurricane track forecasts to perform longterm simulations, for example, one year, when the real time forecasting data are not available.

A statistical model for hurricane strength forecasting based on forecast error percent has also been developed for the simulation program EVACSIM.

CHAPTER 4

MONTE CARLO SIMULATION OF MODU COLLISION PROBABILITY

4.1 Introduction

Simulation is a technique for conducting experiments in a laboratory or on a digital computer in order to model the behavior of a system. If the relationships that compose the system are simple enough, it may be possible to use mathematical methods (such as algebra, calculus, or probability theory) to obtain exact information on questions of interest; this is called an analytic solution. However, many real-world systems are too complex to allow realistic models to be evaluated analytically, and there are few fundamental laws which can be used to predict the response of the system, and these systems must be studied by means of simulation. In a simulation we use a computer to evaluate a system numerically, and data are gathered in order to estimate the true characteristics of the system.

Monte-Carlo simulation is usually used for problems involving random variables of known or assumed probability distributions. Using statistical sampling techniques, a set of values of the random variables is generated in accordance with the corresponding probability distributions. These values are used to obtain a "sample" solution. By repeating the process and generating many sets of simulated data, many sample solutions can be determined. Statistical analysis of the sample solutions is then performed.

Monte-Carlo techniques were first used by U.S. nuclear bomb researchers to test the reaction of atoms during nuclear explosion during World War II. The experiment was conducted in Monte Carlo and that is where its name came from.

Owing to improvements in computing power and in simulation software these years, the simulation's value and usage have increased and the application areas extended to other fields besides physics. In space science, the direct Monte Carlo simulation has been applied to satellite contamination studies (Rault & Woronowicz, 1995). In atmospheric sciences, it has been applied to study the transfer of solar or thermal radiation through atmospheres (Evans, 1993), and to study the impact of various cloud morphologies (roughness, voids, waves, and horizontal spreading) on radiative properties of finite, thin, model cirrus clouds (Chylek & Dobbie, 1995). In environmental geology, it has been used to develop a deep bed filtration simulator that is capable of describing the motion and deposition of suspended particles in the interior of downflow, upflow, and horizontal flow filters and of predicting their collection efficiency at the initial filtration stages (Burganos, Paraskeva and Payatakes, 1995) and to evaluate the uncertainty in 3 existing analytical groundwater pollution transport models (Bobba, Singh and Bengtsson, 1995). There are some other areas of application such as to analysis the regional rainfall frequency in Louisiana (Naghavi and Yu, 1995) and to study the migration of deep-well injected waste in heterogeneous confining layers (Rhee; Reible and Constant, 1993).

Simulation has been used as a tool to evaluate offshore construction alternatives (McCarron, 1971). Chen used a Monte Carlo simulation approach to offshore construction project planning and scheduling (Chen and Rawstron, 1983). Slomski and Vivatrat used Monte Carlo simulation procedures to evaluate risks of Arctic offshore operations (Slomski and Vivatrat, 1986). Wen used Monte Carlo techniques to develop risk models for offshore structures (Wen, 1988). Hu and Gupta used the Monte Carlo simulations and time-domain techniques to include all nonlinear phenomena when they investigated the effects of free surface fluctuation and the nonlinearity of wave kinematics on total wave forces and on the dynamic responses of offshore structures (Hu, Gupta, Zhao, 1995).

MODU movement in a hurricane is a very complicated process. The environmental force and the MODU moving direction are time-dependent variables. In 1992, an analytical method was developed by TRIDENT CONSULTANTS LTD to solve a similar problem, evaluation of the collision probability between Floating Storage Unit (FSU) and platforms around it in Gulf of Thailand (GOT) (Webster, 1992).

In this procedure, the probability that the FSU would collide with a platform was treated as the product of three other probabilities. These were,

- 1) the probability that the FSU would break its mooring,
- 2) the probability that it would move in the direction of a platform, and
- 3) the probability that it would encounter a platform in its direction of travel.

This collision probability may be expressed as a simple equation either for all platforms around it or for each individual platform. It may be calculated on an annual basis as in Equation 4.1 and 4.2, or on a cell and generating storm basis as in procedures developed during the study:

$$P_c^p = P_b \cdot P_d^p \cdot P_e^p \quad (4.1)$$

$$F_c = P_b \cdot \sum (P_d^p \cdot P_e^p) \quad (4.2)$$

where,

F_c : Annual probability of the breakaway FSU colliding with any platforms

P_c : Annual probability of the breakaway FSU colliding with platform p

P_b : Annual probability of FSU breaking away from its moorings

P_d^p : Probability the FSU moves in the direction of platform p, this is equivalent to the wind blowing over the FSU towards the platform

P_e^p : Probability of the FSU encountering platform p

p : Denotes platforms around the FSU

The two equations above can be rewritten by replacing the annual probabilities of breakaway and collision with the probabilities for a particular category of generating storm at a given location in the gird:

$$P_{c_y}^p = P_{b_y} \cdot P_{d_1}^p \cdot P_{e_1}^p \quad (4.3)$$

$$F_{c_y} = P_{b_y} \cdot \sum (P_{d_1}^p \cdot P_{e_1}^p) \quad (4.4)$$

Where, Probabilities refer to individual cells denoted by i and particular generating storm intensities categories denoted by j .

The first of these three probabilities, that the FSU breaks its mooring, P_m , was provided by Webster (1992) in the form of a curve for conditional failure probability of the mooring chains vs. significant wave height. The second, P_d^* , could be assumed to be synonymous with the probability density function for wind direction. The last of the three probabilities, P_d , was calculated using geometric arguments. It was later refined slightly by including some information on the FSUs expected motion after breakaway in the direction.

The procedure is very ideal for the problem in GOT, since the complex of platforms are all located within a 30×70 Nautical miles rectangle. Thus, it is relatively easy to calculate P_d and P_g . But, in Gulf of Mexico, there are relatively larger fields and many more platforms. So a MODU can have a long trip before it collides with a platform. Further, as the hurricane center moves, the associated wind and wave field will also change with time. Thus, the MODU route will be curved in responses to the changing wind and wave field.

Also, there are different mooring failure modes (mooring lines broken and anchors dragging) and different MODU moving modes (free floating and skipping). These factors will have a great influence on the MODU route and on the collision probability. In these cases it would be very difficult to calculate the P_d , P_g . As a result, the process is proposed to be modeled by direct computer simulations using the probability models for

the hurricane parameters, the MODU's movements to the site, and the number of hurricanes.

The MODU movement simulation model is based on:

- 1) available statistics and hindcast results for hurricanes in the Gulf of Mexico since the turn of the century(MMS, 1993);
- 2) numerical models of wind, wave, current and their load effect on a platform; and
- 3) probability models to include the hurricane parameter variability, hurricane model uncertainties, and the spatial geometry.

The input to the simulation model is:

- 1) The location of the MODU and surrounding large facilities, e.g., (X_m, Y_m) and (X_r, Y_r) ; where (X_m, Y_m) are coordinates of MODU's location and (X_r, Y_r) are coordinates of surrounding large facilities;
- 2) MODU parameters, e.g., displacement, draft, and mooring system capacity;
- 3) Hurricane parameters, e.g., $\Delta P, V_r, R_m$, which are the pressure difference, storm translation speed and radius of maximum wind speed;
- 4) Hurricane direction parameters, e.g., X_o, ϕ , which are defined in Figure 4.5.

The output of the model is the probability of collision between the MODU and surrounding large facilities during the considered time period.

4.2 Simulation Modeling

4.2.1 Hurricane Statistics

The hurricane parameters of the most interest are the differential barometric pressure (inside - outside) the hurricane (ΔP), the radius of the maximum wind speed (R) and the storm translation speed (V_t). Based on a statistical analysis of the characteristics of past hurricanes in the Gulf of Mexico along the coastal area of Texas and Louisiana since the turn-of-the-century (MMS, 1993), their mean values, standard deviations, coefficient of variation and the correlation matrix are summarized in Table 4.1 and 4.2. The table values represent the maximum values observed when the storm crossed the shelf. Only storms with R less than 100 nm (nautical mile) are considered.

Table 4.1 Hurricane Moment Statistics (110 Hurricanes Represented)

Parameters	Mean	Variance	St.D	C.O.V.
ΔP (mb)	43.2	431.4	20.8	0.48
R (nm)	26.9	104.1	10.2	0.37
V_t (knot)	11.3	22.1	4.7	0.41

Table 4.2 Correlation Coefficient Matrix

	ΔP (mb)	R (nm)	V_t (knot)
ΔP (mb)	1.000	-0.52	0.122
R (nm)	-0.52	1.000	0.022
V_t (knot)	0.122	0.022	1.000

The fit results are summarized in Figure 4.1. Goodness-of-fit tests were also performed. From the statistics point of view, some of the fit results should be rejected. However, the fit results are still acceptable for engineering applications.

The three parameters, ΔP , R and V_f , are modeled as jointly Lognormal random variables with parameters given in Table 4.3. The logarithmic transforms of these parameters follow a jointly normal distribution. It is pointed out that the Lognormal distribution has been used in almost all previous risk studies of hurricanes(e.g., Batts, et al., 1980; Russell, 1968). It is a convenient model to use, in particular, in treating correlated random quantities.

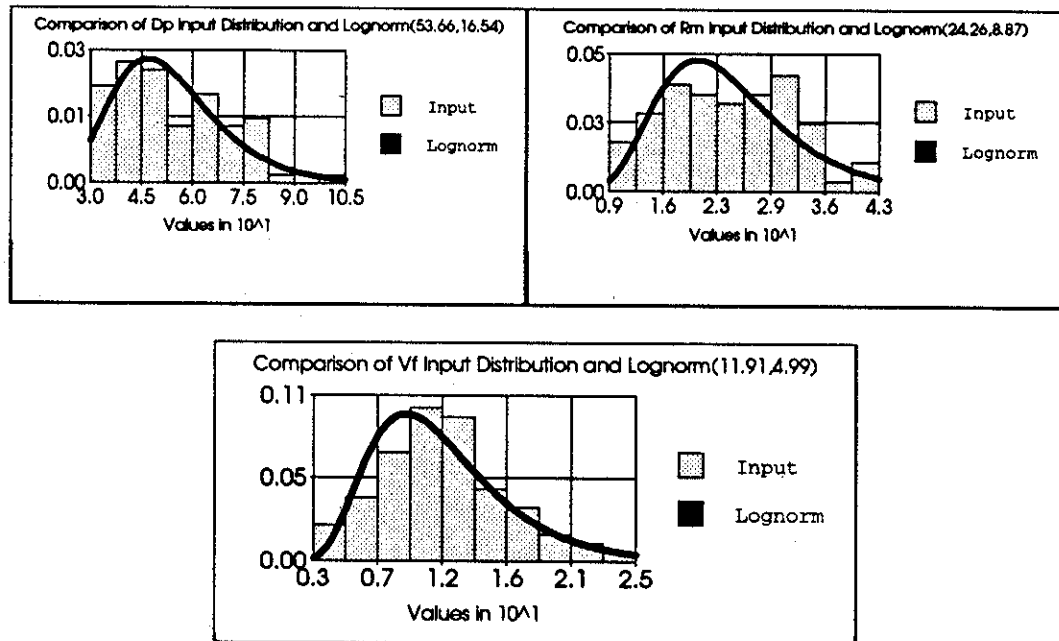


Figure 4.1 Fit Results for Hurricane Parameters

Table 4.3 Hurricane Parameter Distributions

Parameter	ΔP (mb)	R (nm)	V_t (kts)
Distribution	Lognormal	Lognormal	Lognormal
Mean	53.66	24.26	11.99
St. Dev	16.54	8.87	4.99

On the basis of the statistical evaluations performed by Ward, et al.(1978) and Bea (1975), the hurricane track shelf edge crossings, X_s (Figure 4.5), is assumed to be uniform distributed. The hurricane track direction at shelf edge crossing, ϕ (Figure 4.5), is assumed to follow a triangular distribution. The peak value is 101 degrees relative to the coast line orientation (Wen, 1988).

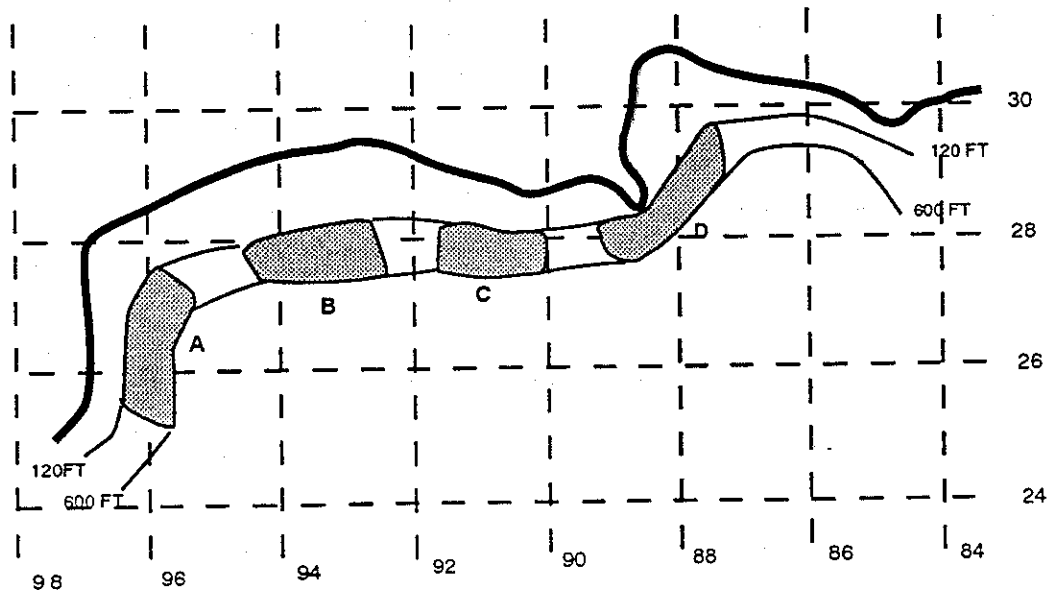


Figure 4.2 Gulf Coastal Water Regions (Ward, et al., 1978)

Previous investigations(e.g., Haring and Heideman, 1978) have shown that the occurrence of hurricanes over time can be approximately modeled as a simple Poisson Process (Bea, 1975). The mean occurrence rate per time is, therefore, the only parameter required of the occurrence in a specified region. From Ward, et al. (1978), the occurrence rates for hurricanes in the Gulf of Mexico regions A, B, C, D in Figure 4.2 are respectively 0.459, 0.563, 0.587, and 0.563 per year. As the widths of the regions are 360 nautical miles, the hurricane occurrence statistics may alternatively be described by the mean rate of the storm tracks crossing the 600ft. depth contour line per year per nautical mile. For example, the occurrence rates at a point in region A, B, C, and D are correspondingly 0.00127, 0.00156, 0.00163, and 0.00156/year-nautical mile. Interpolation may be used to determine the occurrence rate at any given location on the contour line.

4.2.2 Modeling MODU Movement

When a MODU drifts in hurricanes, there are two moving modes that depend on water depth and the MODU draft. They are defined as:

Mode A: Floating $T < d + \Delta d$

Mode B: Skipping $\Delta d + d < T < \Delta d + d + \eta_{\max}$

Mode C: Stopped $T > \Delta d + d + \eta_{\max}$

where, T = MODU draft

d = water depth

η_{\max} = maximum wave height

Δd = surge of sea surface

4.2.3 MODU Moving Distance Modeling

In either Mode A or Mode B, the MODU is modeled as free floating and dragging condition. It is assumed that during each short period of simulation time step, (Δt), the MODU's movement reaches steady-state. Under this assumption, the MODU moves with a steady velocity and the total storm horizontal force is equal to the wave resistance.

4.2.3.1 Case A: MODU Floating

a) Free Floating Condition

During a short period of time (Δt), the MODU is assumed to move with a steady velocity. We assume that the total hurricane horizontal steady force is equal to the viscous drag force on the hull of the MODU. (See Figure 2.4)

$$\begin{aligned} F_{\text{Hurcady}} &= F_{\text{wave}} + F_{\text{wind}} \\ &= F_{\text{Viscous}} = [C_D A_p \rho / 2] [V_{\text{MODU}} - V_{\text{Current}}]^2 \end{aligned} \quad (4.5)$$

where $C_D = 0.7$
 A_p = Projected Area
 $\rho = 64 \text{ lb/ft}^3$
 F_{Wind} = Steady wind force
 F_{Wave} = Mean wave drift force

So:

$$V_{\text{MODU}} = \sqrt{\frac{F_{\text{Wind}} + F_{\text{Wave}}}{C_D A_p \rho / 2}} + V_{\text{Current}} \quad (4.6)$$

$$\text{and, } \Delta_{\text{move}} = V_{\text{MODU}} \Delta t \quad (4.7)$$

where,

Δt = hurricane simulation time period

case A-- MODU Floating

b) Dragging Condition

Here, we also assume the MODU moves with a steady velocity, so the total hurricane horizontal steady force minus anchor dragging force is equal to the viscous drag force.

$$\begin{aligned} F_{\text{steady}} &= F_{\text{wave}} + F_{\text{wind}} - F_{\text{Anchor}} \\ &= F_{\text{Viscous}} = [C_D A_p \rho / 2] [V_{\text{MODU}} - V_{\text{Current}}]^2 \end{aligned} \quad (4.8)$$

where,

$$C_D = 0.7$$

$$A_p = \text{Projected Area}$$

$$\rho = 64 \text{ lb/ft}^3$$

$$F_{\text{Wind}} = \text{Steady wind force}$$

$$F_{\text{Wave}} = \text{Mean wave drift force}$$

So

$$V_{\text{MODU}} = \sqrt{\frac{F_{\text{Wind}} + F_{\text{Wave}} - F_{\text{Drag}}}{C_D A_p \rho / 2}} + V_{\text{Current}} \quad (4.9)$$

and,

$$\Delta_{\text{move}} = V_{\text{MODU}} \Delta t \quad (4.10)$$

Here, the dynamic anchor drag force is assumed as (Bea, 1990):

$$F_{\text{dynamic}} = \bar{\epsilon} F_{\text{static}} \quad (4.11)$$

where, $\bar{\epsilon} = 0.5$, $V_i = 30\%$.

t = hurricane time period

case A--MODU Floating

4.2.3.2 Case B: MODU Skipping

When the MODU moves in the skipping mode, during a wave period, the MODU will move when $T < \Delta d + d + \eta_{max}$, and it will stop when $T > \Delta d + d + \eta$, where Δd , d and η are defined as sea surface surge, water depth and wave height. Since the wave period is short, the MODU can be assumed to be forced by a steady acceleration. The following motion differential equation needs to be solved:

$$F_{Wave} + F_{Wind} + [C_D A_p \rho / 2](V_{Current} - V_{MODU})^2 = M \dot{V}_{MODU} \quad (4.12a)$$

Since V_{MODU} is small in this case and could be neglected, Equation 4.12a can be simplified

to:
$$F_{Wave} + F_{Wind} + [C_D A_p \rho / 2]V_{Current}^2 = M \dot{V}_{MODU} \quad (4.12b)$$

and the moving distance in a wave period can be determined as:

$$\Delta_{move} = \frac{1}{2} \cdot \dot{V}_{MODU} \cdot \Delta t^2 \quad (4.13)$$

4.2.4 MODU Collision Modeling

The surrounding structures are assumed to be located within several large target circles with radius R_c from 0.5 to 5 nm. Collision happens when the MODU runs into one of these circles and collides with structures within the circle. From the simulation, the MODU's route is determined. If the distance between the route and the center of the circle is less than R_c , the MODU has encountered the circle. To determine whether or not the MODU collides with structures within the circle, a pre-calculated simulation was performed.

During the pre-simulation, the MODU is assumed to moving in a straight line within the circle before collision happens. The direction in which the MODU enters the circle is assumed uniformly distributed from 0° – 180° . Target structures are also assumed uniformly distributed within the circle. With a given circle radius and the number of structures within the circle, the distance between these structures and the MODU route is determined. The collision happens if one of these distance is less than safety distance, say 100m.

With a given R_i and N , the process is repeated many times to get the probability of collision on the condition of that the MODU runs into the circle. For different R_i and N , the simulation results are summarized in Figure 4.3.

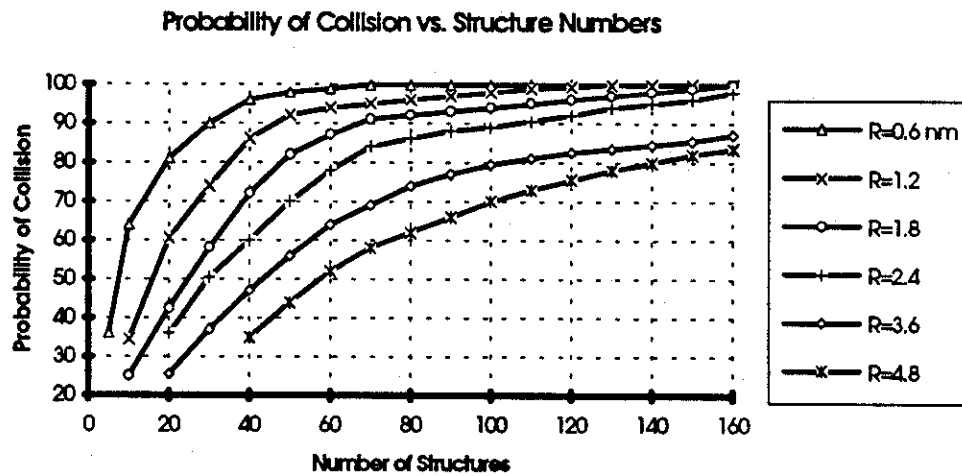


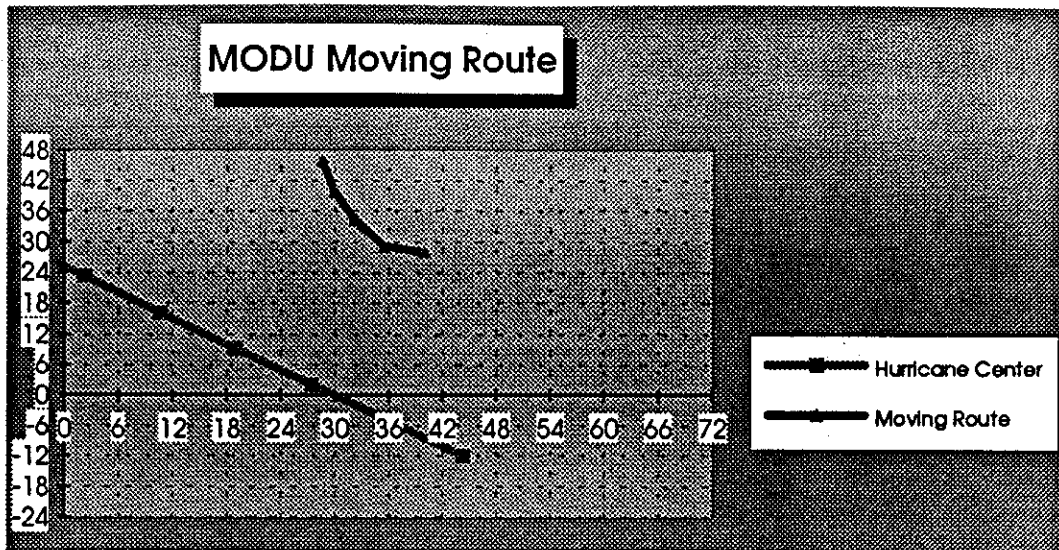
Figure 4.3 Probability of Collision vs. Structure Numbers

Based on the results from the simulation, the following observations can be made:

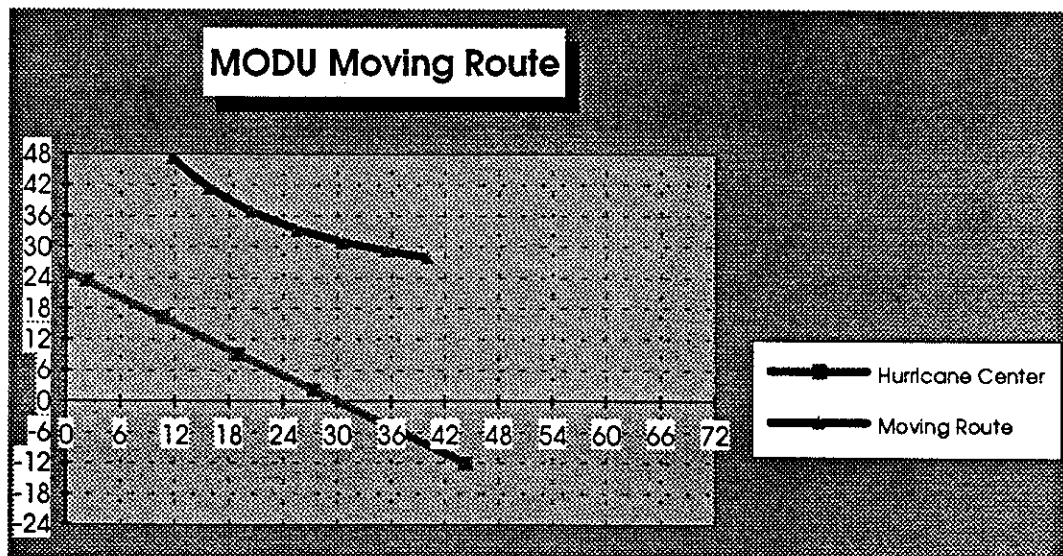
1. $R \leq 2$ nm, the collision probability increases rapidly from 30% to 80% when N increases from 10 to 30. When N is larger than 40, the collision probability is very high and does not change much when N increases.
2. $R \geq 3$ nm, the collision probability increases slowly with N.
3. In both cases, the collision probability increases rapidly at first, then slows down when N is large.
4. The maximum allowable number of structures within a given circle, R, with an acceptable collision probabilities if a MODU runs into the circle can be determined, e.g., for $R=3.6$ nm and acceptable risk is 20%, the allowable maximum number of structures is about 10.
5. For most circles (radius $R=2.4$ nm and number of structures within the circle $N=40$), the collision probability is approximately 60%.

4.2.5 Modeling of Holding after the Collision

During hurricane Andrew, the Zane Barns (Allan, 1988) collided with several platforms after breaking loose from its location. Based on this and similar experience, we know that a MODU may or may not remain at the initial collision location for hours before it starts to move again. As a result of the change in environmental conditions that develop during the holding period, the MODU drift direction could change significantly after collisions. The MODUSIM user can determine whether or not holding happens and how long it is held after a collision. It can be seen from Figure 4.4 that the MODU's moving route changes a lot if it is held for one hour after the first collision.



Holding for 2 hours at the First Collision



No Holding

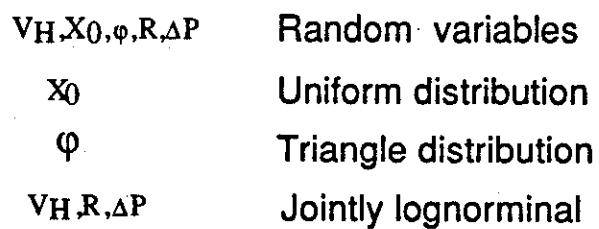
Figure 4.4 Modeling of Holding

4.3 Monte Carlo Simulation

The simulation procedure developed during this research can be summarized as follows:

- 1) Select a reference frame in which the site is located.(See Figure 4.5);
- 2) Generate a random number, n , of hurricanes which occur during the period of consideration, i.e., 1 year, using a Poisson distribution with an occurrence statistics at the location;
- 3) Generate a sets of random variables $X, \Delta P, R, \phi, V_H$ according to the distribution and joint distribution functions given in Section 4.2;
- 4) For each set of the parameters generated in 3), calculated the wind, wave and current force time histories at the site according to the parameter models. If the MODU mooring system is failure, then determine the MODU moving route time history during the hurricane;
- 5) Check if the distance between large facilities and the MODU moving route is smaller than the safety distance;
- 6) Repeat steps 2-5 N times(trials) and record the number of trials in which the collision happens, say c , the relative frequency c/N for large N is the estimate of the probability that the MODU will collide with large facilities in 1 years.

The detailed procedure is illustrated in Figure 4.6 , Figure 4.7 and described in later Sections.



101

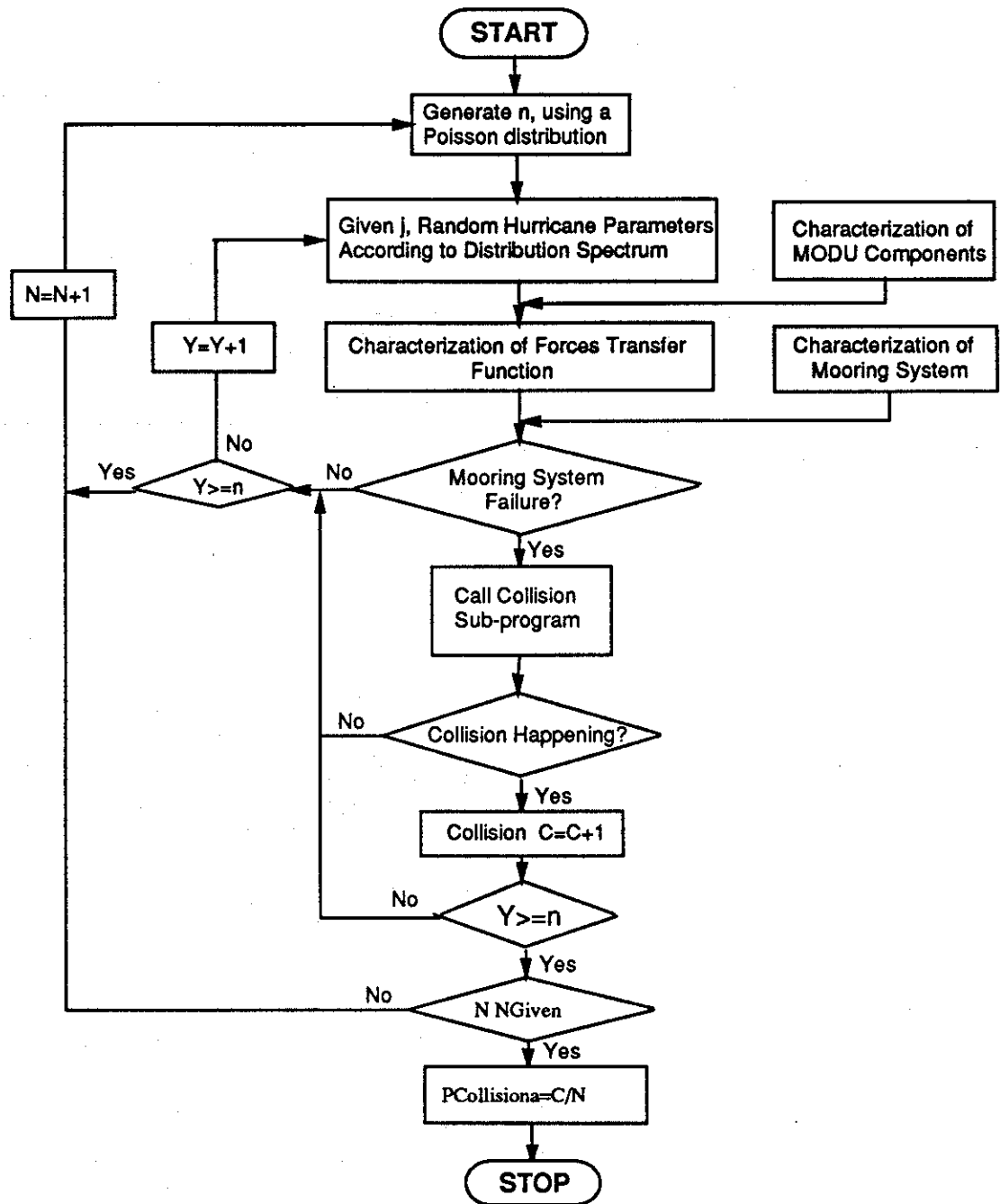


Figure 4.6 Monte Carlo Simulation Procedure

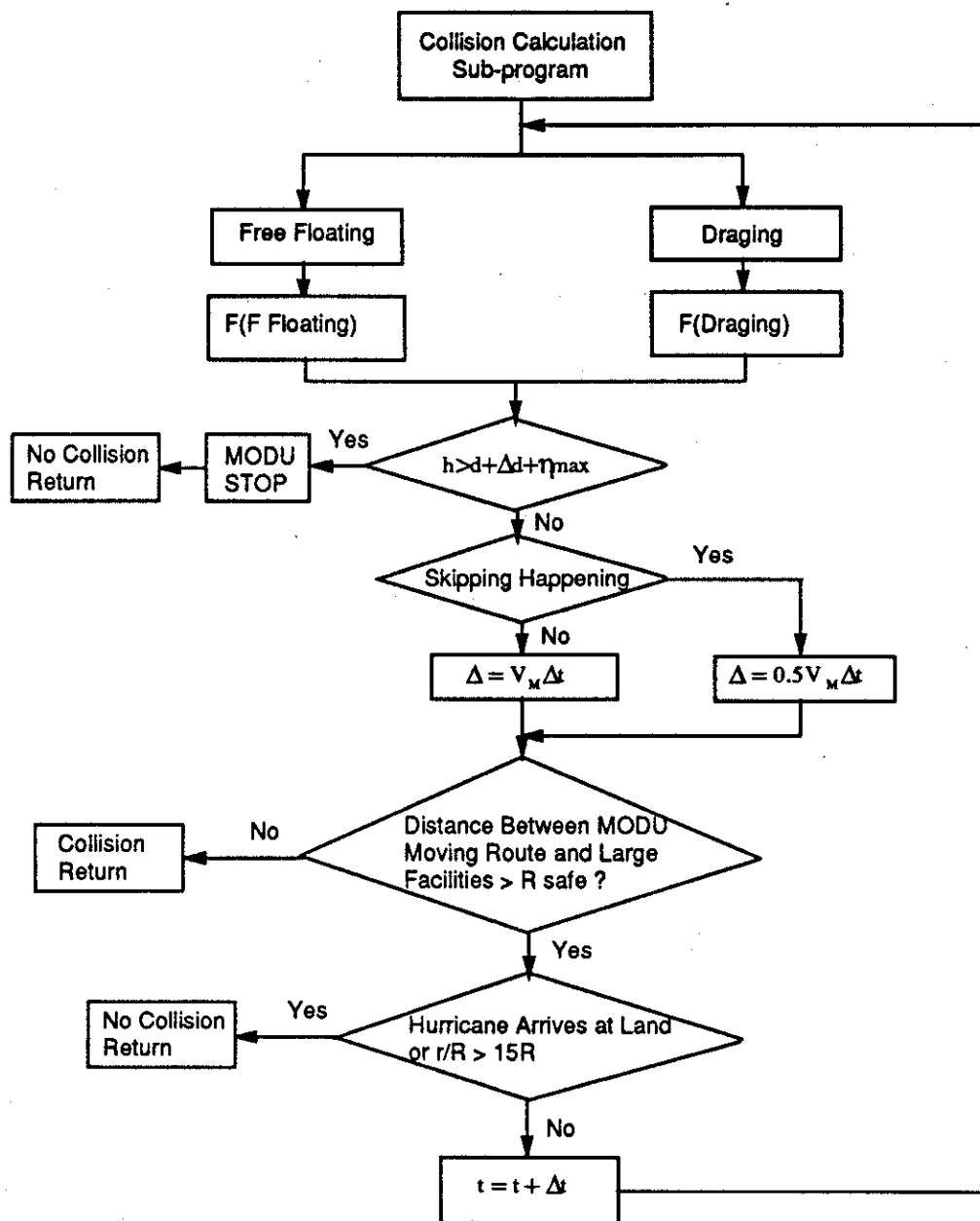


Figure 4.7 Monte Carlo Simulation Procedure

4.3.1 Computer Simulation Approach

The following steps detailed the MODUSIM approach:

- 1) Select a reference frame in which the site is located.(See Figure 4.5)

A reference is selected in which the MODU is located. The X-axis is chosen as parallel to the coastal line, and Y-axis is chosen as perpendicular to the coastal line. The user determined information includes:

- a) Original point of the reference (longitude and latitude);
- b) The width of the reference frame ($X_{max}-X_{min}$);
- c) The distance from X-axis to coastal line;
- d) The water depth at the site of MODU's location;
- e) The MODU's parameters;
- f) The MODU's mooring capacity;
- g) User defined mooring system failure mode.

Based on such information, x and y coordinates of the MODU in the reference frame are determined.

The user also needs to determine the (X,Y) locations of large facility circles around the MODU which are the possible collision targets. The corresponding collision probabilities within these circles can be found from Figure 4.3.

- 2) Generate the number, n , of hurricanes which occur during the period of consideration, i.e., 1 years, within the reference frame using a Poisson distribution with an occurrence statistics at the location, i.e., γ_{λ} . For example, if the reference frame is chosen at area C, with width 100 nm, we know the occurrence rate at a point in region C is 0.00163/year-nm (Figure 4.2), so the occurrence rate within the reference frame is 0.163/year.
- 3) Generate a sets of random variables $X, \Delta P, R, \phi, V_{\lambda}$ according to the distribution and joint distribution functions given in Section 4.2.
- 4) For each set of the parameters generated in 3), calculated the wind, wave and current force time histories at the site according to the parametric models. If the MODU mooring system fails, then determine the MODU's moving route time history during the hurricane.

As in Figure 4.5, the hurricane is assumed to be a storm traveling along a straight line with a given translation speed and direction during each simulation time step, Δt . Changes in the storm strength parameters after shelf edge crossing are not considered.

The coordinates of the hurricane center are:

$$X_H = X_0 + V_H t \cos \phi \quad (4.14)$$

$$Y_H = V_H t \sin \phi \quad (4.15)$$

The coordinate of the mooring MODU and large facilities are (X_m, Y_m) and (X_i, Y_i) ,
($i=1$, to n , where n is the number of large facilities around the MODU).

where, X_0 : Uniform distribution
 φ : Triangular distribution
 $V_H, R, \Delta P$: Jointly log normal distribution

The distance between MODU and the hurricane center is :

$$r = \sqrt{(X_H - X_m)^2 + (Y_H - Y_m)^2} \quad (4.16)$$

The environmental force acting on the MODU are:

a) Wind force: The wind force acting on the MODU is calculated using the procedure given in Section 2.3.3.1. The direction of the wind force γ_{wind} , (polar angle in degree) is given by (refer to Figure 4.5 for definition of γ , β , α , and θ):

$$\gamma_{wind} = \beta_{wind} + \varphi + 90^\circ \quad (4.17)$$

where:

$$\beta_{wind} = \theta + \alpha + 90^\circ \quad (4.18)$$

$$\theta = 90^\circ - \varphi + \arctg \frac{Y_H - Y_m}{X_H - X_m} \quad X_H < X_m \quad (4.19)$$

$$\text{and, } \theta = 270^\circ - \varphi + \arctg \frac{Y_H - Y_m}{X_H - X_m} \quad X_H > X_m \quad (4.20)$$

$$\alpha = 22 + 10 \cos \theta \quad (4.21)$$

- b) Wave force: The wave force is calculated using the procedure given in Section 2.3.3.3. The direction of the wave force γ_{Wave} , (polar angle in degree), is given by:

$$\gamma_{\text{Wave}} = \beta_{\text{Wave}} + \phi - 90^\circ \quad (4.22)$$

where:

$$\beta_{\text{Wave}} = \theta + \alpha + a\left(\frac{r}{R}\right)^b - 90^\circ \quad (4.23)$$

$$a = 144 + 39 \cos \theta - 25 \sin \theta - 15 \cos 2\theta \quad (4.24)$$

$$b = -0.08 \quad (4.25)$$

Here α, θ are the same as in wind force.

- c) Current Force: The current force is calculated using the procedure given in Section 2.3.3.2. Here we assume the direction of the current force is the same as that of the wind force. Then, as shown in Figure 4.8, the total environmental forces acting on the MODU is:

$$\vec{F}_{\text{Total}} = \vec{F}_{\text{Wave}} + \vec{F}_{\text{Wind}} + \vec{F}_{\text{Current}} = \vec{F}_1 + \vec{F}_2 \quad (4.26)$$

$$|\vec{F}_{\text{Total}}| = F_1^2 + F_2^2 + 2F_1F_2 \cos(\gamma_1 - \gamma_2) \quad (4.27)$$

where F_1, F_2 denotes wind and wave forces. The direction, γ_{Total} (polar angle in degree) is:

$$\gamma_{Total} = \gamma_1 + \arccos\left(\frac{F_{Total}^2 + F_1^2 - F_2^2}{2F_{Total}F_1}\right) \quad (4.28)$$

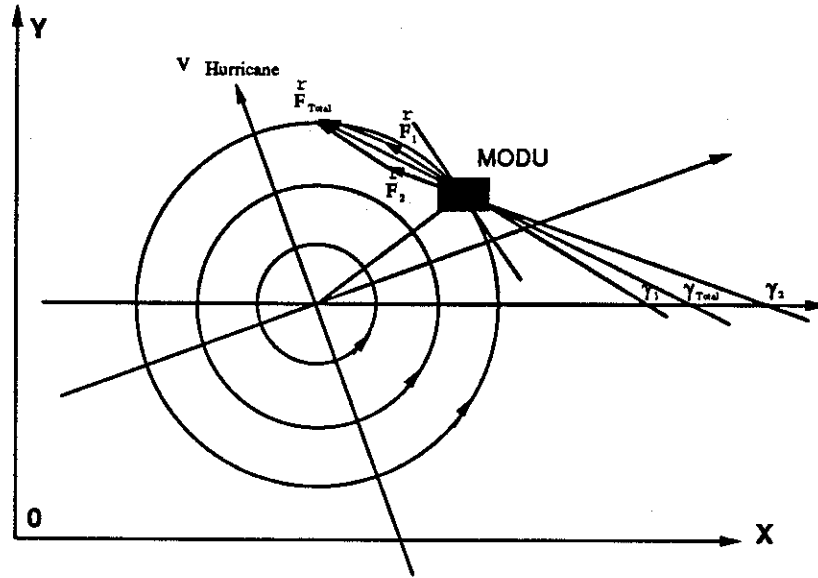


Figure 4.8 Environmental Force Configuration

During the hurricane time history, in each short time period, i.e., 2 hour, we check whether the environmental force exceeds the MODU mooring capacity. If the mooring system fails, then the MODU will move in the direction the same as the direction of the total environmental force, with velocity V_M , where V_M is calculated using the procedure given in Section 4.2.3.

After Δt , i.e., 2 hour, the hurricane center and the MODU will move to a new place.

The new position of the hurricane center and the MODU is:

$$X_H' = X_H + V_H \Delta t \cos \phi \quad (4.29)$$

4.3.2 Variance Reduction Techniques

Statisticians and practitioners have developed several techniques for drawing random samples. The Latin Hyper cube sampling is used in the MODUSIM program. It recreates the input distribution through sampling in fewer iterations when compared with the Monte Carlo method, especially if the input distribution is highly skewed or has some outcomes of low probability.

The key to Latin Hyper cube sampling is stratification of the input probability distributions. Stratification divides the cumulative curve into equal intervals on the cumulative probability scale(0 to 1.0). A sample is then randomly taken from each interval or " stratification" of the input distribution. Sampling is forced to represent values in each interval, and thus, is forced to recreate the input probability distribution.

Stratified sampling procedures involved the definition of a variable y from which the stratification classes G_k can be defined. The random samples for X_i are then stratified by examining y_i corresponding to the i th observation and classifying X_i to be in the k th strata if $y_i \in G_k$. It is assumed that $p_k = P(y \in G_k)$ is known and the sample mean based on stratification is computed as:

$$X_{st} = \sum_k p_k X_k \quad (4.40)$$

where X_k is the sample mean for the k th strata. It can be shown that X_{st} is an unbiased estimator of μ_x . It can also be shown that (Cochran, 1977):

$$\text{Var}[X_{\pi}] = \sum_i p_i^2 \text{Var}[X_i] \leq \text{Var}[X] \quad (4.41)$$

so that a variance reduction may be obtained through stratification. Greater variance reductions are obtained when the absolute differences between the strata means, μ_i , and population mean, μ , are large.

The technique being used during Latin Hyper cube sampling is "sampling without replacement". The number of stratification of the cumulative distribution is equal to the number of iterations performed. For example, for 100 iterations, 100 stratification are made to the cumulative distribution. A sample is taken from each stratification. However, once a sample is taken from a stratification, this stratification is not sampled from again--its value is already represented in the sampled set. For sampling within a given stratification, the program chooses a stratification for sampling then randomly chooses value from within the selected stratification.

4.3.3 Sample size

The simulated data according to Monte-Carlo method should be treated as a sample of experimental observation, and therefore, is subjected to sampling error. The simulation can be modeled as a binomial process. Let Y denote the number of collisions on the N trials,

then $\bar{P}_c = \frac{Y}{N}$ is the unbiased estimation of probability of collision (P_c), which has mean

P_c , variance $\frac{P_c(1-P_c)}{N}$. The standard error of the estimation is:

$$SE(\bar{P}_c) = \frac{\bar{P}_c(1 - \bar{P}_c)}{N} \quad (4.42)$$

The coefficient of variation of the probability based on simulation is:

$$COV = \frac{\sqrt{\frac{\bar{P}_c(1 - \bar{P}_c)}{N}}}{\bar{P}_c} = \sqrt{\frac{1 - \bar{P}_c}{N\bar{P}_c}} \quad (4.43)$$

It is seen that the C.O.V. is dependent on the number of simulations N and the probability of collision, P_c . Therefore, since the estimated probability P_c is small which is usually the case, N should be large enough to decrease the error. For example, for $N=3000$, the coefficient of variation is approximately 10% at $P_c=0.03$. This can be seen in Figure 4.9 and Table 4.4.

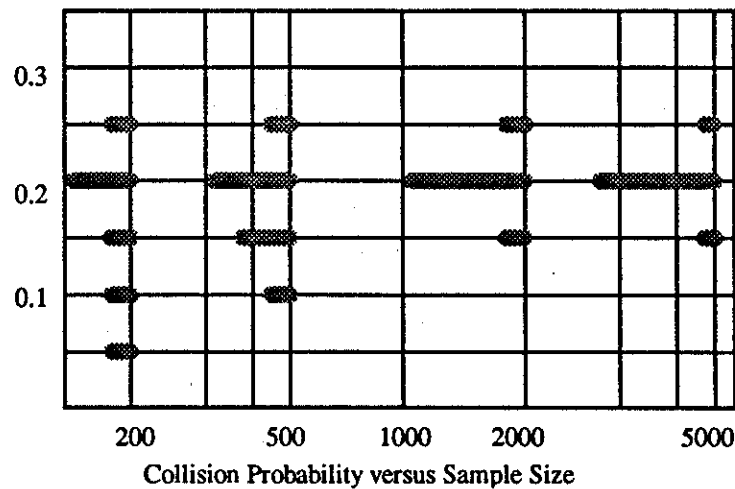


Figure 4.9 Collision Probability vs. Sample Size

Table 4.4 Estimated Collision Probability vs. Sample Size

No.\Sample #	200	500	2000	5000
1	0.006	0.0132	0.018	0.02016
2	0.015	0.0144	0.0219	0.01716
3	0.021	0.0168	0.0174	0.02028
4	0.021	0.0168	0.018	0.02016
5	0.018	0.0156	0.0234	0.01656
6	0.018	0.012	0.0213	0.01908
7	0.021	0.0204	0.0171	0.02232
8	0.018	0.0192	0.0189	0.01908
9	0.024	0.0192	0.0177	0.01704
10	0.012	0.0216	0.0186	0.01812
Mean	0.0174	0.01692	0.01923	0.018996
St.D	0.005254	0.003172	0.002175	0.001805
COV.	0.301929	0.187493	0.113085	0.095016

Simulation has been done based on different sample size, from 200 to 5000. All the simulation input data setting are the same as the verification of Function #1 in Section 4.3.3. It can be seen that when sample size reaches 2000, the COV. is almost 10% and the COV. does not reduce much even when the sample size increases to 5000. Based on the foregoing analysis, the sample size is chosen as 2000 in MODUSIM simulations.

4.4 Parametric and Case Studies

4.4.1 Introduction

The simulation program MODUSIM developed during this research has four major functions:

- #1. Given a MODU's location, estimates the probability of mooring system failure and probability of collision with surrounding structures after mooring failure;
- #2. Given MODU's location and possible coming hurricanes, predicts hurricanes coming routes, estimates the probabilities of mooring failure and the probabilities of collision, and calculates the time to system failure;
- #3. Given a known hurricane's track, straight line or curved, simulates whether the mooring system will break and also the MODU's moving route after mooring failure;
- #4. Given preferred MODU siting location and acceptable radius of siting area, estimates the collision probabilities at eight orientations within the acceptable area and gives a suggestion on the least collision probability location.

For parametric and sensitivity study, Function #1 of MODUSIM was used. The MODU "Zane Barnes", which moved very significant distance during hurricane Andrew in 1992 was used as an example in the parametric and sensitivity study. And in order to have confidence in the estimation of the collision probability, the sample size required, N , was chosen as 2000 as discussed in Section 4.3.3.

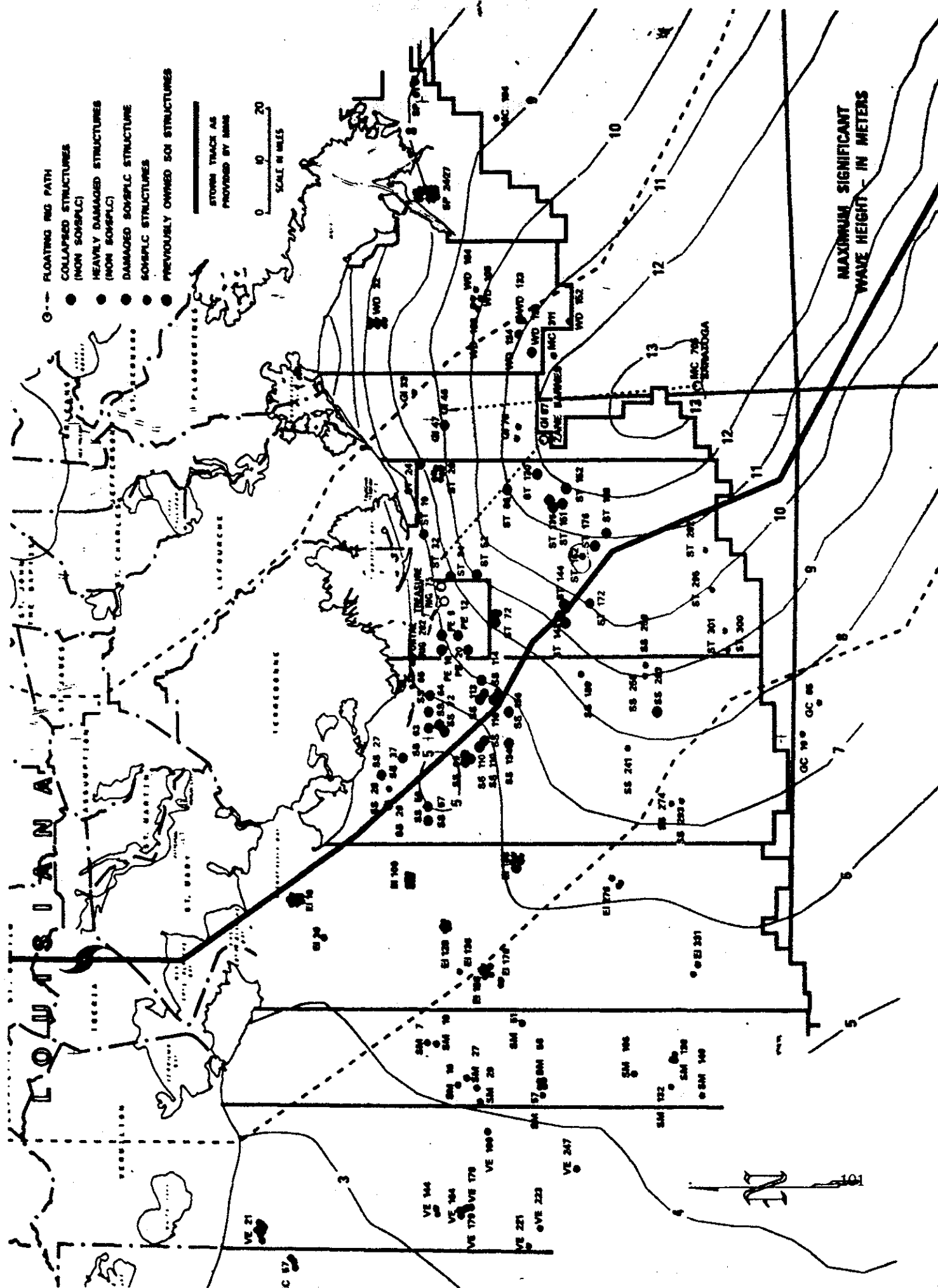
4.4.2 Simulation Setting and MODU's Parameters

The principal dimensions of the semi-submersible drilling unit "Zane Barnes" are summarized in Allan (1988) and Appendix E. Prior to hurricane Andrew, the Zane Barnes was located at La-Grand Isle Block 87 with 170 ft depth of water in the Gulf of Mexico. (Longitude $90^{\circ}5'$, Latitude $28^{\circ}40'$). The storm track of "Andrew" and storm parameters were documented by Oceanweather (1992) and are presented in Figure 4.10.

As the hurricane loading on the MODU is large enough to break the mooring system only when r/R is less than 10, we chose the hurricane parameters during this period as the average of time step 5 and 6 (Figure 4.10). $\Delta P = 82\text{mb}$, $V_p = 11\text{knots}$ and $R = 15\text{nm}$. The hurricane track direction at shelf edge crossing is 140 degrees. The reference frame is selected as in Figure 4.11. The original point is longitude $90^{\circ}30'$ and latitude $28^{\circ}25'$. The simulation began when r/R was 10, ended when the hurricane center reached land or the MODU stopped or, collision happened.

Several different simulation settings were used in the parametric and sensitivity study:

1. The hurricane tracks are assumed to be either straight or curved;
2. Either Airy wave theory or Stokes 5th wave theory is used to calculate the wave kinematics;
3. The MODU is assumed to be either in free floating or in dragging condition after the mooring system fails; and
4. The MODU has different mooring strength and is located in different places.



HURRICANE ANDREW FINAL TRACK

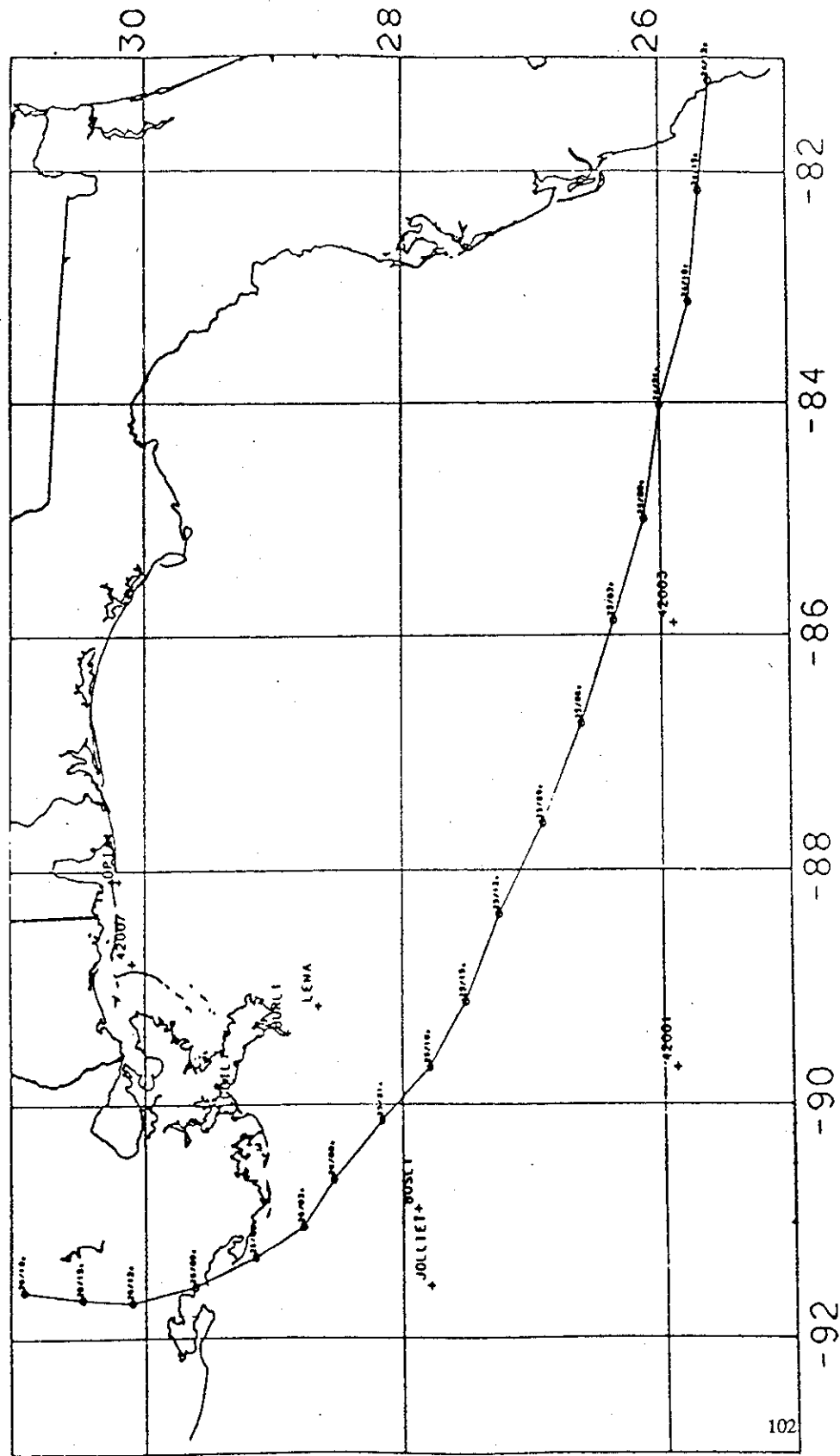


Figure 4.10a Storm Track for Hurricane Andrew

Storm parameters and track used for numerical model
simulation of boundary layer wind field

Typical Cyclone Input Data Project ANDREW JIP
Storm # 9208 Name ANDREW Duration of Hindcast 60 hours

STEP 1 EYELAT = 26 ., DIREC = 280 ., SPEED = 13 ., EYPRES = 947 .,
RADIUS = 9 ., PFAR = 1016 ., SGW = 7 ., AN1 = 120 .,
STEP 2 EYELAT = 26 ., DIREC = 280 ., SPEED = 13 ., EYPRES = 943 .,
RADIUS = 9 ., PFAR = 1016 ., SGW = 7 ., AN1 = 120 .,
STEP 3 EYELAT = 27 ., DIREC = 295 ., SPEED = 13 ., EYPRES = 948 .,
RADIUS = 12 ., PFAR = 1016 ., SGW = 8 ., AN1 = 125 .,
STEP 4 EYELAT = 28 ., DIREC = 295 ., SPEED = 13 ., EYPRES = 944 .,
RADIUS = 15 ., PFAR = 1016 ., SGW = 9 ., AN1 = 125 .,
STEP 5 EYELAT = 28 ., DIREC = 305 ., SPEED = 11 ., EYPRES = 932 .,
RADIUS = 15 ., PFAR = 1016 ., SGW = 11 ., AN1 = 125 .,
STEP 6 EYELAT = 29 ., DIREC = 320 ., SPEED = 10 ., EYPRES = 936 .,
RADIUS = 15 ., PFAR = 1016 ., SGW = 9 ., AN1 = 140 .,
STEP 7 EYELAT = 30 ., DIREC = 340 ., SPEED = 9 ., EYPRES = 958 .,
RADIUS = 15 ., PFAR = 1016 ., SGW = 8 ., AN1 = 155 .,
STEP 8 EYELAT = 30 ., DIREC = 355 ., SPEED = 9 ., EYPRES = 973 .,
RADIUS = 15 ., PFAR = 1016 ., SGW = 8 ., AN1 = 160 .,
STEP 9 EYELAT = 30 ., DIREC = 5 ., SPEED = 8 ., EYPRES = 982 .,
RADIUS = 15 ., PFAR = 1016 ., SGW = 8 ., AN1 = 170 .,
STEP 10 EYELAT = 31 ., DIREC = 5 ., SPEED = 8 ., EYPRES = 990 .,
RADIUS = 16 ., PFAR = 1016 ., SGW = 8 ., AN1 = 175 .

Storm Track Table

STEP	LAT	LONG	SNAP	ROT	(YMDH)
1	25 36	-81 12	1	0	92082412
2	25 41	-82 10		0	2415
3	25 46	-83 09	1	0	2418
4	26 00	-84 03		0	2421
5	26 08	-85 02	2	0	2500
6	26 23	-85 54		0	2503
7	26 38	-86 47		0	2506
8	26 56	-87 38	3	0	2509
9	27 16	-88 24		0	2512
10	27 31	-89 08	4	0	2515
11	27 47	-89 42	5	0	2518
12	28 10	-90 09	5	0	2521
13	28 33	-90 39		0	2600
14	28 47	-91 03	6	0	2603
15	29 09	-91 19		0	2606
16	29 37	-91 34	7	0	2609
17	30 06	-91 42	8	0	2612
18	30 29	-91 40	9	0	2615
19	30 54	-91 36	10	0	102618

Figure 4.10b Storm Parameters for Hurricane Andrew

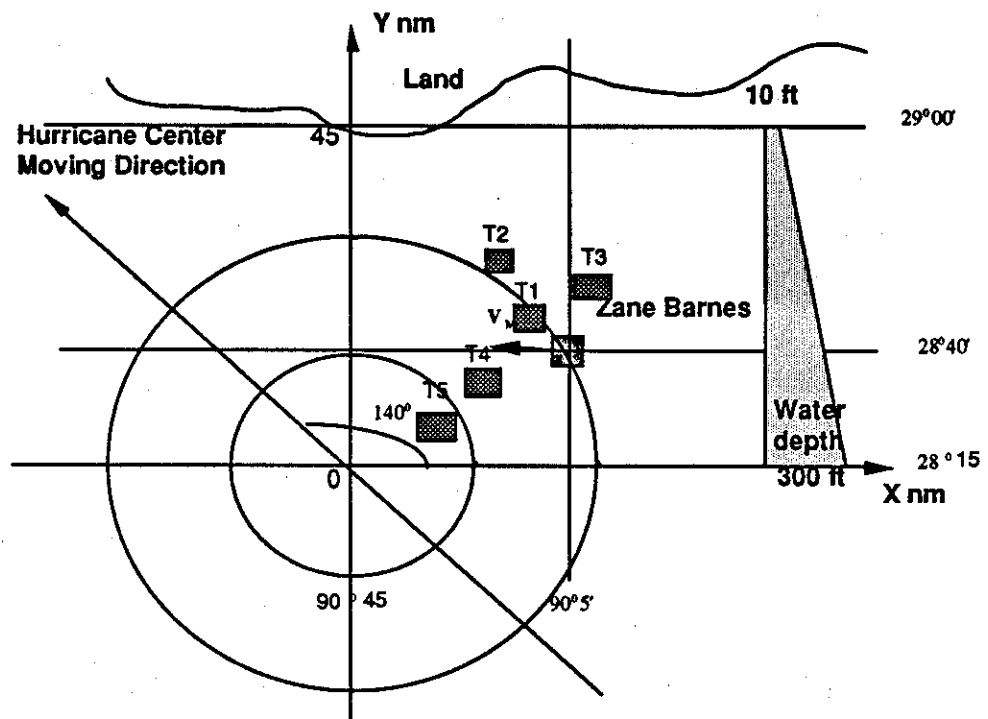


Figure 4.11 Reference Frame in Andrew

4.4.3 Analysis of the Parametric Study Results

Several simulations with different combinations of tracks and wave theory assumptions were performed. The results are summarized in Table 4.4 to Table 4.8. The results include different combinations of assumptions and the probabilities of mooring system failure and the probability of collision, in detail, the probabilities of collision with the first 5 largest target structures are also presented.

Table 4.5 and 4.6 presents a comparison of the results from different assumptions of hurricane tracks (curved and straight) and wave theory (Airy and Stokes) used to calculate the environmental loads. The results shows that the combination of simulation setting 2, "Straight line" assumption and Stokes theory, has the largest probability of collision while combination of setting 3, "Curve" assumption and Airy theory, has the least probability of collision. The results from setting 1 and 4 are very close. This may imply that Straight line assumption and Stokes theory have the effects of increasing the probabilities of collision while the curved track assumption and Airy theory have the effects of decreasing the probabilities of collision. The curved track model and Stokes theory to determine the wave kinematics provide a reasonable model.

Table 4.4 are the results from the assumption of MODU in free floating condition while Table 4.5 are the results from the assumption of MODU in dragging condition. From the results, it can be seen that in a large structure density area, the probability of collision may decrease greatly if anchors are designed to drag prior to any mooring line breaking since in

this case the MODU will not move far. However, if the MODU is to be located near subsea structures that could be damaged by a dragging anchor, the operator may use pile anchors or oversized drag anchors to cause the mooring lines to break first.

Table 4.5 Collision Probability in Free-Floating Condition

MODU NAME					Zane Barnes					
Mooring System										
Mean (Kts):		3500			Number of Mooring Lines:			8		
STD :		1000			Number of Breaking Lines:			8		
Simulation Setting 1 :										
Track Type:		Line			Simulation Number:			3000		
Wave Theory:		Airy			Time Step:			1 Hour		
Simulation Result										
Num	XM	YM	Dep.	P1%	P2%	P3%	P4%	P5%	Pm	Pc
1	40	28	170	1.9	0	0.02	1.8	0.8	8.7%	3.96%
Simulation Setting 2:										
Track Type:		Line			Simulation Number:			3000		
Wave Theory:		Stokes			Time Step:			1 Hour		
Simulation Result										
Num.	XM	YM	Dep.	P1%	P2%	P3%	P4%	P5%	Pm	Pc
1	40	28	170	1.18	0	0	2.64	0.42	10.03%	4.26%
Simulation Setting 3:										
Track Type:		Curve			Simulation Number:			3000		
Wave Theory:		Airy			Time Step:			1 Hour		
Simulation Result										
Num.	XM	YM	Dep.	P1%	P2%	P3%	P4%	P5%	Pm	Pc
1	40	28	170	0.92	0.14	0.02	0.12	0.06	3.3%	1.42%
Simulation Setting 4:										
Track Type:		Curve			Simulation Number:			3000		
Wave Theory:		Stokes			Time Step:			1 Hour		
Simulation Result										
Num.	XM	YM	Dep.	P1%	P2%	P3%	P4%	P5%	Pm	Pc
1	40	28	170	1.58	0.2	0	0.42	0.08	5.3%	2.34%

Table 4.6 Collision Probability in Dragging Condition

MODU NAME					Zane Barnes					
Mooring System										
Mean (Kts):		3500			Number of Mooring Lines:			8		
STD :		1000			Number of Breaking Lines:			6		
Simulation Setting 1 :										
Track Type:		Line			Simulation Number:			3000		
Wave Theory:		Airy			Time Step:			1 Hour		
Simulation Result										
Num.	XM	YM	Dep.	P1%	P2%	P3%	P4%	P5%	Pm	Pc
1	40	28	170	2.34	0.04	0	0.36	0	8.67%	2.78%
Simulation Setting 2:										
Track Type:		Line			Simulation Number:			3000		
Wave Theory:		Stokes			Time Step:			1 Hour		
Simulation Result										
Num	XM	YM	Dep.	P1%	P2%	P3%	P4%	P5%	Pm	Pc
1	40	28	170	2.24	0.02	0	0.5	0	10.02%	2.8%
Simulation Setting 3:										
Track Type:		Curve			Simulation Number:			3000		
Wave Theory:		Airy			Time Step:			1 Hour		
Simulation Result										
Num	XM	YM	Dep.	P1%	P2%	P3%	P4%	P5%	Pm	Pc
1	40	28	170	1	0.06	0.02	0.08	0	3.26%	1.16%
Simulation Setting 4:										
Track Type:		Curve			Simulation Number:			3000		
Wave Theory:		Stokes			Time Step:			1 Hour		
Simulation Result										
Num.	XM	YM	Dep.	P1%	P2%	P3%	P4%	P5%	Pm	Pc
1	40	28	170	1.6	0	0	0.02	0	6.5%	1.62%

Table 4.7 Collision Probability vs. Mooring Capacity Simulation Results

MODU NAME					Zane Barnes						
Simulation Setting :											
Track Type:		Curve			Simulation Number:				3000		
Wave Theory:		Stokes			Time Step:				1 Hour		
Mooring System 1:											
Mean (Kts):		2500			Number of Mooring Lines:				8		
STD :		750			Number of Breaking Lines:				8		
Simulation Result											
Num	XM	YM	Dep.	P1%	P2%	P3%	P4%	P5%	Pm	Pc	
1	40	28	170	2.1	0.08	0	1.04	0.1	8.2%	3.5%	
Mooring System 2:											
Mean (Kts):		3500			Number of Mooring Lines:				8		
STD :		1000			Number of Breaking Lines:				8		
Simulation Result											
Num	XM	YM	Dep.	P1%	P2%	P3%	P4%	P5%	Pm	Pc	
1	40	28	170	0.64	0.06	0	2.3	0.48	10.2%	3.82%	
Mooring System 3:											
Mean (Kts):		4500			Number of Mooring Lines:				8		
STD :		1300			Number of Breaking Lines:				8		
Simulation Result											
Num	XM	YM	Dep.	P1%	P2%	P3%	P4%	P5%	Pm	Pc	
1	40	28	170	1.74	0.1	0	0.4	0.04	5%	2.36%	
Mooring System 4:											
Mean (Kts):		2500			Number of Mooring Lines:				8		
STD :		750			Number of Breaking Lines:				6		
Simulation Result											
Num	XM	YM	Dep.	P1%	P2%	P3%	P4%	P5%	Pm	Pc	
1	40	28	170	2.14	0.02	0	0.06	0	8.3%	2.22%	
Mooring System 5:											
Mean (Kts):		3500			Number of Mooring Lines:				8		
STD :		1000			Number of Breaking Lines:				6		
Simulation Result											
Num	XM	YM	Dep.	P1%	P2%	P3%	P4%	P5%	Pm	Pc	
1	40	28	170	1.28	0	0	0.06	0	6.3%	1.34%	
Mooring System 6:											
Mean (Kts):		4500			Number of Mooring Lines:				8		
STD :		1300			Number of Breaking Lines:				6		
Simulation Result											
Num	XM	YM	Dep.	P1%	P2%	P3%	P4%	P5%	Pm	Pc	
1	40	28	170	0.84	0.02	0	0	0	4.5%	0.86%	

Table 4.8 Strategy Simulation Result in Free Floating Condition

MODU NAME					Zane Barnes					
Mooring System										
Mean (Kts):		3500			Number of Mooring Lines:			8		
STD :		1000			Number of Breaking Lines:			8		
Simulation Setting:										
Track Type:		Curve			Simulation Number:			2000		
Wave Theory:		Stokes			Time Step:			1 Hour		
Simulation Result										
Num	XM	YM	Dep.	P1%	P2%	P3%	P4%	P5%	Pm	Pc
1	40	38	99	0.39	1.23	0	0.27	0.09	7.05%	2.91%
2	47.07	35.07	120	0.3	0.48	0.78	0.09	0.03	5.95%	2.4%
3	50	28	17	0.72	0.21	0.57	0.27	0.12	6.95%	2.16%
4	47.07	20.9	220	0.69	0.03	0.09	0.6	0.24	5.75%	1.83%
5	40	18	240	0.15	0	0	0.87	0.81	6.55%	2.22%
6	32.9	20.9	220	0.06	0	0	0.81	1.05	6.2%	2.31%
7	30	28	170	0	0	0	3.3	0	5.5%	3.3%
8	32.9	35.07	120	0	3.3	0	0.03	0	6.2%	3.51%
9	40	28	170	2.01	0.09	0	0.48	0.03	5.65%	2.67%

Table 4.7 summarize the results from different assumed mooring capacities given a curved storm track and Stokes theory to calculate wave kinematics. The mean value of the mooring capacity was changed from the specified normal value of 3500 kips up and down 30% (upper range largest reasonable mooring strength). The collision probability remains almost the same. Within this range, the mooring strength is not important to the collision probability. It is found that anything more intense than about a one year hurricane storm will cause breakaways. The difference in mooring strength only results in a different

MODU moving route. In high structure density areas, it seems that mooring strength is not important to the collision probability. However, when the surrounding structures are far from the MODU, this difference may change the probability of collision a lot. In this case, it is still useful to test the various mooring systems for different mooring strength.

Table 4.9 Strategy Simulation Result in Dragging Condition

MODU NAME					Zane Barnes					
Mooring System										
Mean (Kts):		3500			Number of Mooring Lines:			8		
STD :		1000			Number of Breaking Lines:			6		
Simulation Setting:										
Track Type:		Curve			Simulation Number:			3000		
Wave Theory:		Stokes			Time Step:			1 Hour		
Simulation Result										
Num	XM	YM	Dep.	P1%	P2%	P3%	P4%	P5%	Pm	Pc
1	40	38	99	0.12	0.18	0	0	0	6.6%	0.36%
2	47.07	35.07	120	0	0	0.24	0	0	5.7%	0.36%
3	50	28	170	0.06	0	0.48	0	0	5.7%	0.54%
4	47.07	20.9	220	0.06	0.06	0	0	0	5.7%	0.12%
5	40	18	240	0	0	0	0.12	0.06	4.9%	0.24%
6	32.9	20.9	220	0	0	0	0.9	0.12	7%	1.2%
7	30	28	170	0	0	0	3.42	0	6.3%	3.42%
8	32.9	35.07	120	0	2.94	0	0	0	6.3%	2.94%
9	40	28	170	1.14	0	0	0	0	6.1%	1.14%

Table 4.8 and 4.9 summarize results from the effect of another important factor, the MODU site. User inputs the best preferred MODU siting place and the acceptable radius of siting area. The program automatically calculates the collision probability at eight orientations within the acceptable area. (Figure 4.12). The results give a suggestion on where to locate the MODU to have the least risk of collision with surrounding facilities.

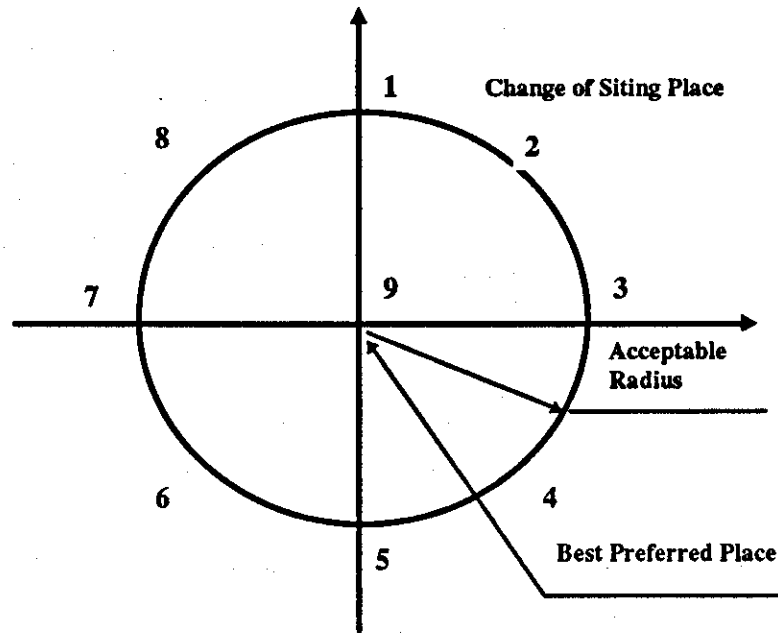


Figure 4.12 Changing MODU's Site

The results show that the collision probability is very sensitive to the location of the large target structures around the MODU. The target structures in this study are all located to the North-West of the MODU (Figure 4.11). It is obvious that locations 1, 2, 7, 8 (Figure 4.12) have the largest collision probability while location 4 has the least collision probability. In the area where the target structures are not located in a regular pattern, it would be very difficult to determine where to site the MODU to have the least risk. In such cases, the results from the simulation program could be of great help in identifying the best MODU location.

Also, it can be seen that the probability of mooring failure is very close in different locations, while the collision probabilities are different. These results imply that once a hurricane comes, the mooring system will fail. The difference in sitting location only results in different MODU moving routes, and different collision probabilities.

The study shows that should a MODU mooring failure occur, collision with a platform was likely. This may due to the high density of platforms within the area. However, a series of simulations was conducted varying the location of MODU and the distance from the MODU to the closest target circles. The results of these simulations show that the most likely collision target circle around the MODU is Target 1 and 4, those which are located at north-west to the MODU (storm tracks are generally from the south east). So the MODU should be moored as far as possible from the north-west target circles in this case. For example, if Zane Barnes were moored at (47,20) instead of (33,35) which is about 20 NM to the south-east, the probability of collision would be reduced to about 50% of its previous value (Table 4.8).

4.4.4 Case Studies

Thorough verification studies on MODU "Zane Barnes" have been performed. The following summarizes results from MODUSIM Functions #1 through #4 simulations performed on the Zane Barnes.

4.4.4.1 Function #1

The MODU's location and system configuration are the same as in the parametric studies. The mean mooring capacity is 3500 kips and it is assumed that the MODU is in the free floating condition after the mooring lines break. Based on the curved track assumption and with Stoke's 5th theory used to determine the wave kinematics, the probability of mooring system failure is 5.3% and the probability of collision with the surrounding structures is 2.3%.

4.4.4.2 Function #2

Given the incoming hurricane with the data from Andrew, with forecast times beginning at the different distance between the hurricane center Zane Barnes, the probabilities of collision have been determined. The results are summarized in Table 4.10 and Figure 4.13.

It can be seen from the results that when the hurricane was 600 nm away, the MODU was safe in the following 48 hours and the probability of collision (P_c) increased rapidly after 48 hours. When the hurricane was 400 nm away, the MODU was safe in the following 24 hours and P_c increased rapidly between the 24 to 36 hours, then P_c stayed at high level after that. When the hurricane was 200 nm away, the P_c always stayed at high level. The same thing happens to the probability of mooring failure, P_m (Figure 4.13).

Table 4.10 Simulation Result of Forecast Probability

Distance	200 nm		400 nm		600 nm	
Hour\Type	Pa_Moor	Pa_Coll	Pa_Moor	Pa_Coll	Pa_Moor	Pa_Coll
12	18.4	10.6	0	0	0	0
24	55	21.8	0.8	0.36	0	0
36	56	22.2	21.8	15	0	0
48	57.6	22.9	40	18	4.2	1.8
72	60	23.4	43.4	18.7	30	14

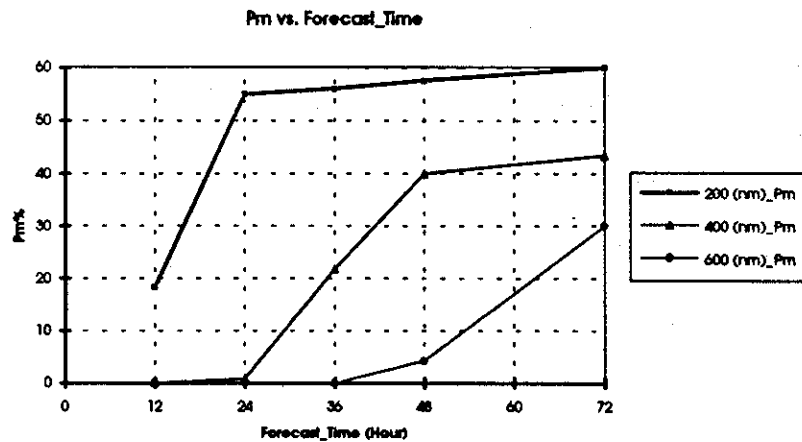
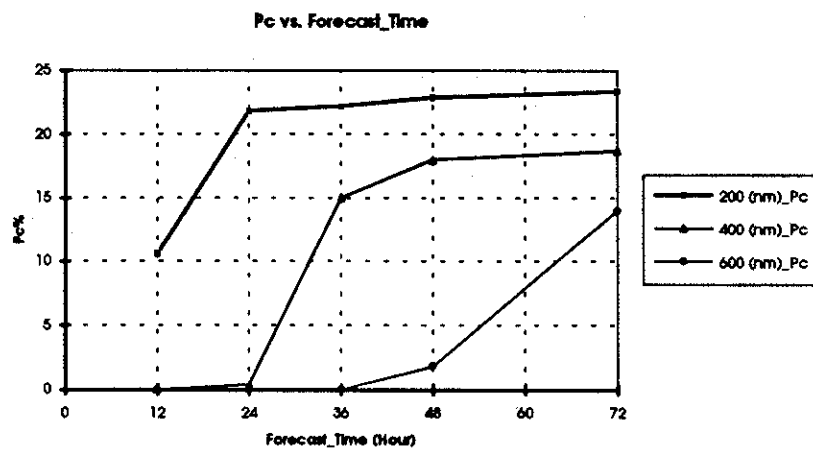


Figure 4.13 Probability of Failure vs. Forecast Time

4.4.4.3 Function #3

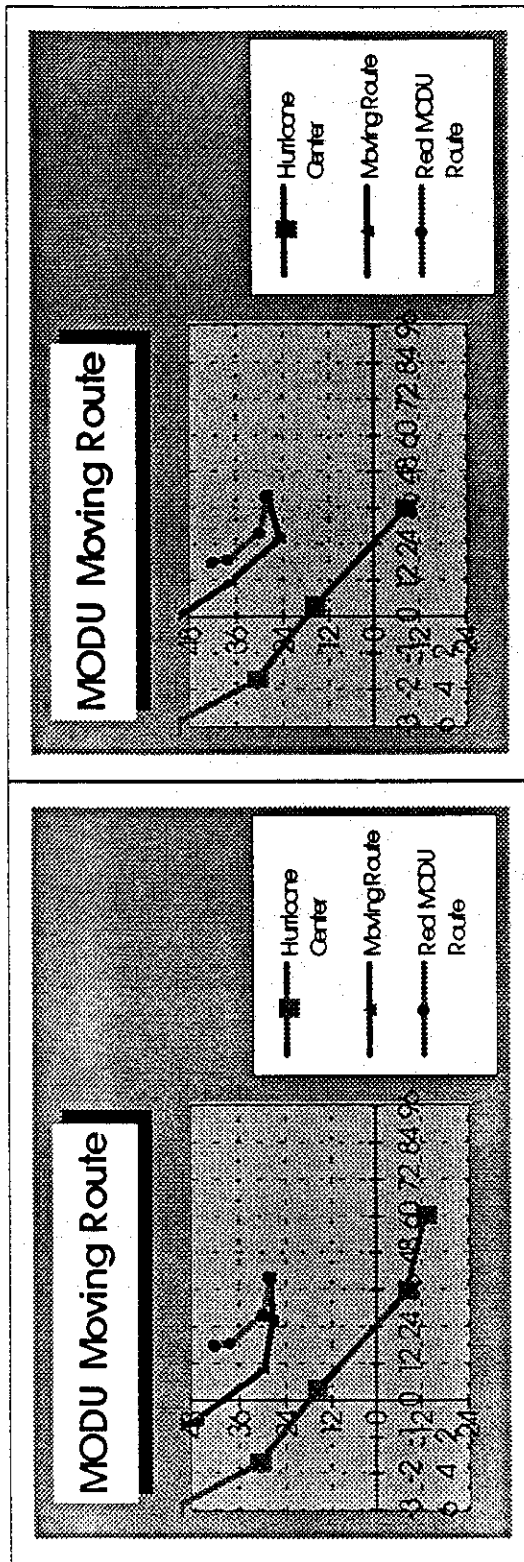
To verify Function #3, the Zane Barnes was driven to northwest for about 30 nm, stopped at South Timbalier (Block 32) in a water depth of 45 ft. It was in free floating at first and in skipping when the water depth was less than the draft. Different values of mooring capacity were assumed in the simulations. The results are in Figure 4.14.

The mean mooring capacity in Figure 4.14a is 3500kips, 4500kips in Figure 4.14b and 5500kips in Figure 4.14c. In Figure 4.14d, the MODU was held for an hour following each collision, and the result from this assumption is the closest to the real route. This may imply that the mooring capacity of Zane Barnes was around 4500kips and it was held for about an hour after each collision during its travel.

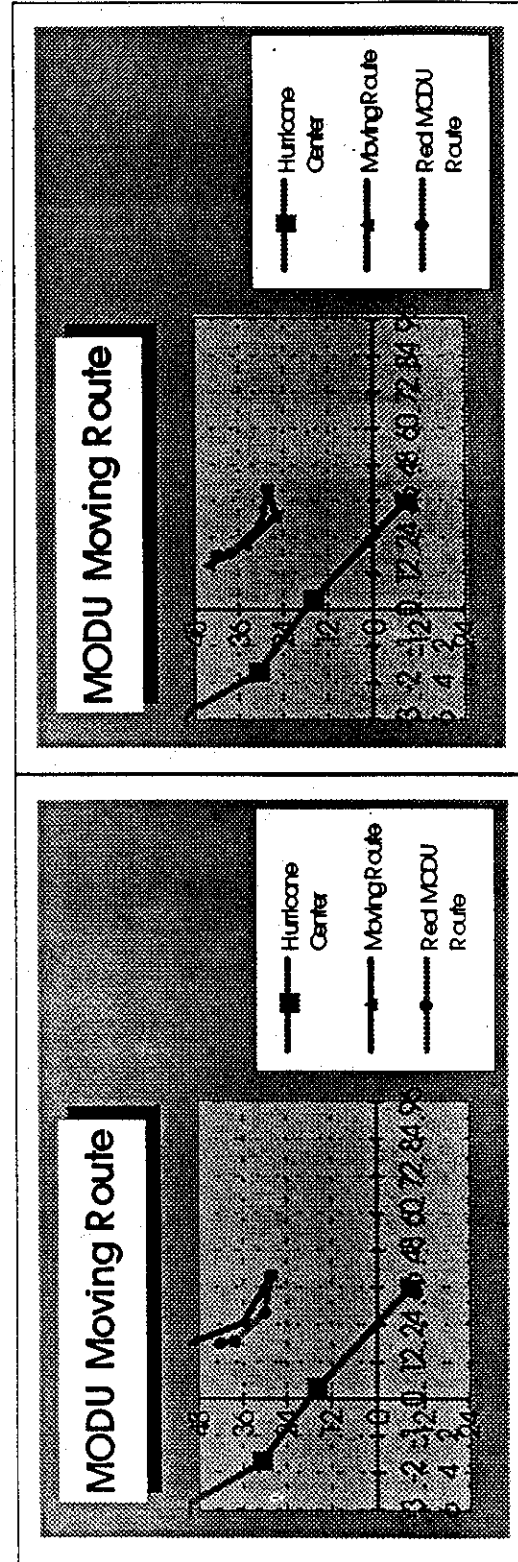
Another three MODUs from Gulf of Mexico are also utilized to verify MODUSIM. The Zapata Saratoga, which moved from Miss Canyon 705 to Grand Isle 47 during Andrew, was simulated in free floating condition. Treasure 75, which was ballast on bottom and moved 4 miles from South Pelto 7, and Ocean Now Era, which was moved 800 ft from Grand Isle 103, were simulated in dragging condition with two mooring lines dragging. (See Figure 4.15 and Figure 4.16). It was found that results from MODUSIM agreed very well with the real route.

4.4.4.4 Function #4

For application of Function #4, refer to Table 4.8 and 4.9.



a. Mooring Capacity 3500kips

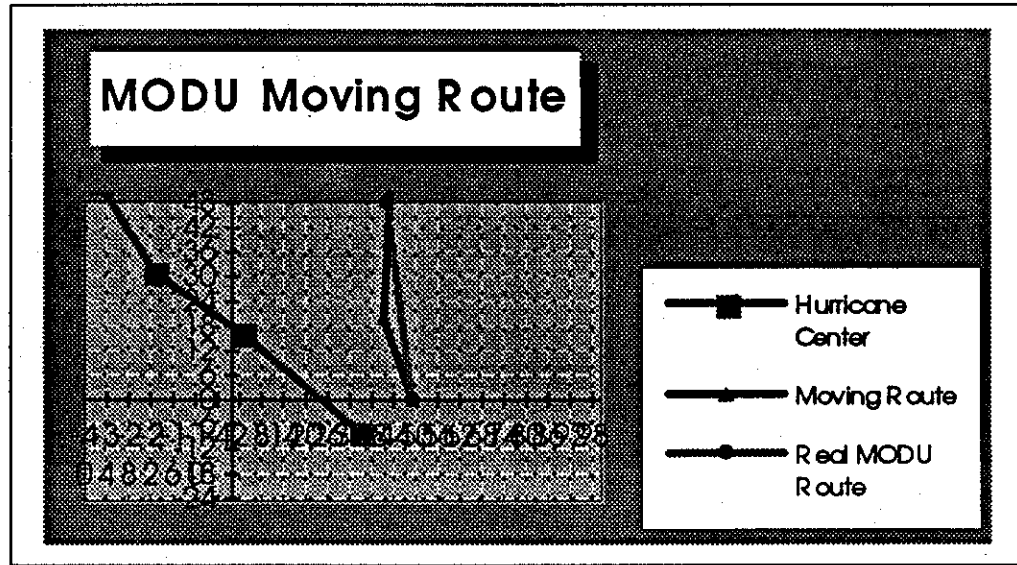


c. Mooring Capacity 5500kips

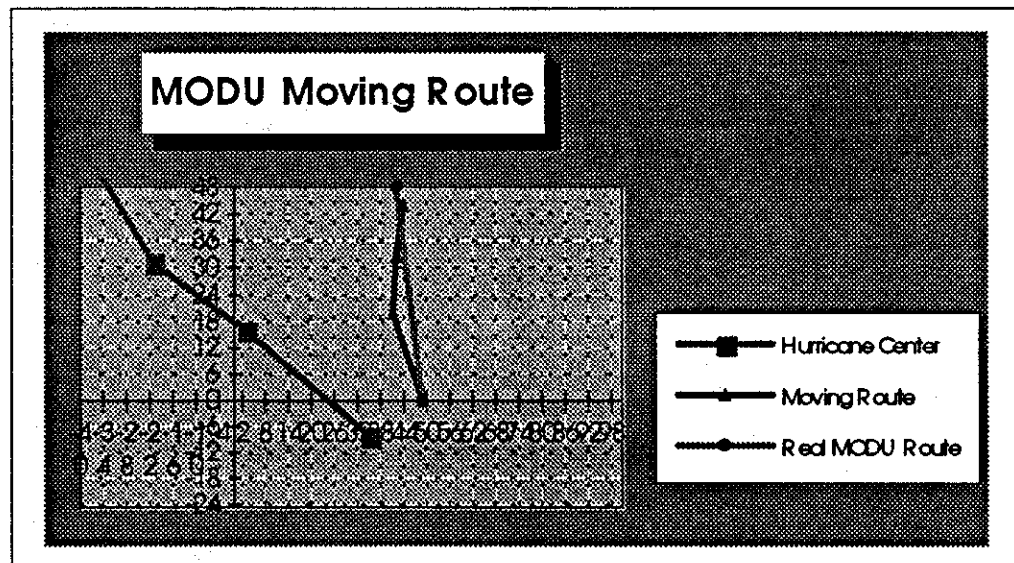
b. Mooring Capacity 4500kips

d. 4500kips, Holding Th each Collision

Figure 4.14 Simulated Moving Route of Zane Barnes in Hurricane Andrew

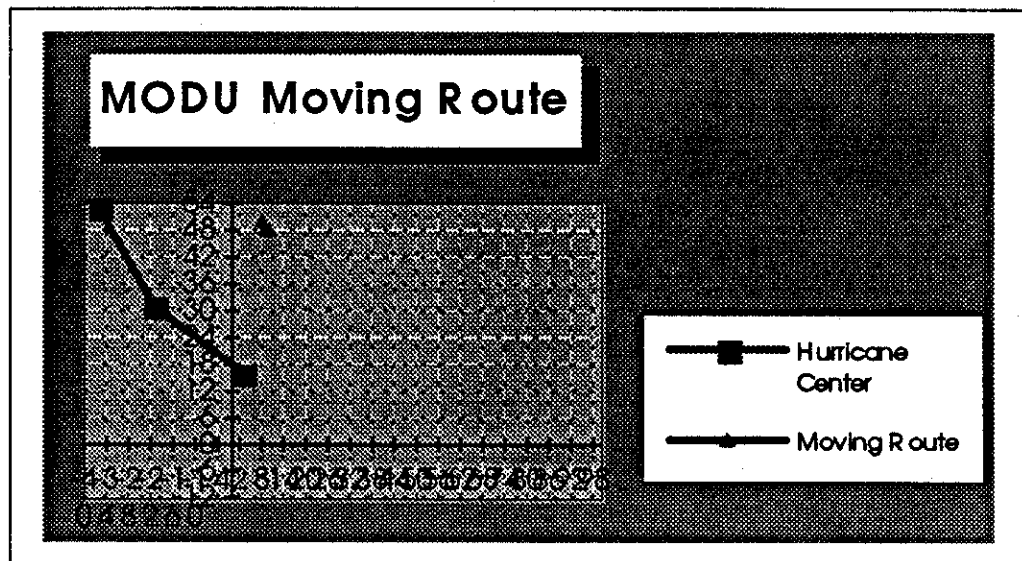


a. Mooring Capacity 4000 kips

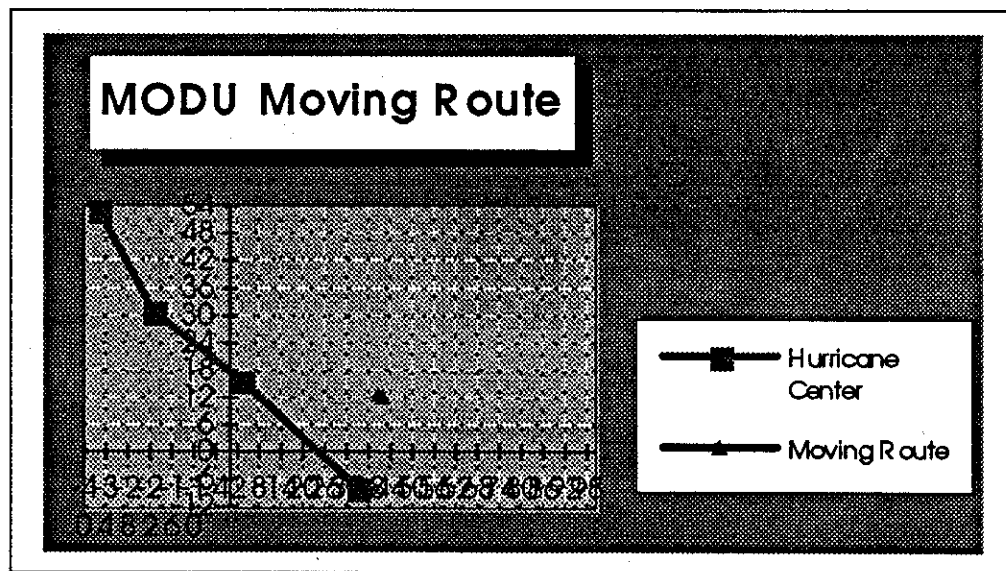


b. Mooring Capacity 4000 kips, Holding 1h Each Collision

Figure 4.15 Simulated Moving Route of Zapata Saratoga in Hurricane Andrew



a. Treasure 75, Ballast on Bottom, Moved 4 miles from South Peito 7



b. Ocean Now Era, Mooring Capacity 3000 kips,
Moved 800 ft from Grand Isle 103

Figure 4.16 Simulated Moving Route of Treasure 75 and Ocean Now Era in Hurricane Andrew

4.5 Simulations of the Movement of Bottom-Founded Platforms

4.5.1. Modeling Jack-up

The analytical and simulation model was extended to include analysis of the movements of bottom-founded MODUs (jack-up). The jack-up rig used in this research is a realistic amalgamation of several different existing deep water jack-up rigs. Properties such as flexural stiffness of the legs, overall dimensions and hull weights were averaged to yield an average harsh environment jack-up rig.

The rig has three independent square lattice truss legs supported at the sea floor by large spud cans. The principal properties of this average rig are summarized in Table 4.11. The centerline to centerline dimension between chords (vertical leg posts) is 39.6 ft. Each of the four chords has a cross sectional area of steel equal to 1.59 ft².

The structure is idealized as a planar assemblage of individual elements. The single degree of freedom model is idealized as consisting of three elements. The first element represents the two aft legs of the unit. The second element represents the hull, and the third element represents the fore leg. The element representing the 2 aft legs has twice the area, stiffness and moment capacity of the single fore leg listed in Table 4.12. The hull was assumed to have 5 times the stiffness of the legs.

Each node of the structure can have three degrees of freedom, translation in the horizontal and vertical, and rotation. The nodes can be controlled so as to have a zero displacements

Table 4.11 General Dimension of Average Jackup Rigs

GENERAL DIMENSIONS AND CHARACTERISTICS OF AVERAGE JACK-UP RIG

Length overall	230.0 ft
Width overall	250.0 ft
Depth of hull	33.0 ft
Length of spud legs	480.0 ft
Distance between centerlines of aft and fore legs (longitudinal)	160.0 ft
Distance between centerlines of aft legs (transverse)	190.0 ft
Diameter of spud can	55.0 ft
Footing area of spud can	2376 sq ft
Weight of hull	30,370 kips
Moment of inertia of legs	2487 ft ⁴
Rotational stiff. of jack housing and hull	1.5*10 ⁸ k•ft/rad
Structural damping	2-5 %
Equivalent leg diameter ($C_D * D$)	9.97 ft
Projected area for wind loading	16000 sq ft
Flexural Stiffness of legs (EI/L)	2.361x10 ⁷ kip•ft
Shear Area of Leg	3.5 sq ft
Yield Moment	6.528x10 ⁵ kip•ft
Plastic Moment	6.763x10 ⁵ kip•ft
Ultimate Moment	7.433x10 ⁵ kip•ft
Yield axial load	3.297x10 ⁴ kips
Ultimate axial load	4.601x10 ⁴ kips
Balance Points for Axial Load - Moment Interaction Curve	
Yield axial load	1.319x10 ⁴ kips
Yield moment	5.288x10 ⁵ kip•ft
Ultimate axial load	1.840x10 ⁴ kips
Ultimate moment	6.026x10 ⁵ kip•ft

or rotations relative to the ground, or two nodes can be constrained to have identical displacements. The single degree of freedom model, shown in Figure 4.17, constrains the nodes at the foundation (nodes 1 and 4) to have zero displacements in the horizontal, vertical and rotational directions (i.e. fixed end conditions). The nodes representing the leg-hull connection (nodes 2 and 3) are constrained to have identical horizontal displacements, zero vertical displacements and zero rotational displacements. By constraining nodes 2 and 3 to have identical displacements, the only motion possible is in the X direction shown in Figure 4.17.

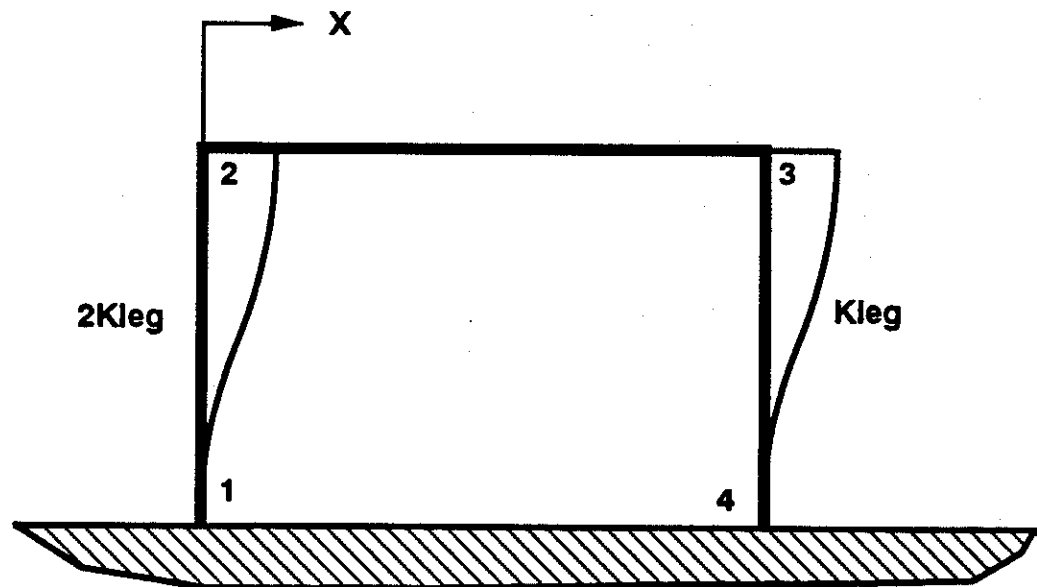


Figure 4.17 Jack-up: Single Degree of Freedom Model

The mass was distributed equally among the three legs. Since the element between nodes 1 and 2 represents the two aft legs of the unit, $2/3$ of the rig is located at node 2. The remaining $1/3$ of the rig mass is located at node 3.

The static wave forces were computed at one second intervals using Morison's equation with a drag coefficient (C_D) equal to 1.1 and inertia coefficient (C_M) equal to 1.2. The wave forces were computed using linear wave theory or Stoke's 5th theory. Current velocities were included in computing the hydrodynamic forces on the jack-up rig. The result of this process is a time history of the static wave forces acting on the jack-up at one second intervals.

The direction of approach of the waves was assumed to be orthogonal to a line between the two aft legs of the rig (parallel to the longitudinal centerline). This was done in order to induce the maximum loading in the single fore leg.

The yield moment of the leg section was computed assuming a linear stress distribution across the leg section. The yield moment was defined as the moment which resulted in the tension edge of the section reaching yield stress (36 ksi), as shown for the yield moment in Figure 4.18. The plastic moment was computed assuming the chord sections were fully yielded and the stress distribution was as shown for the plastic moment in Figure 4.18.

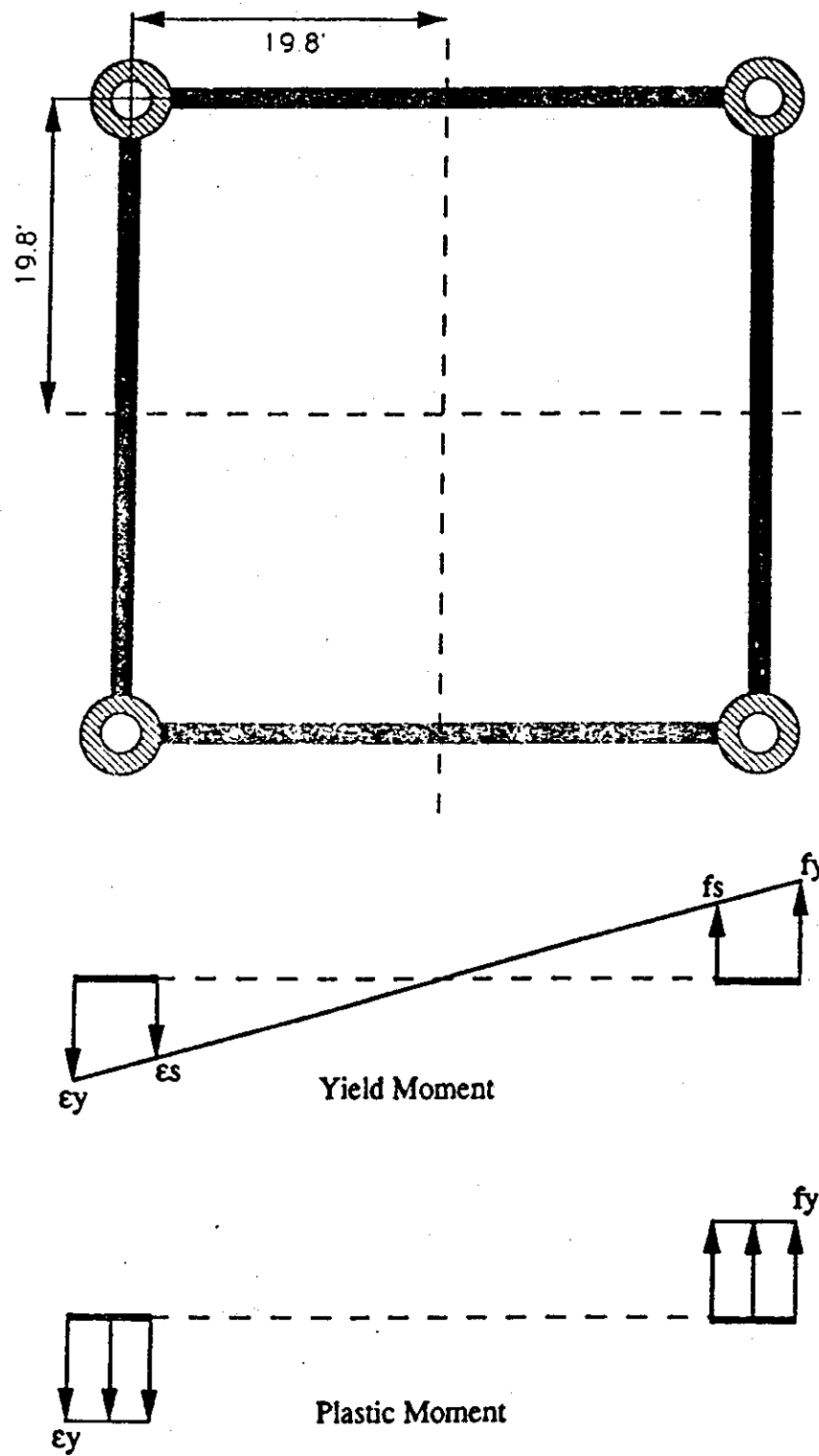


Figure 4.18 Definition of Yield Moment

4.5.2 Foundation Capacities

The capacity of the foundation is determined by its ability to withstand the vertical and horizontal loads transmitted to it by the jack-up unit. The vertical capacity is developed by the shear strength of the soil beneath the footing. The horizontal capacity is developed by the combination of sliding resistance and developed passive pressure of the soil as the footing applies increasing horizontal stresses to the soil.

The horizontal sliding resistance is the summation of the frictional resistance and the mobilized passive pressure of the soil as the footing reacts against it. The frictional resistance can be computed using Equation 4.44, assuming undrained soil conditions. In computing the sliding resistance, the mean value of the remolded shear strength of the soil was used. The resulting sliding resistance of the foundations are: for the Gulf of Mexico, sliding resistance ranges between 2590 kips and 1295 kips. The range in the sliding resistance is due to the potential variation in the effective area of the footing due to spud can rotations. As was computed in the bearing capacity analysis the effective area of the foundation can be approximately 50% of the static area.

$$H = S_v A \quad (4.44)$$

Passive pressure is the pressure that is developed by soils to resist movement when a load is applied to the soil mass. The fundamentals of bearing capacity discussed above are based on the development of passive pressure to resist the vertical loads. The mobilized passive pressure to resist the horizontal loads can be estimated using Equation 4.45.

$$\overline{\sigma}_p = K_p \overline{\sigma}_v + 2c\sqrt{K_p} \quad (4.45)$$

The coefficient of passive pressure K_p is defined in Equation 4.46.

$$K_p = \tan^2(45 + \phi / 2) \quad (4.46)$$

For clays with the angle of internal friction (ϕ) equal to zero, K_p is equal to 1.0. The value of the cohesion (c) (c and S_u are used interchangeably) is that of the initial shear strength of the soils, 0.5 ksf for the Gulf of Mexico. The resulting maximum passive pressures that could be developed by this foundation is 4.2 ksf for the Gulf of Mexico locations. The project area of the spud can is 412.5 ft². The resulting load capacities per spud can are 1730 kips for the Gulf of Mexico location (Table 4.12).

Table 4.12 Foundation Capacities of GOM

	Median Value	Standard Deviation
Moment	662071 (kip-ft)	0.106
Axial Load	41409 (kip)	0.117
Horizontal	3391 (kip)	0.40

4.5.3 Failure Modes of Jack-up

There are four principal failure mechanisms due to environmental loading on the jack-up: horizontal displacements, bearing capacities, overturning and leg failure. The occurrence of any one of these failure modes would render the jack-up unserviceable. Based on this, the jack-up system can be modeled as a system of elements in series, in which the

probability of failure of the entire system is the probability of failure of the most likely to fail element.

Overturning has been traditionally computed as the point at which the vertical reaction at the seafloor on the weather side leg is equal to zero. Typically, no consideration has been given to the transient nature of the wave loading. The duration of loads which are capable of causing the rig to overturn is relatively short, and the instant this load is removed, the rig returns to equilibrium. Realistically overturning can only occur if the center of gravity of the rig is pushed beyond the line of action of the vertical reaction of the leeward footing. This of course assumes that the rig will not suffer a bearing failure or a collapse of the leeward leg. The overturning failure is more an indication of the potential of inducing a failure into the system due to other components picking up the additional load and exceeding their capacity. Since overturning is not a realistic failure mode it will not be considered in further discussion. Also, the effects of the vertical capacities are not important due to the effects of pre-loading on the foundation. During pre-loading, the soil beneath the footing is consolidated under loads higher than those experienced during operations, hence as long as the vertical loads on the foundation remain below the pre-load no significant further consolidation should occur. The intent of pre-loading the foundation is to replicate the expected maximum loading the foundation would experience during an extreme event. There will be however, a small amount of settlement of the foundation due to further or secondary consolidation of the soils beneath the footings, however this occurs over a long period of time and is not a storm response.

As the preliminary nature of the study in this area, the evaluation of the rig will concentrate on the horizontal foundation failure modes and leg failure.

a. Leg Failure

The ultimate shear that can be resisted by a leg is obtained based on bending moment capacities of the leg. The interaction of bending moment and axial force (**M-P**) is taken into account. The maximum bending moment and axial force that can be developed in a leg is limited by local buckling of leg cross-sections.

The vertical dead loads of the decks are assumed to be equally shared between the deck legs. The vertical live loads in the legs caused by the lateral overturning forces are computed and summed to define the axial loading in each leg.

Due to relatively large axial loads (weight of the decks and topside facilities) and large relative displacements (deck bay drift) at collapse, $P - \Delta$ effect play a role in reducing the lateral shear capacity and hence is taken into account.

To derive a realistic estimate of $P - \Delta$ effect without leaving the framework of a simplified analysis, it is assumed that the deck is rigid. The analysis is done using the direct stiffness method, with the nodal displacements as unknowns. The equilibrium condition to be solved is given as:

$$P = K \cdot \Delta \quad (4.47)$$

where P is the lateral load and K is defined as:

$$K = \sum_{leg} \frac{12EI}{h^3} \quad (4.48)$$

Where,

E=Elastic Modules

I=Moment of inertia about the axis of bending for the leg

h=Height of the leg

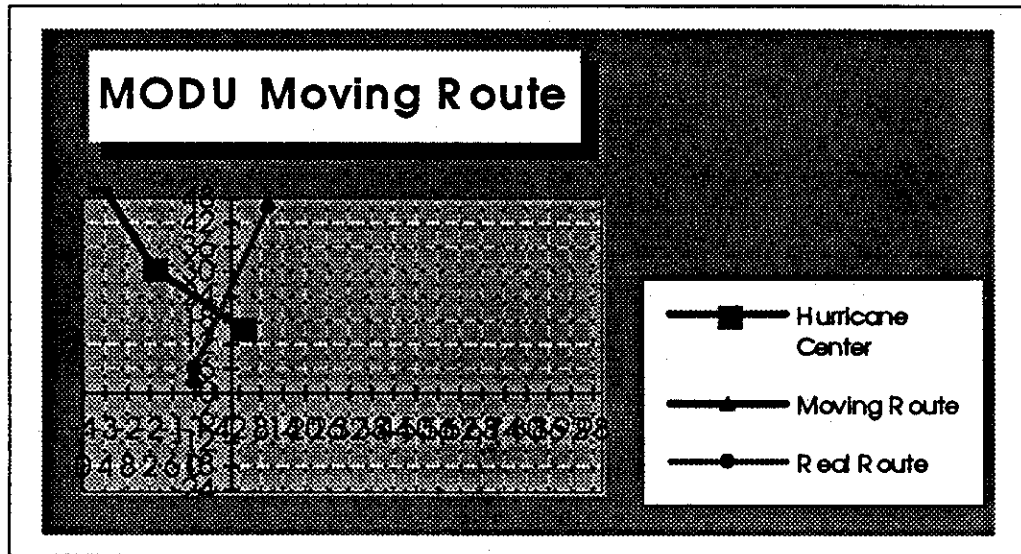
b. Horizontal Displacement

During a wave period, if the total lateral force is larger than the foundation horizontal capacity, the Jack-Up will move forward and backward. And in the shallow water condition, the forward wave force generally is large than the backward wave force, the Jack-up will move step by step along the wave propagate direction. Here for a simplified analysis, it is assumed that the MODU's moving time is quarter wave period forward and quarter wave period backward during one wave period. The moving distance during a wave period is defined as:

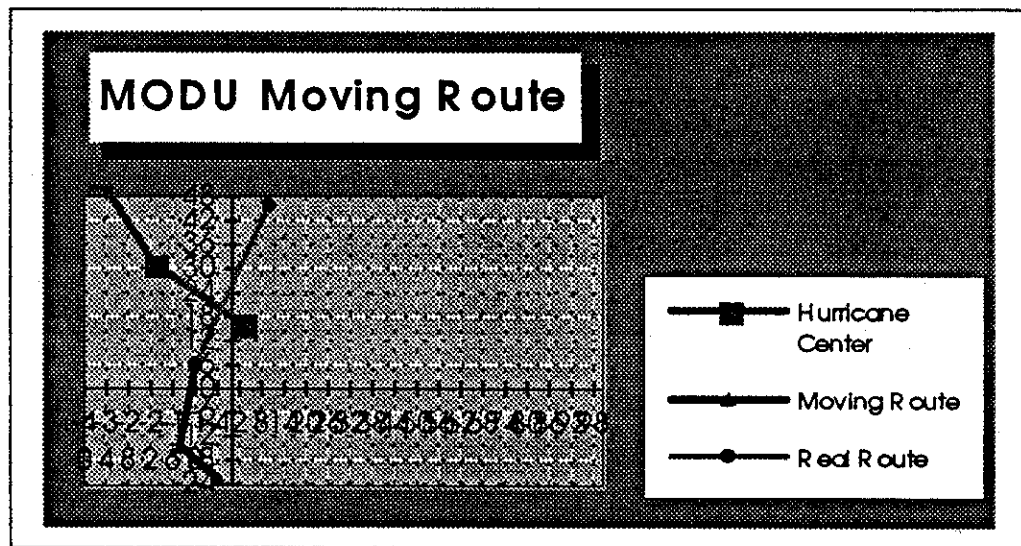
$$S_{wave_period} = \frac{1}{2} \cdot a \cdot \left(\frac{T}{4}\right)^2 \quad (4.49)$$

4.5.4 Example of Martin 3 Jack-up in Hurricane Andrew

During hurricane Andrew, Jack-up Martin 3 broke legs and moved from Ship shoal 263 to South Timbale. The result from MODUSIM (Figure 4.19) did not agree with the real route. We may find out from Figure 4.19 that if the Martin 3 legs were broken before Andrew reached the Jack-up, the Martin 3 would always move to deep water by the environmental force. Since the Martin 3 moved to shallow water in fact, this implies that the Jack-up legs were broken after Andrew passed the Jack-up location. Because the maximum environmental forces happened when Andrew reached the Martin 3, MODUSIM would assume that the Jack-up legs were broken at that time and so the resulting moving route would be different from the real one. From this point of view, MODUSIM needs to be improved to simulate cases in which low cycle fatigue results in degradation in the capsizing of Jack-up's legs.



a. Foundation Horizontal Failure



b. Leg Broken

Figure 4.19 Example of Martin 3 Jack-up in Andrew

CHAPTER 5

SIMULATION MODEL FOR EVACUATION PROCEDURES

5.1 Introduction to Project Management

Project management is the planning, organizing, and managing of tasks and resources to accomplish a defined objective, usually with constraints on time and cost. Managers of almost any fact of business can use project management concepts and tools to manage their work. If the project involves more than a few tasks, or if one has several resources to track, one can benefit from project management practices.

The goal of project management is to achieve a specific objective within a given deadline and budget. An objective can be as simple as planning the design and production of a corporate sales brochure, or as complex as designing and building a community in space. In each case, one must break the project into easily manageable tasks or activities, schedule the tasks, and then track tasks as the work progresses. The tasks are the building blocks of project management. One can also assign resources, such as people and equipment, to accomplish these tasks.

Project management can help one answer various scheduling, resource, and cost questions, such as:

- How long will this project take?
- If a particular task is delayed, will the project be delayed?

- Which tasks are critical to meeting the schedule?
- Do I have enough resources to complete the project as scheduled?
- What are the resource costs for the project?

The following is a brief overview of some of the most significant achievements in developing project management techniques. Each of these achievements has influenced the development of project management software:

Critical Path Method (CPM)

The process of computerizing project management began in the 1950s. Du pont Corporation, in an effort to improve its project scheduling techniques, developed a scheduling system called the critical Path method, or CPM scheduling. CPM is a mathematical model that calculates the total duration of a project based on individual task duration's and dependencies, and identifies which task are critical. This model is the fundamental scheduling method used in project management software today, including Microsoft project, which has been used to develop EVACSIM.

Program Evaluation Review Technique (PERT)

During the 1950s, the United States Navy faced the huge challenge of developing the Polaris Missile project, a submarine-based weapons system. Lockheed, the primary contractor on the project, developed the PERT scheduling system, which uses statistical probabilities to calculate expected duration of activities. Today, a PERT chart (sometimes called a network chart) refers to the graphic representation of task relationships.

Gantt Chart

In a separate evolution of project management systems, Henry L. Gantt developed a graphic charting system to depict activities across a timescale. Initially called bar charts, these charts have since been renamed Gantt charts in honor of the inventor of the system. The Gantt chart in Microsoft Project can be used to build a project, as well as to track and report it.

5.2 Background of Simulation Model

Safety and cost effectiveness are the determining factors in achieving a successful hurricane evacuation project. The success is measured by the safe completion of the evacuation at minimum cost within the time. Whether or not this is accomplished depends largely on how accurately management foresees the problem and evacuation options during the planning as well as the execution phases of a hurricane evacuation project. The management decisions are further complicated by unpredictable weather and equipment downtime.

In order to help management in its decision-making, various ways of predicting downtime, ranging from gut-feeling to sophisticated computer simulation programs, have been developed, both by oil companies and contractors. The work by McCarron (1971), Burke (1977), Hoffman (1978), Chen (1983), and Praught (1982) are a few examples of industry's efforts in this area since the early days of North Sea construction projects. Slomski and Vivatrat used Monte Carlo simulation procedures to evaluate risks of Arctic

offshore operations (Slomski and Vivatrat, 1986). Moore (1994) proposed to develop the early warning systems to safe and effective evacuation of platforms.

Storm forecasting is an important factor in safe and effective evacuation of platforms. These years, weather forecasting reliability of the tracks and intensities of severe storms has been improving. Forecasting are continually updating hypotheses and developments resulting in decreasing uncertainty levels over time (Moore, 1993). However, as discussed in Chapter 3, there are a great uncertainties associated with the storm forecasting, and these uncertainties create a number of problems for decision makers.

As a result of these uncertainties, it is important to determine the criteria for platform evacuations and securing operations. Evacuation and securing criteria can be based upon a number of factors such as:

- wave heights,
- wind speeds,
- storm distance,
- storm direction,
- storm forward speed,
- type of MODU,
- capacity of unit and mooring to withstand extreme loading,
- availability of evacuation and securing vessels and helicopters,
- distance from the unit to shore,

- the number of personnel to evacuate.

An evacuation simulation model would be useful to develop early warning systems for offshore platforms in storm conditions. For offshore operations, early warning signals come in the form of storm forecasting. If the lead time to respond to a storm is too short, securing operations and evacuations are more hazardous and the potential for accidents are more prevalent. If evacuations are made too early, they may have been in error resulting in unnecessary costs and loss of work time. Operating under high intensity or unpredictable weather conditions, effective weather forecasting is an essential factor to operational reliability. Good weather forecasts at early stages allow sufficient alert time for preparation and evacuation ahead of oncoming storms.

The current hurricane alert procedures used by the oil company usually include several alert phases which are based on the distance from the storm center. The following is an example of the evacuation system for the MODU Zane Barnes (R & B, 1988):

- Phase I - Green Alert: A tropical depression (winds 23-33 knots), a tropical storm (winds 34-63 knots), or a hurricane (winds greater than 75 knots) is identified at 750 nautical miles of the grilling location.
- Phase II - Yellow Alert: A tropical depression, storm or hurricane has moved to 500 nautical miles of the drilling site (or 650 NM if it has a closing speed greater than 15 knots).

- Phase III - Red Alert: The outer edge (gale force winds) of a tropical depression, storm, or hurricane has moved to approximately 250 NM or 24 hours from the location.

These kinds of hurricane preparedness and evacuation policies based on cyclonic storm positions are widely accepted by current oil company. But due to the unpredictable nature of the intensity and the track of the storm, consequently, most storms that resulted in evacuation, did not substantially impact the area of operation. The hurricane either recurved away from the area of operation or just had minimal intensity.

The average cost of a typhoon evacuation includes helicopter mobilization and operations costs, onshore room, board and transportation for evacuated personnel and associated rig downtime costs. The cost is almost \$500,000 per evacuation. As drilling operations expand significantly, the evacuation costs will increase rapidly during storm season. Also there is an inherent risk of evacuating large number of offshore personnel by helicopters or ships in uncertain weather conditions. All these factors, (ex., safety concerns, financial impact and schedule delays), indicate a need to improve hurricane evacuation planning.

The computer simulation program EVACSIM developed during the research can simulate different kinds of evacuation operations and calculate the probability of safe evacuation based on hurricane forecasting, different evacuation start time, available resources and alternative evacuation procedures. The evacuation simulation model is based on:

- 1) Available statistics and hindcast results for hurricane forecast in the Gulf of Mexico;
- 2) Real-time 72 hour hurricane strength and track forecasts;
- 3) Probability models to include the hurricane strength and track forecast errors;
- 4) Real hurricane evacuation operations and procedures performed on MODUs;
- 5) Available evacuation resources and different weather-relative workable time periods of these resources based on the resources shut down environmental criteria.

Results from this model are intended to assist in developing decision criteria for MODU securing and evacuations. The simulation results can be helpful to answer the following questions:

- Given the evacuation start time, how long will it take to complete safely?
- At different evacuation start times, what is the failure probability of these evacuations?
- What is the best evacuation start time based on acceptable risk and cost?
- What is the most reliable and cost-effective evacuation procedure?

In this way, the platform operator can evaluate the latest start evacuation time to have the least risk and avoid un-necessary evacuations.

5.3 Development of the Simulation Model

A logical development of the state of the art in evacuation studies is to generate modeling techniques for the entire evacuation sequence, taking into consideration of evacuation procedures as well as equipment availability and downtime.

The evacuation sequence can be modeled by a network of activities. The network consists of a collection of branches and nodes. The branches represent the activities and the nodes represent milestones or events associated with the project. Simulation of a evacuation sequence thus involves stepping through the network from start to finish using a computer.

A typical evacuation network consists of branches and nodes to represent activities and milestones. Each activity emanates from one node and terminates at another. A node is realized when all activities terminating at that node are realized. Only then are the subsequent activities scheduled. in this manner, all the sequential as well as parallel job activities can be simulated by stepping through the network from start using a computer.

Figure 5.1 shows a logic flow chart of an evacuation simulation process.

In performing a simulation, the project definition in terms of the network described in the preceding are input to the computer program. Beginning at the desired starting time, the hurricane forecast from national weather forecast center or through hindcast weather time histories are used as a basis for decision-making.

Each activity on the network is performed sequentially or in parallel, with the time required being dictated by statistics based on the input activity duration estimates. The operation is periodically interrupted by the occurrence of bad weather or equipment

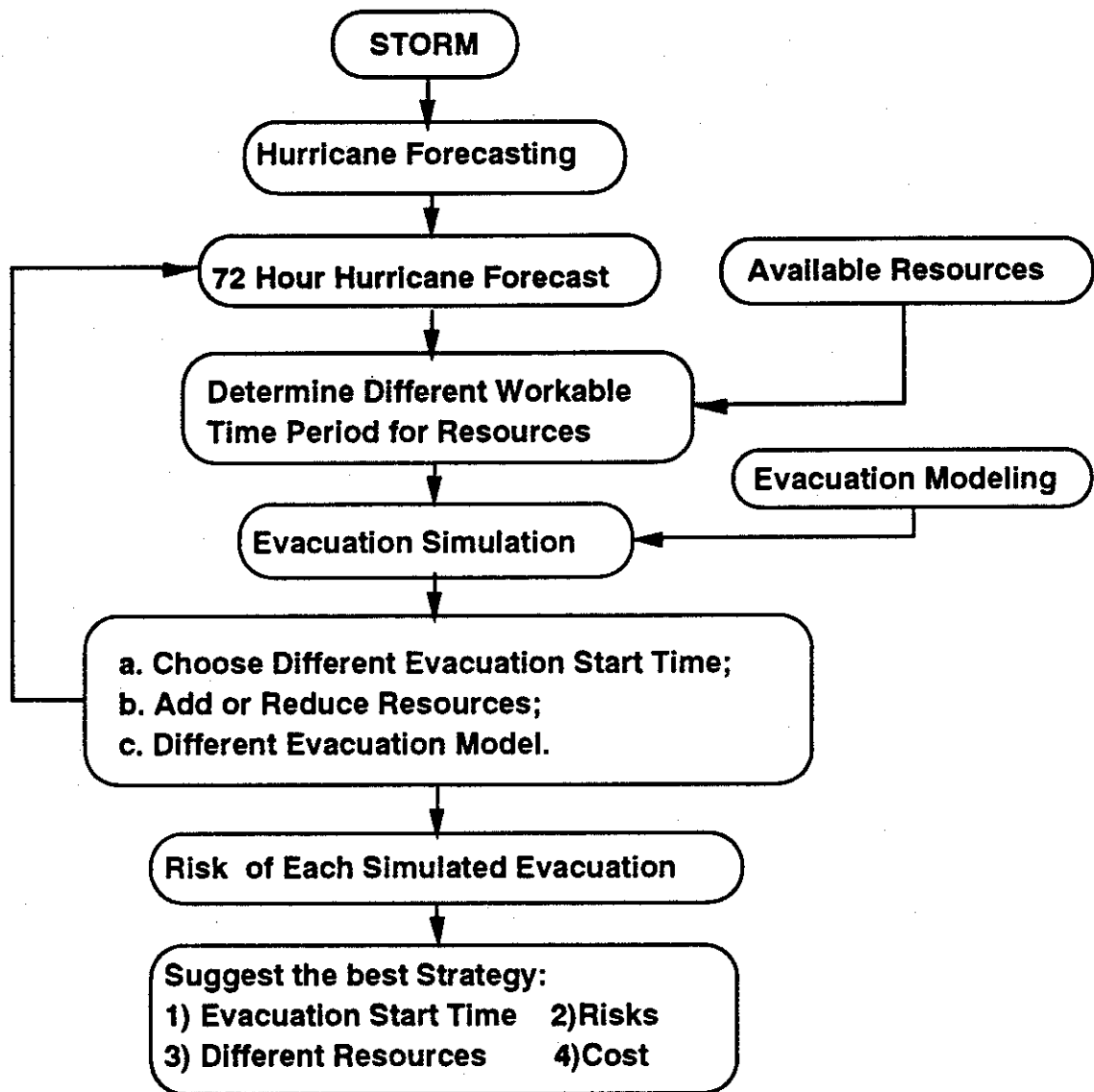


Figure 5.1 Probabilistic Simulation Procedure

downtime, which is generated using random number generation in accordance with the statistics of hurricane history. The process continues until the entire evacuation project is complete.

5.4 Shutdown Criteria

The ability to perform tasks offshore is normally controlled by the environmental conditions and the motion responses of the MODU. Each task is limited by specific interactions between the MODU motions and the function being performed. Usual attempts to quantify the criteria-limiting operations generally considered a wave height or wind speed for a particular operation. These were indirect functions derived from operator experience based on visually observed conditions. Even through this type of criteria is generally applicable to one MODU type only and is subject to many flaws such as variation in performance with wave direction relative to the vessel and the frequency distribution of wave energy, these criteria are useful, however, as they form a basis for preliminary estimation with a minimum of effort.

The environmental criteria used in the simulation model is wind speed and wave height. Based on the forecast data from National Hurricane Forecast Center, the workable time period of different resources are determined. As the simulation is resource-driven, that means the duration of each sub-task is determined by the associated resource workable time, the duration of whole evacuation process can be determined.

There is another shut-down criteria model in the EVACSIM, un-separable worktime of some resources. Like the other offshore projects, some of the tasks during the evacuation procedure may not be separated. That means, if it starts, it must continuously perform until it finishes, and, if it stops, it must be start again from the beginning. For example, we assume sending a helicopter from land to platforms takes 3 hours, if the helicopter can not land when it arrives the platform because of bad weather, it must fly back to land. That means the whole process needs to be repeated again. And the minimum duration is 3 hours which is the fastest evacuation operation time and the maximum is 5 hours (the fuel can last that long).

In the simulation model, each sub-task can be defined as must-continuous or may-not-continuous, and also may be given a minimum and a maximum completion duration. The minimum duration is defined as the minimum time to finish the task and the maximum duration is defined as the maximum time to finish the task, in helicopter example, 3 and 5 hours. This will be the shut-down criteria added to the results of helicopter workable time period from hurricane forecast.

5.5 Simulation Procedure

In order to examine evacuation procedures and decisions, it is important to develop models of these operations. An exhaustive model of securing and evacuation systems can be complex. These models should be simple enough to understand, yet detailed enough to include the important factors involved in the operation. For platform securing and

evacuations tasks in this research, Microsoft Project 4.0 was used to build the evacuation process model.

Microsoft Visual Basic is used to generate the input file of MS Project and to determine the workable time of resources. Because the different resource workable time periods are dependent on hurricane forecasting from MODUSIM or national hurricane forecasting center, the whole evacuation duration and cost will change with the different evacuation start times. Thus the risk and cost from different evacuation start time can be compared and optimum decision may be suggested.(Figure 5.1)

The deterministic result is just a most probable case of the evacuation duration histogram. The results of a single simulation are not meaningful because these results are valid only for the particular weather and activity duration of that run. Since the weather as well as the activity duration are probabilistic, the simulation is generally repeated many times to provide a statistically reliable sample for performance evaluation. With the simulation in probabilistic region, the useable length of simulation results is extended despite the increasing uncertainties in hurricane forecast and the relative threat to different evacuation start times can be compared.

The simulation procedure is as follows:

- a. Creating the evacuation model

This is the most important phase of the simulation. It includes defining the tasks and their duration, setting up relationships between the tasks, and, if one is going to track resource usage, assigning resources to the tasks. All of the project's later phases are directly based on the information you provide when you create the project;

- b. Inputting hurricane forecast data and determining the workable time periods of different resources based on input hurricane data. The input file of hurricane forecast data is *pdata.txt*. Please refer to EVACSIM Menu for detail. The detailed procedure of determining workable time period for resources, which is programmed in Visual Basic, is presented in Figure 5.2.

- c. Performing deterministic simulations at different evacuation start times;

The deterministic simulation procedure is presented in Figure 5.3.

- d. Performing Monte Carlo simulation at different evacuation start time.

In the Monte Carlo regime, random environmental conditions are generated based on hurricane hindcast data and the 72 hurricane forecast (Section 3.5), the simulation is repeated numerous times in order to provide a statistically reliable sample for performance evaluation. The correlation between each 12 hour data is assumed as 0.8. Usually 100 simulations at different evacuation start time are sufficient to provide information for predictions with a satisfactory degree of confidence. The probability of

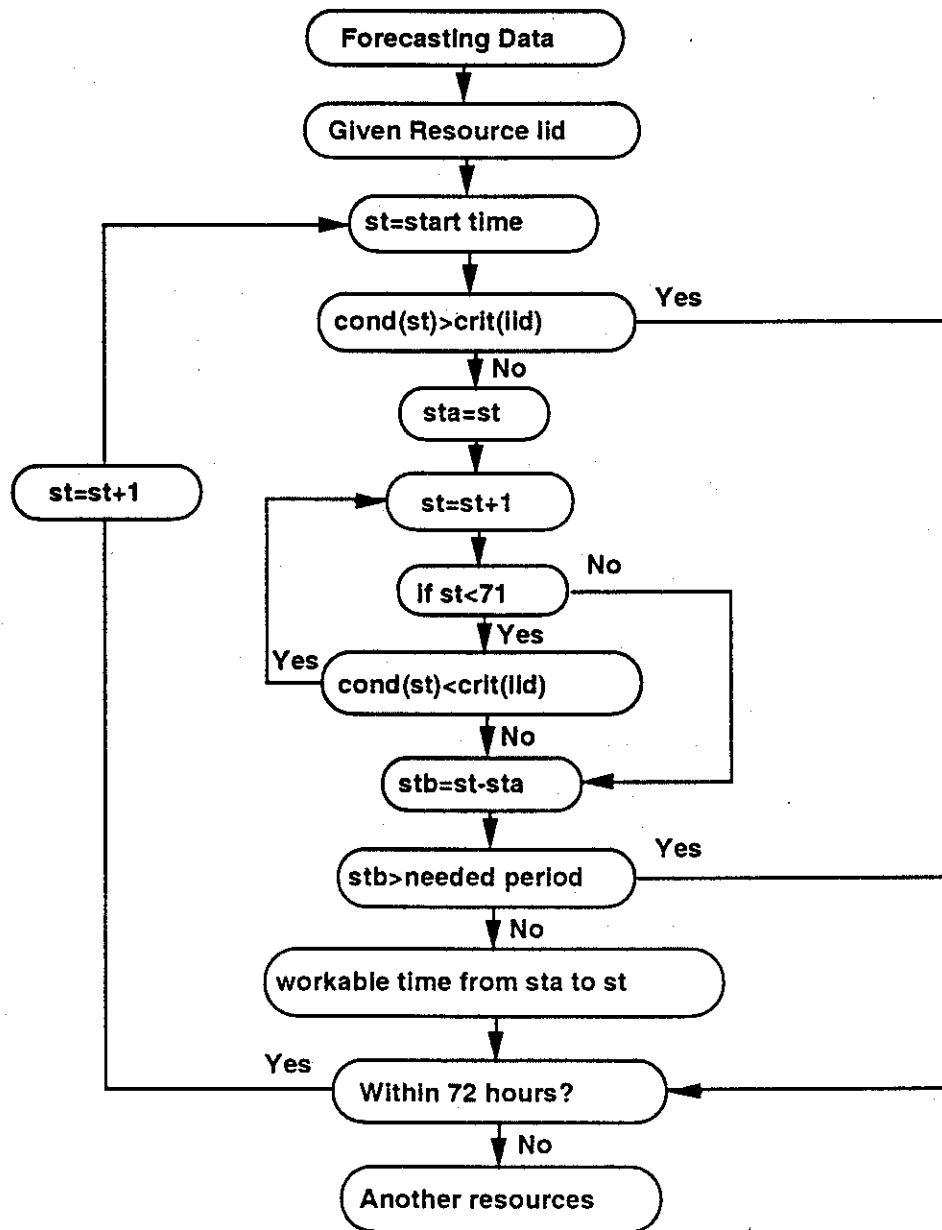


Figure 5.2 Procedure of Determination Resource Workable Time Period

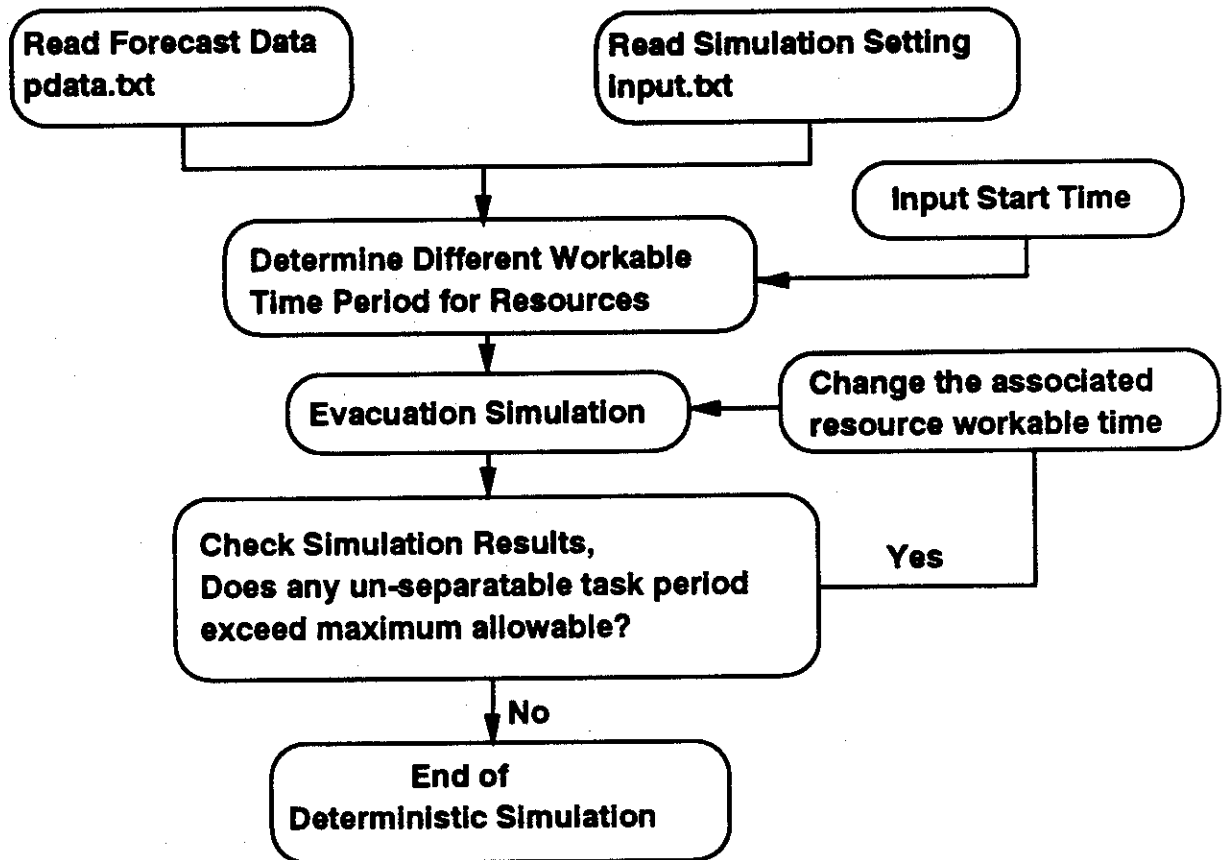


Figure 5.3 Deterministic Simulation Procedure

evacuation failure is defined as the number of failure in each simulation divided by the number of simulations.

The probabilistic simulation procedure is summarized in Figure 5.1.

- e. Upon completion of all simulations, the records for the duration, weather downtimes, critical path for each simulation, are accumulated and histograms are generated. Suggestions on evacuation decision may be given.

Histograms and statistics on evacuation duration, equipment/weather downtime, waiting time, total project cost and critical path indices for each activity, are some of the outputs available to help make management decisions. The usefulness of the model is illustrated by a case study based on a real evacuation procedure performed on Zane Barnes.

5.6 Case Studies

In order to explore the effect that each of the factors has on the results, a series of runs have been carried out where one parameter has been varied at a time. The main factors examined are:

- different evacuation start time;
- number of available resources;
- type of available resources, ex., helicopters or crew boats;
- different evacuation alternative.

Following is the simulation process of a real evacuation procedure performed on Zane Barnes:

a. Creating the evacuation model;

In Figure 5.4, the whole evacuation operations are modeled as tasks and sub-tasks from top to down. The needed duration and the associated resources of each sub-task are also presented. Input file *Input.txt* contains the all resources shut down criteria and some imagine resources defined as “control resources” which are used to control project process through the control of workable time period. Please refer to EVACSIM Menu for a detailed explanation of *Input.txt*.

b. Input hurricane forecast data and determine workable time period of different resources;
Input file *pdata.txt* includes environmental condition inputs, ex., 72 hour wind speed and wave height forecast, Figure 5.5. Run Visual Basic to determine the workable time period.

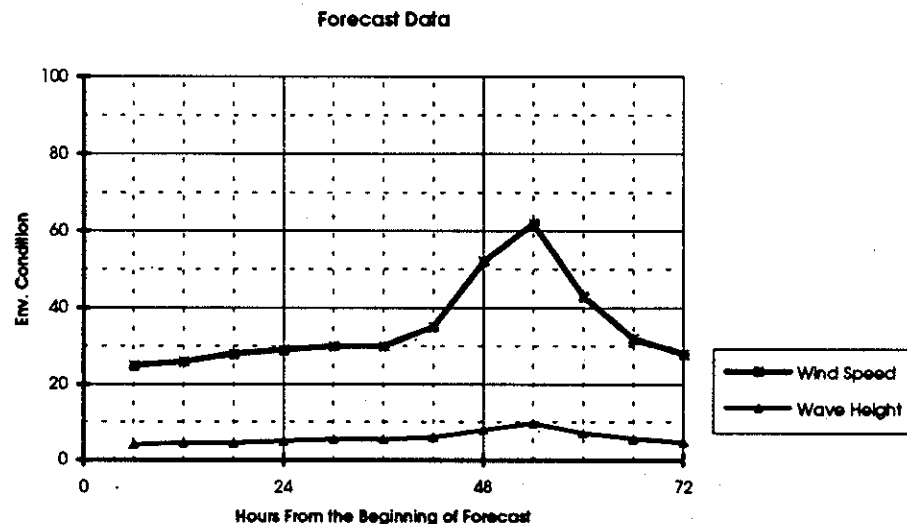


Figure 5.5 Example of Input Environmental Forecasting Data

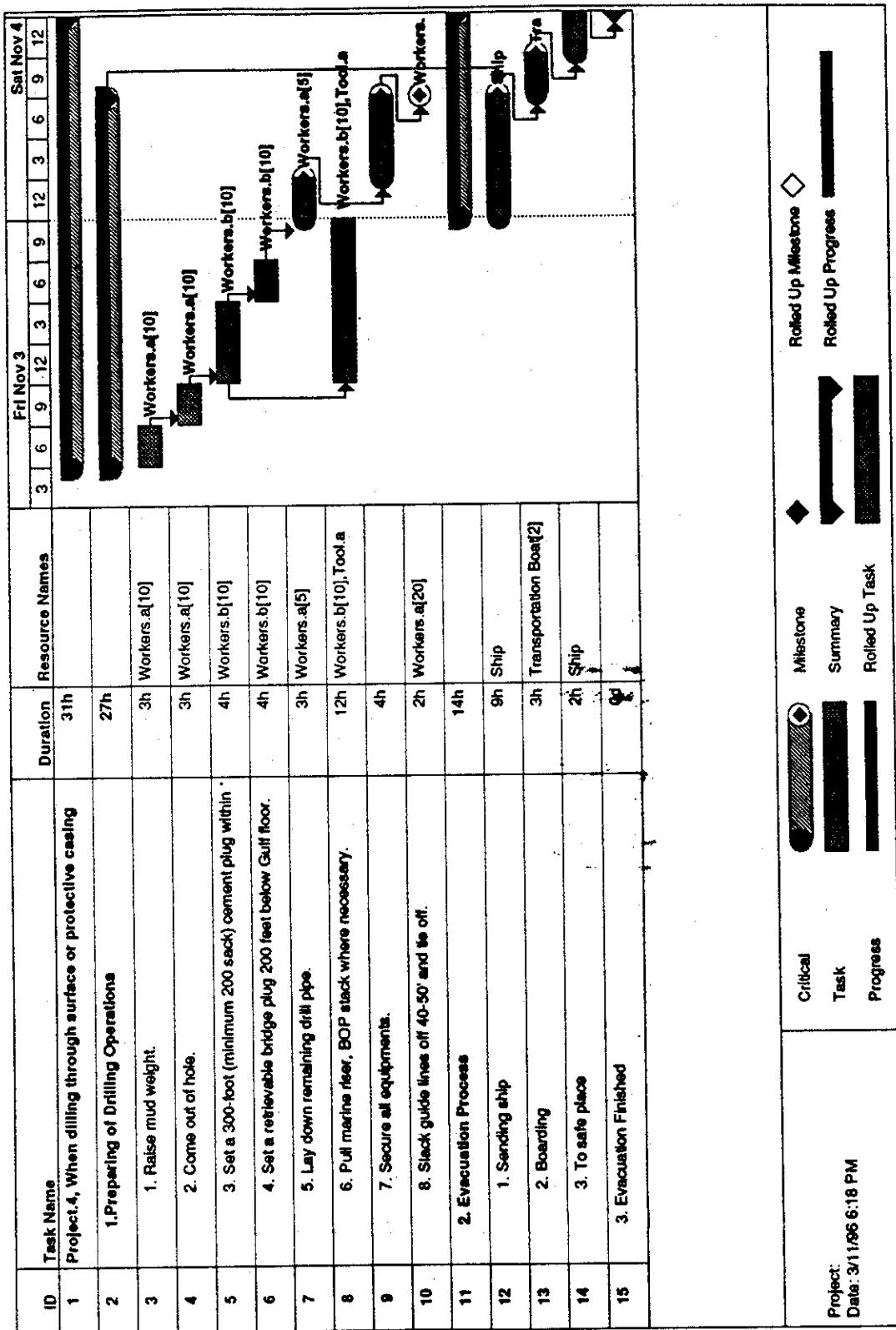


Figure 5.4 Modeling of Whole Evacuation Operations

c. Performing deterministic simulations at different evacuation start time;

From the deterministic results, it can be found that if the evacuation starts at six to twelve hours from the forecast beginning time, it took nearly 30 hours to safely finish the whole evacuation process. It took longer if the start time was getting late. It seems that the whole project won't be safely finished if the evacuation started after 18 hours from the forecast beginning time. (Figure 5.6)

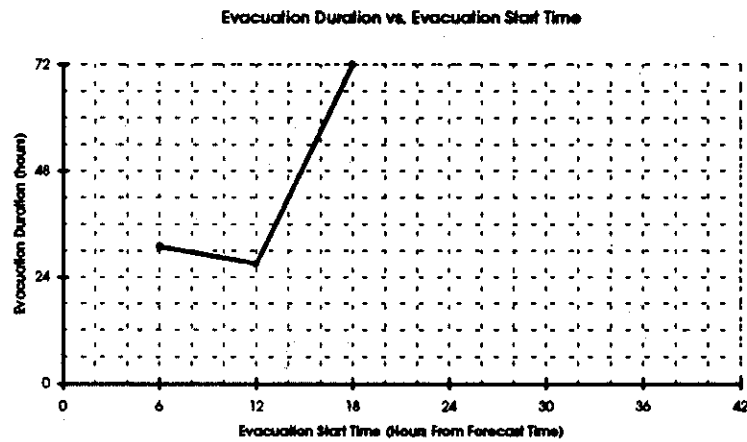


Figure 5.6 Simulation Result for One Transportation Boat

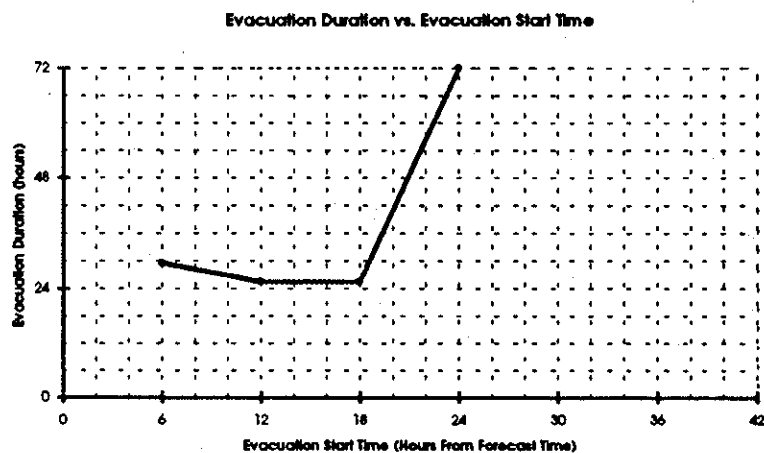


Figure 5.7 Simulation Result for Two Transportation Boat

Also, from the simulation, it is found that the critical point during the evacuation procedure is Task 13. (Boarding). Boarding is the transfer of people to the crew boat.

If the task duration can be reduced to half by either supplying crew boat or increasing the people transfer speed, the simulation result will be different (Figure 5.7). Now one can wait 6 hours more before one has to start the evacuation. This will give the platform operator more time to make decision, and most importantly, the hurricane may change direction or its strength may decrease rapidly during this period. In this case, an unnecessary evacuation may be avoided.

d. Performing Monte Carlo simulation at different evacuation start time;

The probability of evacuation failure vs. different start time is generated as in Figure 5.8.

The case that there are two crew boats is also simulated. The simulation result is presented in Figure 5.9.

It can be found from Figure 5.8 that the probability of failure is about 20% if the evacuation starts 6 to 12 hours from the forecast beginning time. The failure probability increases rapidly to almost 40% if the evacuation start time is 18 hours from the forecast beginning time. If the evacuation were to begin after 36 hours from forecast time, the failure probability would be about 60%. From Figure 5.9, the failure probability is not increased rapidly compared with that in Figure 5.8. This is mainly due to the duration of the On Board task is reduced to half as before, 1.5 hours, and since this is the critical point

of the whole evacuation, the failure probability at 18 hours is only 10%, much less than before. Also, at 36 hours, the failure probability is 50%, a little less than before.

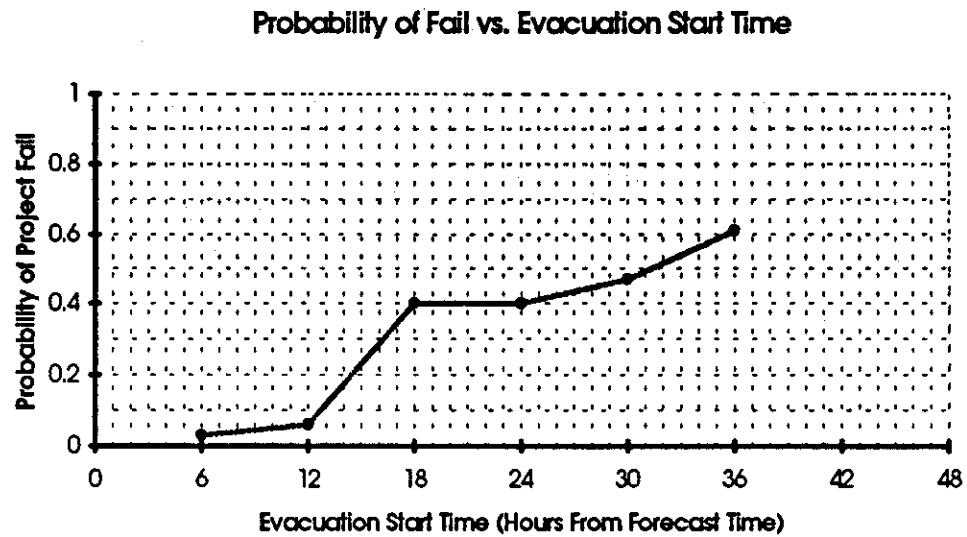


Figure 5.8 Probabilistic Simulation Result

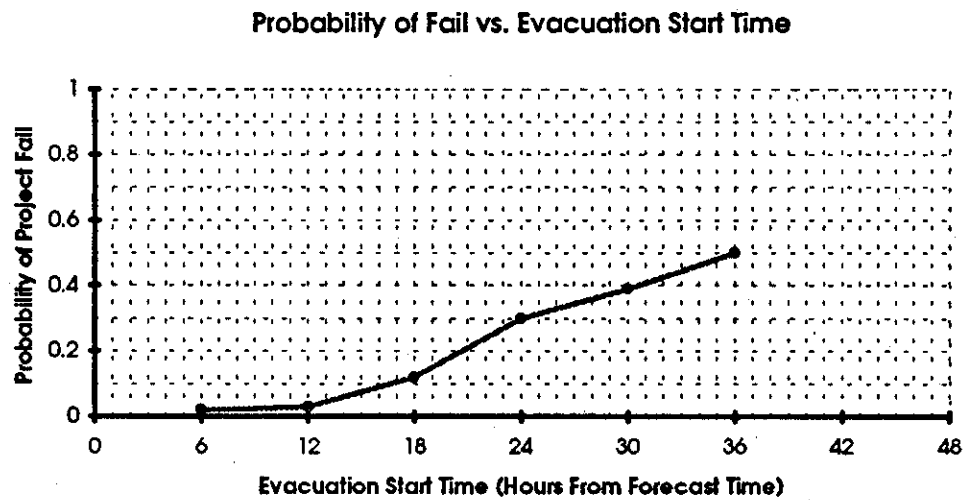


Figure 5.9 Probabilistic Simulation Result

Several different evacuation alternatives can be simulated based on the same environmental input and available resources, and the results can be compared. The safest and most cost effective method can be suggested. Dependent on how much risk the platform owner/operator can take, EVACSIM can be used to evaluate when and how to start the evacuation.

5.7 Possible Areas of Application

Due to the general and powerful nature of the simulation program, many areas of application in offshore weather-sensitive projects are envisaged. The application ranges from technical evaluation of vessel operability characteristics to project management and economic studies. The following is a list of some of the possible areas of application:

Vessel selection:

- Provide cost estimates for alternative construction scenarios.
- Compare activity shutdown sea-state sensitivities on project schedule and cost.
- Estimate probable weather downtime.
- Uncover incompatibility of activity duration from "Critical path" point of view.
- Demonstrate effect of weather forecast uncertainties.
- Help in making optimum construction scenarios and vessel selection.

Operations Risk Assessment:

- Provide risk assessment.

- Help formulate contingency plans.
- Establish optimum design criteria for equipment.
- Investigate effect of weather forecast uncertainties on decision-making requirements.
- Evaluate new concepts on basis of expected risk level.

Equipment logistics:

- Evaluate equipment replacement policy that is weather sensitive.
- Establish optimum level of service to drilling/production operations.
- Identify critical pieces of equipment from overall project point of view.

Project scheduling planning:

- Assess effect of individual operations decision.
- Provide a realistic "critical path."

Bid preparation/evaluation:

- Compare construction vessel spread alternatives.
- Evaluate various rate structures and lump-sum bids.

5.8 Summary

An computer simulation program EVACSIM was developed which is utilized to help evaluate operational and evacuation systems for MODUs in hurricane conditions.

The evacuation simulation model is based on: 1) available statistics and hindcast results for hurricane forecast in the Gulf of Mexico; 2) Real time 72 hour hurricane strength and track forecast; 3) Probability models to include the hurricane strength and track forecast errors; 4) Real hurricane evacuation operations and procedures performed on MODUs; 5) Available evacuation resources and different workable time periods of these resources based on the resources shut down environmental criteria.

The simulation can be performed in deterministic and probabilistic region. And an example application of the simulation model to a real evacuation procedure performed on Zane Barnes was presented as a verify case study. The results were reasonable.

Results from this model are intended to assist in developing decision criteria for MODU securing and evacuations. The simulation results is helpful to the following questions:

- Given the evacuation begin time, how long will it take to safe complete?
- At different evacuation start time, what is the failure probability of these evacuations?
- What is the best evacuation start time based on acceptable risk and cost?
- What is the best reliable and cost-effective evacuation procedure?

CHAPTER 6

CONCLUSIONS AND RECOMMENDATIONS

6.1 Summary

A simulation model has been developed to predict the movements of MODUs in the Gulf of Mexico during hurricanes. A Monte-Carlo simulation model (MODUSIM) has been developed to enable prediction of the probability of collision between MODUs and surrounding large facilities. The variability of hurricane parameters and their correlation, the storm spatial geometry, shallow water shoaling effects, and modeling and parameter estimation uncertainties are considered. To verify the model, the MODU Zane Barnes, Zapata Saratoga and Treasure 75, which all moved a significant distance during hurricane Andrew, were used. The simulation results closely matched the information on the performance of the semi-submersible MODUs during hurricane Andrew. Also, the probability of collision between a MODU and the surrounding structures has been determined.

From this study, it has been found that the best way to reduce collision probabilities is to design anchors to drag prior to any mooring line breaking. In this case, the MODU will not move far because of the large dynamic dragging force. However, if the rig is to be located near subsea structures that could be damaged by a dragging anchor, the operator may use pile anchors or oversized drag anchors to cause the mooring lines to break first.

Another effective way is to change the MODU's siting location. Using MODUSIM, the best place with the least collision probability can be determined. For example, if Zane Barnes were moored at (47,20) instead of (33,35) which is about 20 NM to the south-east, the probability of collision will be one half of before (Table 4.8).

It seems that within practical limits mooring strength is not important to the collision probability. It has been found that a hurricane with an intensity greater than about a one year hurricane return period can cause breakaways. To reduce the collision probability in half, one needs to increase the mooring capacity by almost three times.

The recommended procedure to choose a best place to site MODUs is as follows:

- 1) Determine the large target structures in the area which are of interest;
- 2) Determine the best MODU site and the acceptable radius of the sitting area;
- 3) Using the MODUSIM function "Strategy", determine the best place to site the MODU within the acceptable area;
- 4) Change the mooring line failure mode (Free floating or Dragging) and mooring capacity with the MODU located at the best place to get the acceptable collision risk level.

Another simulation model (EVACSIM) has been developed to examine evacuation procedures and decisions. Monte-Carlo techniques has been utilized to predict the probability of evacuation failure. The uncertainties in hurricane forecast, the different

evacuation start time, the different available resources and associated environmental or operational shut-down criteria were considered. A real hurricane evacuation procedure performed on Zane Barnes was used to verify the simulation model. The simulation results were reasonable and easy to understand.

EVACSIM simulation results can be used to compare the relative threat to different evacuation start time, to give platform operators confidence to choose appropriate evacuation start times, and to avoid un-necessary evacuations. These results should be helpful in developing decision plans and criteria for MODU securing and evacuations.

6.2 Recommended Future Work

Potential research topics for further studies have been identified during the present research. These are listed and briefly discussed in the following:

- **Perform Further Verification Studies on MODUSIM**

The verification studies performed during this research include 4 Gulf of Mexico MODUs. Although the results are extremely encouraging, additional studies on MODUs with different configurations would help increase the confidence in the MODUSIM.

- **Further Refine Jack-up and Foundation Modeling**

At present stage, MODUSIM includes a very simple procedure to model jack-up MODUs and their foundations. The next step in refining the procedure would be to include more detailed analyze of structure failure mechanics and foundation capacity.

- **Develop a Professional Version of MODUSIM**

Based on a simultaneous development and verification/calibration approach, the present version of MODUSIM has been developed during the second year of this research. The program runs in EXCEL4.0. It has the potential to be further developed and include additional features that enhance the speed and user-friendliness of the program. The most efficient way to do so would be to rewrite MODUSIM in Visual Basic 4.0.

- **Perform Further Verification Studies on EVACSIM**

The evacuation verification studies performed include only one evacuation procedure for the MODU Zane Barnes. More verification studies need to be performed to include the effects of different evacuation procedures. More parametric and sensitivity studies are needed.

- **Further Refine the Uncertainties in EVACSIM**

The simulation program EVACSIM currently only considers the major uncertainties in the evacuation process, and the uncertainties associated with hurricane forecast. Additional work is need to consider the uncertainties involved in the evacuation operations, e.g.,

equipment availability and reliability, operational risk, human error factors and other unpredictable factors which influence the duration of sub-tasks and the reliability of the evacuation. The estimate may be assigned a probability density function, determined by various distributions to account for the random variations. Probabilistic simulation results from the refined model should be more informative and be more helpful in developing MODU securing and evacuation plans.

• Develop Parametric Early Warning System Model for MODUs in Gulf of Mexico Hurricane Conditions with the Information from MODUSIM and EVACSIM

The reliability of warning systems are dependent upon the ability to forecast danger and to effectively respond to it. Future work needs to be done to develop an early warning systems for MODU securing and evacuation in GOM hurricanes. The MODUSIM and EVACSIM can be integrated together to be a part of an early warning system.

REFERENCE

Alfredo H-S. Ang and Wilson H. Tang, "Probability Concepts in Engineering Planning and Design, Volume II--Decision, Risk, and Reliability."

Allan, R.J.: "Integrated Motion, Stability and Variable Load Design of the Trendsetter Class Semisubmersible 'Zane Barnes'". Offshore Technology Conference, Texas, May 2-5 1988. OTC 5625.

American Petroleum Institute, 1991. "Recommended Practice for Design, Analysis, and Maintenance of Mooring for Floating Production Systems. API Recommended Practice 2FP1 (RP 2FP1). First Edition. Washington, D.C..

American Petroleum Institute, 1993. "Recommended Practice for Planning, Designing and Constructing Fixed Offshore Platforms - Load and Resistance Factor Design (RP 2A-LRFD)." First Edition, July, Washington, D.C.

American Petroleum Institute (1994). Recommended Practice for Design and Analysis of Stationkeeping System for Floating Structures. Washington, D.C..

Atkinson, A. C.: The Computer Generation of Poisson Random Variables, Appl. Statist., 28: 29-35 (1979).

Baker, M.J.: "Structural Reliability Theory and Its Applications". Springer-Verlag, Berlin, Heidelberg, New York, 1982.

Bea, R.G. 1973. "Wave Forces, Comparison of Stokes Fifth and Stream Function Theories." Engineering Note No. 40, Environmental Mechanics, April.

Bea, R.G.: "Gulf of Mexico Hurricane Wave Heights". Journal of Petroleum Technology. September 1975. 1160-1171.

Bea, R.G., Lai, N.W., 1978. "Hydrodynamic Loadings on Offshore Structures." Proceedings, Offshore Technology Conference, OTC No. 3064. Houston, TX.

Bea, R.G.: "Gulf of Mexico Shallow-Water Wave Heights and Forces". Offshore Technology Conference, Texas, May 2-5, 1983. OTC4586.

Bea, R.G., Pawsey, S.F., Litton, R.W., 1986. "Measured and Predicted Wave Forces on Offshore Platforms." Proceedings, Offshore Technology Conference, OTC No. 5787. Houston, TX.

Bea, R.G.: "Review of Tropical Cyclone Parameters for Goodwyn A Platform Environmental Criteria" Report to Woodside Offshore Petroleum Ltd. Perth, Western Australia. February 1989.

Bea, R.G.: "Wind & Wave Forces on Marine Structures". CE/NA 205B Class Notes. Department of Civil Engineering and Department of Naval Architecture & Offshore Engineering, University of California, Berkeley.

Bea, R.G.: "Reliability Based Design Criteria for Coastal and Ocean Structures". Australia, 1990.

Bea, R.G., Young, C., 1993. "Loading and Capacity Effects on Platform Performance in Extreme Condition Storm Waves & Earthquakes." Proceedings, Offshore Technology Conference, OTC No. 7140. Houston, TX.

Bea, R.G. and Mortazavi, M., 1995. "Screening Methodologies for Use in Platform Assessments and Requalifications." Final Report, Department of Civil Engineering, University of California at Berkeley.

Bobba, A.G.; Singh, V.P.; Bengtsson, L., "Application of uncertainty analysis to groundwater pollution modeling". Environmental Geology, v 26 p 89-96, September 95.

Bratley, P., B. L. Fox, and L. E. Schrage: A Guide to Simulation, 2d ed., Spring-Verlag, New York (1987).

Burganos, V. N.; Paraskeva, C. A.; Payatakes, A.C., "Monte Carlo network simulation of horizontal, upflow and downflow depth filtration". AIChE Journal, v 41 p 272-85, February 95.

Burke, B.D., "Downtime Evaluation for Operations from Floating Vessel in Waves", SNAME Spring Meeting/STAR Symposium, San Francisco, Calif., May 1977.

Carr, Lester E.; Elsberry, Russell L., "Systematic and integrated approach to tropical cyclone track forecasting part 1., approach overview and description of meteorological basis". Naval Postgraduate School, Monterey, California.

Chen, Henry; Rawstron, Phil. "Systems Approach to Offshore Construction Project Planning and Scheduling". Marine Technology, v 20, No. 4, Oct. 1983, pp. 332-347.

Chylek, Petr; Dobbie, J. Steven. "Radiative properties of finite inhomogeneous cirrus clouds: Monte Carlo simulations". Journal of the Atmospheric Science. v 52 p 3512-22, October 15, 1995.

Cochran, W.G., "Sampling Techniques", Third Edition, John Wiley, 1977.

Cooper, C. K., Parametric Models of Hurricane-Generated Winds, Waves, and Currents in Deep Water. Conoco Inc.

Dean, R.G., 1977. "Hybrid Method of Computing Wave Loading." Proceedings, Offshore Technology Conference, OTC 3029, Houston TX, May.

Det Norske Veritas, 1993. "WAJAC. Wave and Current Loads on Fixed Rigid Frame Structures." DNV SESAM AS. Version 5.4-02.

Draft Recommended Practice for Design, Analysis, and Maintenance of Mooring for Floating Production Systems. API Recommended Practice 2FP1 (RP 2FP1). First Edition, May 1, 1991.

Elsberry, Russell L.; Frank, William M.; Holland, Greg J.; Jarrell, Jerry D.; Southern, Robert L., "A Global View of Tropical Cyclones". Based largely on materials prepared for the International Workshop on Tropical Cyclones, Bangkok, Thailand, November 25 to December 5, 1985.

Evans, K. Franklin. "Two-dimensional radiative transfer in cloudy atmospheres: the spherical harmonic spatial grid method". Journal of the Atmospheric Sciences, v 50 p 3111-24, September 15, 1993.

Fenton, J.D., 1985. "A Fifth Order Stokes Theory for Steady Waves, "ASCE Journal of Waterway, Port, Coastal and Ocean Engineering, Vol. 111, No. 2, pp.216-234.

Fishman, G. S.: Estimating Sample Size in Computer Simulation Experiments, Management Sci., 18: 21-38 (1971).

Glynn, P. W.: Stochastic Approximation for Monte Carlo Optimization, Proc. 1986 Winter Simulation Conference, Washington, D. C., pp. 356-365 (1986).

Grosenbaugh, L. R.: More on Fortran Random Number Generators, Commun. Assoc. Comput. Math., 12: 639 (1969).

Hahn, G. J., and S. S. Shapiro: Statistical Models in Engineering, John Wiley, New York (1967).

Hammersley, J. M., and D. C. Handscomb: Monte Carlo Methods, Methuen, London (1964).

Haring, R.E., and Heideman, J.C. (1980). "Gulf of Mexico Rare Return Periods", Journal of Petroleum Technology, Society of Petroleum Engineers, Dallas, TX.

Heidelberger, P.: Variance Reduction Techniques for the Simulation of Markov Processes, I: Multiple Estimates, IBM J. res. Develop., 24:570-581 (1980).

Heideman, J.C., Weaver, T.O., 1992. "Static Wave Force Procedure for Platform Design." Proceedings of Civil Engineering in the Oceans V, College Station, Texas, American Society of Civil Engineers, New York.

Hindcast Study of Hurricane Andrew (1992), Offshore Gulf of Mexico. Oceanweather Inc. Cos Cob, ct. November 1992.

Hoffman, D. and Fitzgerald, V., "System Approach to Offshore Crane Ship Operations", Trans. SNAME, Vol 86, 1978.

Hu, Sau-Lon Janes; Gupta, Manish; Zhao, Dongshen. "Effects of wave intermittency/nonlinearity on forces and responses". Journal of Engineering Mechanics. v 121 p 819-27, July 95.

Law, Averill M.; Keiton, W.David, "Simulation Modeling and Analysis". Second edition, McGraw-Hill Series in Industrial Engineering and Management Science.

L'Ecuyer, P.: Random Numbers for Simulation, Commun. Assoc. Comput. Mach., 33: (1990).

McCarron, J.K., "Computer Simulation as a Tool for Evaluating Offshore Construction Alternatives". OTC Paper 1353, Offshore Technology Conference, Houston, Tex., 1971.

McDonald, D.T., Bando, K., Bea, R.G., Sobey, R.J., 1990. "Near Surface Wave Forces on Horizontal Members and Decks of Offshore Platforms." Final Report, Coastal and Hydraulic Engineering, Dept. of Civil Engineering, University of California at Berkeley, Dec.

McDonald, David T., "Reliability Evaluation of a Jack-up Drilling Unit in the North Sea and in the Gulf of Mexico." MS Thesis, Department of Civil Engineering, University of California, Berkeley.

Mehrdad Mortazavi, "A Probabilistic Screening Methodology for Use in Assessment and Requalification of Steel, Template-Type Offshore Platforms". Ph.D Dissertation, Department of Civil Engineering, University of California at Berkeley.

Moore, W.H., 1993. "Management of Human and Organizational Error in Operations of marine Systems." Ph.D Dissertation, Graduate Division, Univ. of Cal. at Berkeley.

Morison, J.R., O'Brien, M.P., Johnson, J.W., Schaff, S.A., 1950. "The Force Exerted by Surface Waves on Piles." Petrol. Trans. AIME, Vol. 189, pp 149-154.

Naghavi, Babak; Yu, Fang Xin. "Regional frequency analysis of extreme precipitation in Louisiana". Journal of Hydraulic Engineering, v 121, p 819-27, November 95.

Noble Denton, 1991. "Climate of Environmental Extremes Tropical Storm Areas", Final Report. Report No., L14839/NDWS/HDL

Oceanweather Inc. (1992). Hindcast Study of Hurricane Andrew - Offshore Gulf of Mexico. Cos Cob, CT.

Oppenlander, Joseph C.; Oppenlander, Jane E., "Storage lengths for left-turn lanes with separate phase control". ITE Journal, v 64 p 22-6, January 94.

Petrauskas, C., Botelho, D.L.R., Krieger, W.F., and Griffin, J.J., 1994. "A Reliability Model for Offshore Platforms and its Application to ST 151 H and K Platforms During Hurricane Andrew (1992)." Proceedings of the Behavior of Offshore Structure Systems, Boss '94, Massachusetts Institute of Technology.

Petrauskas, C., Heideman, J.C., Berek, E.P., 1993. "Extreme Wave-Force Calculation Procedure for the 20th Edition of API RP-2A." Proceedings, Offshore Technology Conference, OTC 7153, Houston, Texas, May.

Petrauskas, C., Heideman, J.C., and Berek, E.P., 1993. "Extreme Wave Force Calculation Procedure for 20th Edition of API RP 2A." Proceedings, Offshore Technology Conference, OTC 7153, Houston, TX.

Praught, M and Devlin, P., "Evaluating Offshore Construction Activities Using a Project Simulation Program". SNAME, Northern California, Section, Nov. 1982.

Preston, D., 1994, "An Assessment of the Environmental Loads on the Ocean Motion International Platform," MS Thesis, Department of Naval Architecture and Offshore Engineering, University of California, Berkeley, USA.

Pritsker, A. Alan B. and Claude Dennis Pegden, "Introduction to Simulation and SLAM."

Rault, Didier F. G.; Woronowicz, Michael S., "Application of direct simulation Monte Carlo to satellite contamination studies". Journal of Spacecraft and Rockets, v 32 p 392-7 May/June 95.

R & B, Gulf of Mexico Hurricane Evacuation Procedures, Zane Barnes, 1988.

Rhee, Seung-Whee; Reible, Danny D.; Constant, W. David. "Stochastic modeling of flow and transport in deep-well injection disposal systems". Journal of Hazardous Materials, v 34 p 313033, August 93.

Ripley, B. D.: Stochastic Simulation, John Wiley, New York (1987).

Rubinstein, R. Y.: Simulation and the Monte Carlo Method, John Wiley, New York (1981).

Sargent, R. G.: A Tutorial on Validation and Verification of Simulation Models, Proc. 1988 Winter Simulation Conference, San Diego, Calif., pp. 33-39 (1988).

Sarpkaya, T, Isaacson, M., 1981. "Mechanics of Wave Forces on Offshore Structures" Van Nostrand Reinhold Company.

Schruben, L. W.: Establishing the Credibility of Simulations, Simulation, 34: 101-105 (1980).

Shannon, R. E.: Systems Simulation: The Art and Science, Prentice-Hall, Englewood Cliffs, N.J. (1975).

Shore Protection Manual, Coastal Engineering Research Center, Department of The Army. Volume I & II.

Skjelbreia L., Hendrickson J., "Fifth Order Gravity Wave Theory." Proceedings 7th Conference of Coastal Engineering, pp. 184-196. Honolulu HI: 1961.

Stephen Slomski and Vitoon Vivatrat, "Risk Analysis for Artic Offshore Operations". Marine Technology, v 23, No. 2, April 1986, pp.123-130.

Technica Consulting Scientists & Engineers. "Risk Assessment of Emergency Evacuation from Offshore Installations".

Thoft-Christensen, P., Baker, J., 1982. "Structural Reliability Theory and Its Applications." Springer-Verlag.

Trident Consultants Ltd., 1992, "Quantitative Risk Assessment of a Typhoon Contingency Plan for Offshore Operations in the Gulf of Thailand".

U.S. Minerals Management Services, Hurricane track database, 1993.

Wagner, H. M.: Principles of Operations Research, Prentice-Hall, Englewood Cliffs, N.J. (1969).

Ward, E.G., Borgman, L.E., and Cardone, V.J. (1979). "Statistics of Hurricane Waves in the Gulf of Mexico", Journal of Petroleum Technology, Society of Petroleum Engineers, Dallas, TX.

Webster, W.C. and Thorsen Th.L., 1992. "Studies of the UNOCAL's Floating Vessels in the Gulf of Thailand".

Welch, P. D.: The Statistical Analysis of Simulation Results, in The Computer Performance Modeling Handbook, S. S. Lavenberg, ed., pp. 268-328, Academic Press, New York (1983).

Wen, Y.K.: "Environmental Event Combination Criteria, Phase I, Risk Analysis". Research report for the Project PRAC-87-20 entitled "Environmental Event Combination Criteria". July 1988. Department of Civil engineering, University of Illinois at Urbana-Champaign.

Wen, Y.K.: "Environmental Event Combination Criteria, Phase II, Design Calibration and Directionality Effect". Research report for the Project PRAC-88-20 entitled "Environmental Event Combination Criteria". February 1990. Department of Civil engineering, University of Illinois at Urbana-Champaign.

Williams, M.D.; Brown, M.J.; Cruz, X., "Development and testing of meteorology and air dispersion models for Mexico City". Atmospheric Environment (Oxford, England), v 29 no21, p 2929-60, November 95.

Woodward-Clyde Consultants (1982). Shallow Water Wave Force Criteria Study, Gulf of Mexico, Prepared for McMoran Offshore Exploration Co., P.O. Box 6800, Metairie, Louisiana 70009.

Ying, J. and Bea, R.G., "Development and Verification of a Computer Simulation Model for Evaluation of Siting strategies for Mobile Drilling Units in Hurricanes." MS Thesis 1994, Department of Naval Architecture and Offshore Engineering, University of California, Berkeley, USA.

Ying, J. and Bea, R.G., "Development and Verification of a Computer Simulation Model for Evaluation of Siting strategies for Mobile Drilling Units in Hurricanes." Phase II Report 1995, Department of Naval Architecture and Offshore Engineering, University of California, Berkeley, USA.

Ying, J. And Bea, R.G., "Simulation Model for Development of Siting Strategies for Mobile Offshore Drilling Units", Proceedings of the 6th International Offshore and Polar Engineering Conference, Los Angeles, California, USA, 1996.

Appendix A MODUSIM
MODU Movement Simulation Program
User Manual

MODUSIM

MODU Movement Simulation Program

Copyright 1996

This software is provided "as is" by the Marine Technology and Management Group (MTMG) at University of California at Berkeley to sponsors of the research project *Securing Procedures for Mobile Drilling Units in the Gulf of Mexico Subject to Hurricanes*. Any express or implied warranties of merchantability and fitness for a particular purpose are disclaimed. In no event shall the MTMG be liable for any direct, indirect, incidental, special, exemplary, or consequential damages (including, but not limited to, procurement of substitute goods or services; loss of use, data, or profits; or business interruption) however caused on any theory of liability, whether in contract, strict liability, or tort (including negligence or otherwise) arising in any way out of this software, even if advised of possibility of such damage.

A1. Introduction

A1.1 Introduction

MODUSIM is a computer simulation program developed for simulating the MODU's movement in hurricanes. It is based on simplified load, capacity and movement calculation procedures developed for the joint industry - Government sponsored research project called "*Securing Procedures for Mobile Drilling Units in the Gulf of Mexico Subject to Hurricanes*".

This research has been performed at the University of California at Berkeley, Department of Naval Architecture and Offshore Engineering by Research Assistant Jun Ying under supervision of Professor Robert Bea. The theoretical background of MODUSIM is documented in previous chapters of this report.

A1.2 Application Range of MODUSIM

MODUSIM can be applied to typical semi-submersible drilling units with generic geometry's and some special types of Jack-up platforms. The loading and mooring capacity has been calibrated to platforms located in 0 - 300 ft water depth. At this stage, MODUSIM is expected to give some reasonable results. For information on other limitations of the program, please refer to next sections of this appendix.

A1.3 Program Structure

The program is developed using Microsoft Excel Software. The following Excel files are bounded together under the workbook named MODU.xlw:

- Welcom1.xls
- MODUSIM.xlm
- modu.xls
- Stokev.xls
- Dbase.xls
- Coll.xlm
- Result.xls
- Route.xlc
- Histogram.xlc

A1.4 Installation

A1.4.1 Backup Disk

Before any installation begins, it is always a good practice to backup the program diskette in the back of the report. We assume you are already familiar with DOS commands or Windows operation. For example, in DOS you will need the DISKCOPY command to make backup copies of your program disk.

A1.4.2 System Requirements

To run MODUSIM 2.0, you must have a 486 or higher based PC with 8MB RAM at least, MS DOS 5.0, Windows 3.0, EXCEL 4.0 and @RISK 3.0.

A1.4.3 Installation

To install MODUSIM 2.0, first copy all the files in the attached disk to your hard drive under the directory "c:\MODUSIM". Then you can open the file 'MODU.XLW' directly from EXCEL4.0 & @Risk3.0. Or you can specify the program group name, item name, and the path of MODUSIM to windows. Type WIN to execute Windows, select New from File menu in program Manager to add the program group. The following window will appear, select Program Group and then OK.

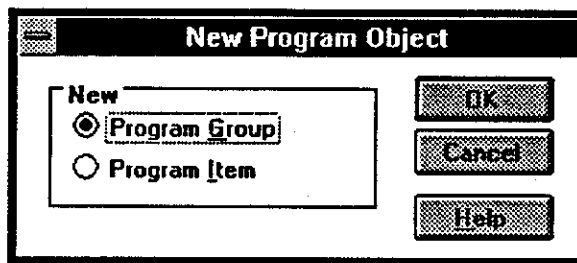


Figure A1.1: Select 'Program Group' for the MODUSIM program.

Next the following window will appear. Fill in the Description and Group File as indicated. Then select OK.

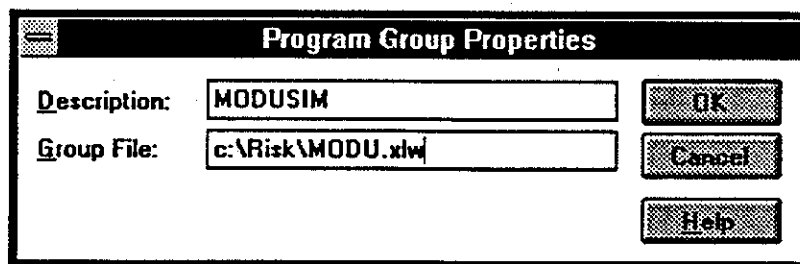


Figure A1.2: Specify the group name and the filename and path.

Notice that a new program group MODUSIM has been created in your Microsoft Windows. Now you can double click the icon to start MODUSIM.

A2. Input Data

A2.1 Introduction

After double clicking the MODUSIM icon, the main window will pop up like the following Figure 2.1. The menu bar can be changed to general Excel 4.0 menu bar by "Ctrl+M" and back to MODUSIM by "Ctrl+A". Those users who are not familiar with windows operation are recommended to following the step-by-step directions in this chapter. Here, for example, let's say we have a MODU named "Zane Barnes".

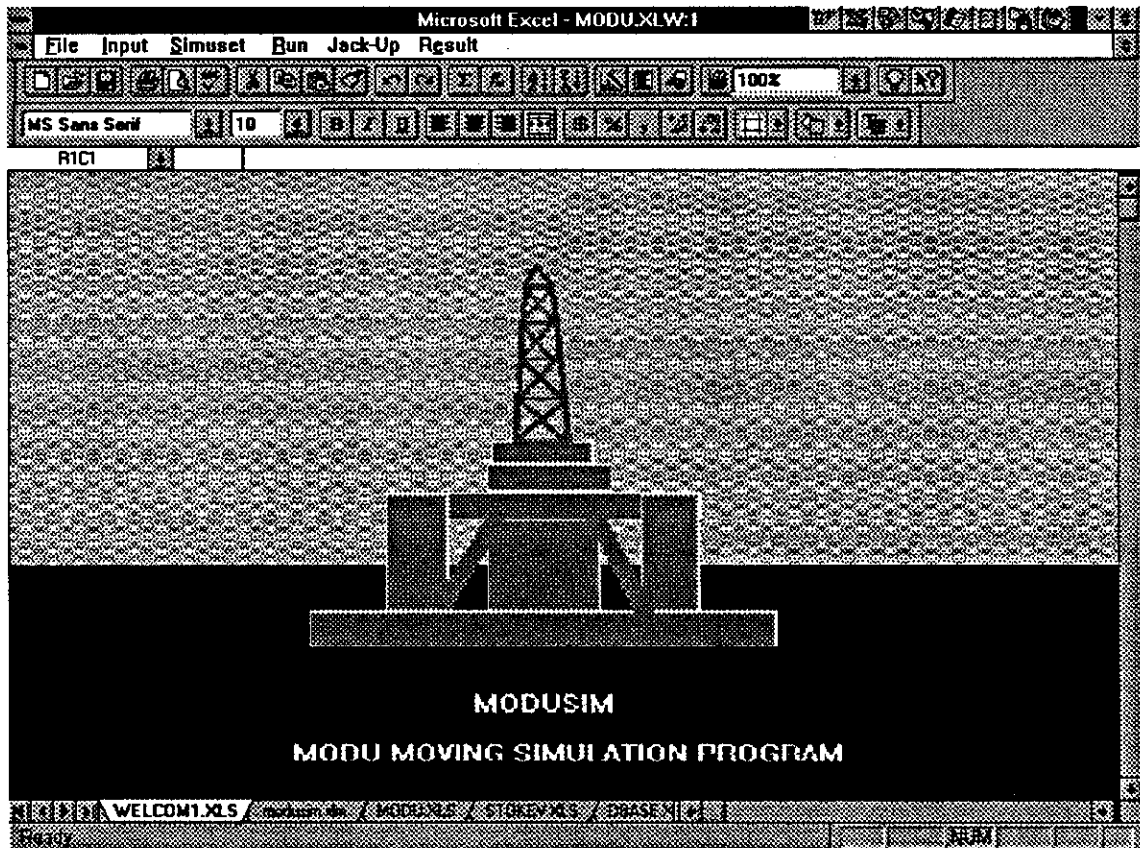


Figure A2.1 MODUSIM is popped up.

There are principally two ways of data input in the program:

- a) by stepping through the input menu and defining the necessary parameters or
- b) by opening an input file that has been originally created by stepping through the input menu and subsequently saved.

There are three commands under the **File** menu. **Open Input File** command allows to open the saved simulation input and result file. **Save Input As** command allows to save the current simulation setting and simulation result.

SIMULATION RESULT

MODU NAME:		ZANE BARNES			
LOCATION:		MOORING CAPACITY		FAILURE MODE	
X	Y	MEAN	STD.	NOM	NOB
50	28.1	3500	1000	8	6
Probability of collision:			0.0114		
Target 1	Target 2	Target 3	Target 4	Target 5	Mooring
0.0048	0.0006	0.0048	0.0006	0	0.09

Figure A2.2 Saved Simulation Result

Click **Exit** to quit the application.

Warning: All the current simulation setting and results will be lost if you leave the program. Save the simulation setting and results if necessary.

The data that needs to be defined by the user is subdivided into five principle categories:

- General MODU Information
- Mooring System Information
- Simulation Setting Data
- Execute the Program
- General Jackup Information

A2.2 General MODU Information

There are five commands under **Input** Menu to input the required information.

MODUINF command allows to input the MODU's general information. The dialogue box

'MODU INFORMATION' will pop up when **MODUINF** command is selected.

MODU INFORMATION

? MODU NAME: ZANE BARNES OK Cancel

MODU PARAMETERS

DISPLACEMENT (LT):	50715
DRAFT (FT):	60
DIAMETER OF CORNER CAISSON (FT):	45
DIAMETER OF CENTRE CAISSON (FT):	72
LENGTH OF PONTODN (FT):	370
HEIGHT OF PONTODN (FT):	40
WIDTH OF PONTODN (FT):	20
EQUIVALENT WIND AREA (FT ²):	25000

Figure A2.3 Input MODU General Information

To input the information, you can click on the certain box with mouse or type 'ALT' + 'Underline letter'. For example, to input **DISPLACEMENT**, type ALT+D When you finished, click **OK**, or you can click **Cancel** to cancel the dialogue.

MODULOC command allows to input coordinates of MODU's initial location. When **MODULOC** command is selected, the dialogue box 'MODU LOCATION' will pop up.

MODU LOCATION	
INPUT TYPE	
<input checked="" type="radio"/> KEYBOARD	<input type="radio"/> CHART
<input type="button" value="OK"/> <input type="button" value="Cancel"/>	
KEYBOARD	
X COORDINATE (NM):	40
Y COORDINATE (NM):	28
WATER DEPTH (FT):	170
DIST TO LAND (NM):	52
CHART	
X COORDINATE (NM):	50
Y COORDINATE (NM):	28.1
WATER DEPTH (FT):	169.291666
DIST TO LAND (NM):	52

Figure A2.4 Input MODU Initial Location

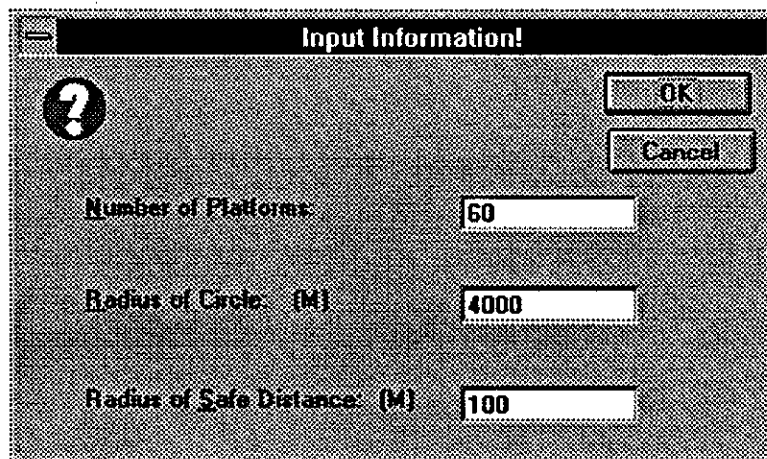
In the group of **Input Type**, if **Keyboard** is selected, the information will be input from keyboard to the box in the group of **keyboard**. The input information includes X, Y coordinates, water depth of MODU location and the distance from X-axis to coast. If **Chart** is selected, next command **LOCHART** need to be selected to input information

from chart. It is recommended that **Keyboard** function is used to input the initial location and **Chart** function is used to change the location of MODU.

If **Chart** was selected in the **MODULOC** command, **LOCHART** command need to be selected, and the chart 'MODU Moving Route' will pop up. To change the location of the MODU, click on the MODU while hold down **CTRL**, then drag MODU to wherever you want it to be sited.

LARGE FACILITY INFO command allows to set up the simulation for probability of collision within target circles. 'LARGE FACILITY INFORMATION' dialogue box will pop up when it is selected.

- **Number of Platforms:** Structure number within the target circle.
- **Radius of Circle:** Radius of target circle
- **Radius of safe Distance:** The safety distance between the MODU and structures.



Input Information!	
Number of Platforms:	60
Radius of Circle: (M)	4000
Radius of Safe Distance: (M)	100

Figure A2.5 Input Target Circle Information

Note here, the location of target circles is determined by the user from file [MODU.xlw]modu.xls. You can choose as many as 5 target circles.

CALCU PROB command allows to begin the simulation of collision within the target circle. When the simulation is completed, a dialogue box will pop up the calculation result. A pre-calculated curve about the probability of collision within the target circle with $R=0.6$ to 4.8 NM is presented in Figure 4.3. For a target circle with given radius and number of structures, the probability of collision can be found from the curve.

A2.3 Mooring Capacity Information

Mooring Command under **Input** menu allows to input mooring system information. The dialogue box 'Mooring System' will pop up when **Mooring** command is selected.

The image shows a software dialog box titled "MOORING SYSTEM". In the top left corner, there is a question mark icon. In the top right corner, there are "OK" and "Cancel" buttons. The dialog is divided into two main sections. The first section is titled "MOORING CAPACITY" and contains two input fields: "MEAN VALUE (KIPS)" with the value "3500" and "STANDARD DEVIATION" with the value "1000". The second section is titled "FAILURE MODE" and contains three input fields: "NUMBER OF MOORING LINES" with the value "8", "NUMBER OF BREAKING LINES" with the value "8", and "DYNAMIC DRAGGING COEFF. :" with the value "0.5".

Figure A2.6 Input Mooring System Information

In the group of **MOORING CAPACITY**, input the mean value and standard deviation of mooring strength; in the group of **FAILURE MODE**, input the total number of mooring lines, number of broken lines while failure and the dynamic dragging coefficient of anchor while they are dragging in the bottom of the sea.

A2.3 Simulation Setting Data

There are five commands under the **Simuset** menu to define the required data:

SIMUTYPE command allows to set up the simulation. The dialogue box 'SIMULATION TYPE' will pop up when **SIMUTYPE** is selected.

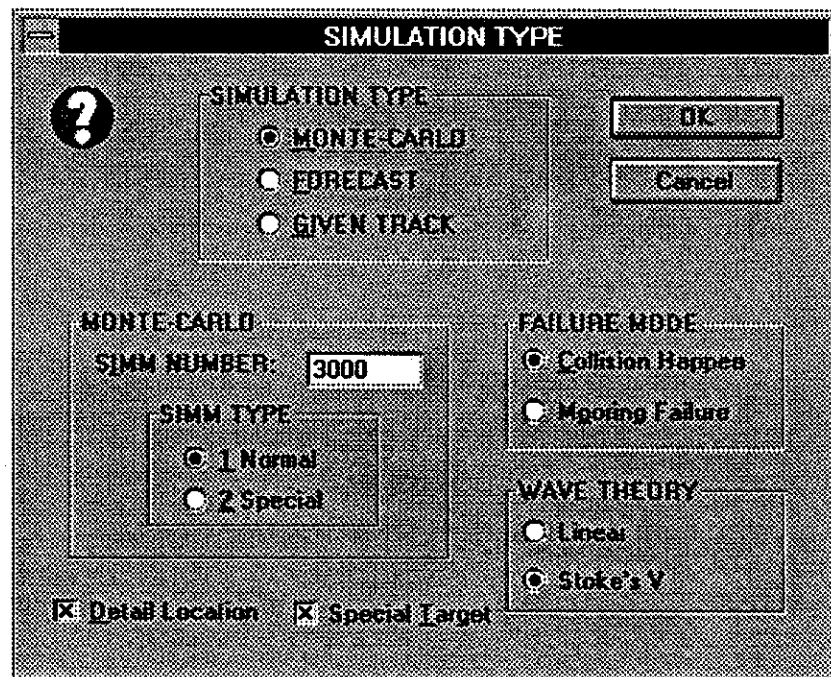


Figure A2.7 Set Up the Simulation

Following are the selected combinations to get the specific MODUSIM functions mentioned in Chapter 4.

Function A:	Monte-Carlo+Normal;
Function B:	Forecast+Normal;
Function C:	Given Track;
Function D:	Monte-Carlo+Normal.

Click **Collision Happen** to define failure mode as collision happens. Click **Mooring Failure** to define failure mode as mooring lines break. Select wave theory as **Linear** or **Stoke's 5th** theory. Check **Detail Location** to include the MODU information within target circles. Check **Special Target** to calculate the probability of collision within a given target.

HURRICANE PARAMETER

? **TRACK TYPE**
☐ STRAIGHT LINE ☒ CURVE

SPECIAL HURRICANE PARAMETER

TRACKS CROSSING CONTOUR	(NM)	30
TRACK DIRECTION	(DEGREE)	140
PRESSURE DIFFERENCE	(MB)	81
RADIUS OF MAXIMUM WIND SPEED	(NM)	10
STORM FORWARD SPEED	(KTS)	11
STORM STARTING DISTANCE	(NM)	400

FORECAST TIME TYPE
☐ 12 Hour
☐ 24 Hour
☐ 36 Hour
☐ 48 Hour
☒ 72 Hour

OK
Cancel

Figure A2.8 Input Hurricane Parameters

If **Forecast** is selected, the given hurricane parameters should be input in the following 'Hurricane Parameter' dialogue box. Check **Straight Line** or **Curve** to determine the type of hurricane tracks in the simulation. Select forecast time type for Function B.

If **Forecast** is selected, the following 'Env. Data Simulation Setting' dialogue box will pop up after the 'Hurricane Parameter' dialogue box. Select **Env.Forecast** to perform environmental condition forecast.

The image shows a software dialog box titled "Env. Data Simulation Setting". On the left is a circular icon with a question mark. To its right is a section labeled "Env. Setting" containing two radio buttons: "No Env. Forecast" (which is selected) and "Env. Forecast". Further right are "OK" and "Cancel" buttons. Below this is a section labeled "Critical Env. Data" containing four input fields: "Max. Wind Speed (knot):" with the value "50", "Current Velocity (knot):" with the value "2", "Wave Height (ft):" with the value "40", and "Acceptable Risk %:" with the value "10".

Figure A2.9 Environmental Simulation Settings

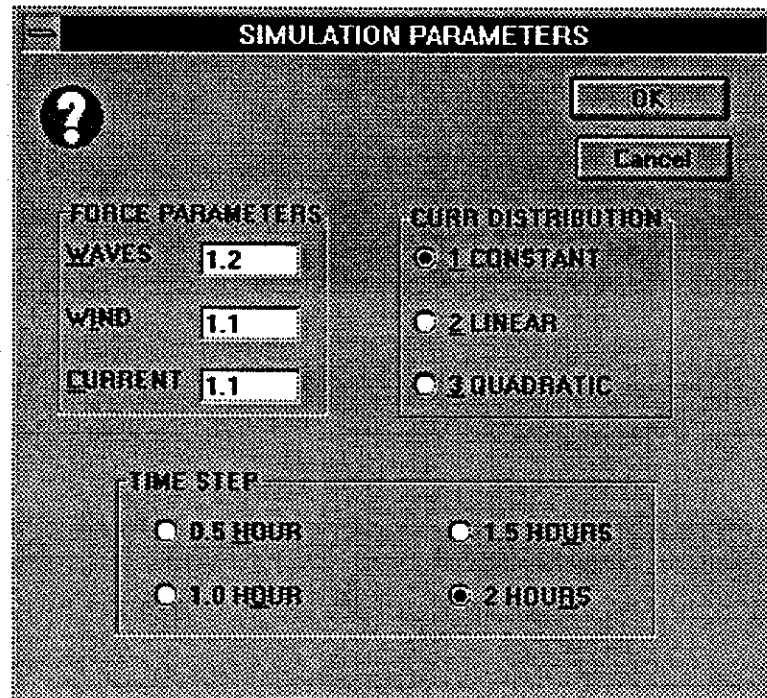
If **Given Track** is selected, the 'Given Hurricane Track' dialogue box will pop up after the 'Simulation Type' dialogue box. Input the general hurricane information in the group of **Hurricane Parameter**. There are at most eight points that can be input to describe the hurricane track. DT is the time step between the adjacent points.

	XH	YH	DT		XH	YH	DT
1	183	-93	3	2	138	-62	3
3	93	-48	3	4	60	-13	3
5	35	-8	3	6	3	16	3
7	-21	31	3	8	-36	53	3
9				10			

Figure A2.10 Given Hurricane Track Information

SIMUPARA command allows to input calculation coefficients. The dialogue box 'SIMULATION PARAMETERS' will pop up when it is selected. Input the wind, wave and current force coefficients in **FORCE PARAMETERS**, Select the type of current

velocity distribution in **CURRENT TYPE**, Select the time step between the re-calculation of environmental forces in **TIME STEP**.



The image shows a dialog box titled "SIMULATION PARAMETERS". It contains several input fields and radio button options. In the top right corner, there are "OK" and "Cancel" buttons. A question mark icon is located in the top left corner. The dialog is divided into three main sections: "FORCE PARAMETERS", "CURR DISTRIBUTION", and "TIME STEP".

Section	Parameter	Value / Option
FORCE PARAMETERS	WAVES	1.2
	WIND	1.1
	CURRENT	1.1
CURR DISTRIBUTION	1 CONSTANT	<input checked="" type="radio"/>
	2 LINEAR	<input type="radio"/>
	3 QUADRATIC	<input type="radio"/>
TIME STEP	0.5 HOUR	<input type="radio"/>
	1.0 HOUR	<input type="radio"/>
	1.5 HOURS	<input type="radio"/>
	2 HOURS	<input checked="" type="radio"/>

Figure A2.11 Input Calculation Coefficients

RAND PARA command allows to input probability distributions of random parameters. The dialogue box 'RANDOM PARAMETER' will pop up when **RAND PARA** command is selected.

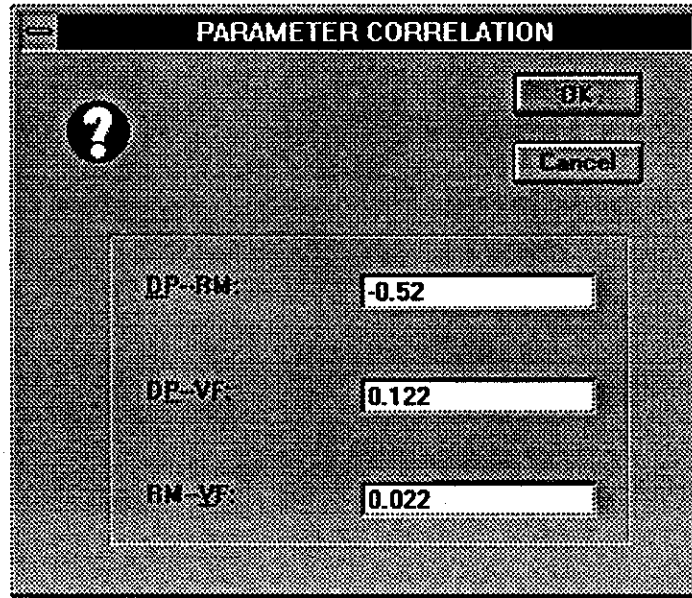
RANDOM PARAMETER		
<div> <div>?</div> <div>OK</div> <div>Cancel</div> </div>		
PN POISSON LAMBDA <input type="text" value="0.131"/>	FI TRIANG (DEGREE) MINIMUM <input type="text" value="0"/> MOST LIKELY <input type="text" value="101"/> MAXIMUM <input type="text" value="180"/>	XO UNIFORM (NM) MINIMUM <input type="text" value="-20"/> MAXIMUM <input type="text" value="60"/>
DP LOGNORM (MB) MEAN <input type="text" value="53.64"/> STD <input type="text" value="16.14"/>	RM LOGNORM (NM) MEAN <input type="text" value="24.16"/> STD <input type="text" value="7.85"/>	VT LOGNORM (KTS) MEAN <input type="text" value="11.8"/> STD <input type="text" value="4.5"/>

Figure A2.12 Input Random Parameter Information

Note here, Lamta is the hurricane occurrence rate at a point in the selected reference per year per nautical mile.

PARA CORRELATE command allows to input correlation among random parameters.

The dialogue box 'PARAMETER CORRELATION' will pop up when it is selected.



PARAMETER CORRELATION

?

OK

Cancel

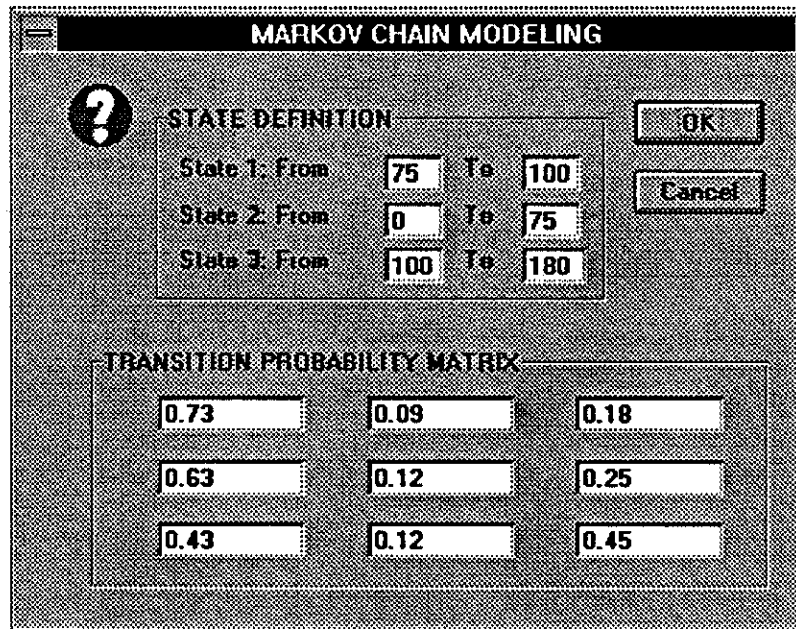
DP-RM: -0.52

DP-VF: 0.122

RM-VF: 0.022

Figure A2.13 Input Correlation Coefficients among Random Parameters

Markov Modeling command allows to input the definition of states in Markov chain model and the transition probability matrix.



MARKOV CHAIN MODELING

?

OK

Cancel

STATE DEFINITION

State 1: From 75 To 100

State 2: From 0 To 75

State 3: From 100 To 180

TRANSITION PROBABILITY MATRIX

0.73	0.09	0.18
0.63	0.12	0.25
0.43	0.12	0.45

Figure A2.14 Input Markov Model Setting

A2.4 Execute the Program

There three commands under **RUN** menu:

RESET command allows to reset the program before each simulation.

RUN command is clicked to begin the simulation. Before click **RUN**, you should set up @RISK simulation parameters. The recommended @RISK simulation settings is as in Figure 2.12. After the simulation is completed, a dialogue box will pop up.

The image shows the 'Simulation Settings' dialog box for @Risk. It contains several sections with various settings:

- Iterations:** 3000, **Simulations:** 1. Buttons: ☒ OK, ☒ Cancel.
- Random Number Generator Seed:** 0. ☐ Pause on Error, ☐ Update Display.
- ☐ Allow Multitasking.
- Sampling Type:** ☒ Latin Hypercube, ☐ Monte Carlo. ☐ Collect Distribution Samples?
- Standard Recalc:** ☐ Expected Value, ☒ Monte Carlo, ☐ True EV.
- Convergence:** ☐ Monitor Convergence? Check Every 100 Iterations. ☐ Auto-Stop Simulation? Stop When All Output Percent's Change Less Than 1.5 %.
- Execute Macro:** ☐ Execute Macro? ☐ Before simulation, ☐ Before sampling/ worksheet recalc, ☐ After sampling/ worksheet recalc, ☐ After simulation. Macro name: [text box].

Figure 2.15 @Risk Simulation Setting

Strategy command allows to do strategy simulation to determine the best place to site the MODU within the acceptable area.

A2.5 General Jackup Information

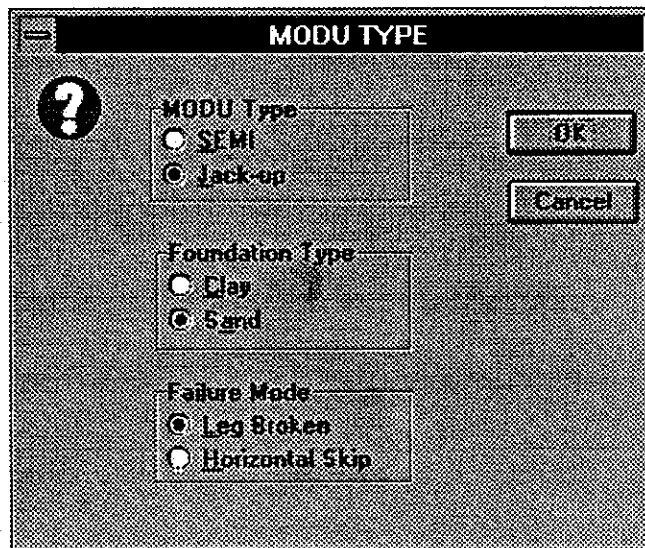
The MODUSIM has been updated to simulate the movement of bottom founded MODUs.

There are three command under the **Jackup** menu.

Jackup Type command allows to determine the MODU type, foundation type and failure mode.

Jackup Info allows to input the general information of the jack-up.

Capacity allows to input the foundation capacity and leg capacity.



The image shows a dialog box titled "MODU TYPE". On the left side, there is a circular icon containing a question mark. The dialog box contains three sections, each with a label and two radio button options:

- MODU Type**:
 - ☐ SEMI
 - ☒ Jack-up
- Foundation Type**:
 - ☐ Clay
 - ☒ Sand
- Failure Mode**:
 - ☒ Leg Broken
 - ☐ Horizontal Skip

On the right side of the dialog box, there are two buttons: "OK" and "Cancel".

Figure A2.16 Jackup Type Input Information

JACK-UP INFORMATION

? Jack-Up Name:

Jack-Up Parameters

Weight (kips):	<input type="text" value="30370"/>
DRAFT if Floating (FT):	<input type="text" value="10"/>
Number of legs:	<input type="text" value="3"/>
Length Overall (FT):	<input type="text" value="230"/>
Width Overall (FT):	<input type="text" value="250"/>
Equivalent Leg Diameter (Cd*D) (FT):	<input type="text" value="9.97"/>
Footing Area of Spud Can (FT^2):	<input type="text" value="2376"/>
Projected Area for Wind Loading (FT^2):	<input type="text" value="16000"/>
Moment of Inertia of Legs (FT^4):	<input type="text" value="829"/>
Material Elastic Modulus E:	<input type="text" value="4320000"/>

Figure A2.17 General Jackup Input Information

Leg Capacity

? **Foundation Capacity**

Horizontal Capacity for Clay (kip):

STD:

Friction Angle if Sand:

Leg Capacity

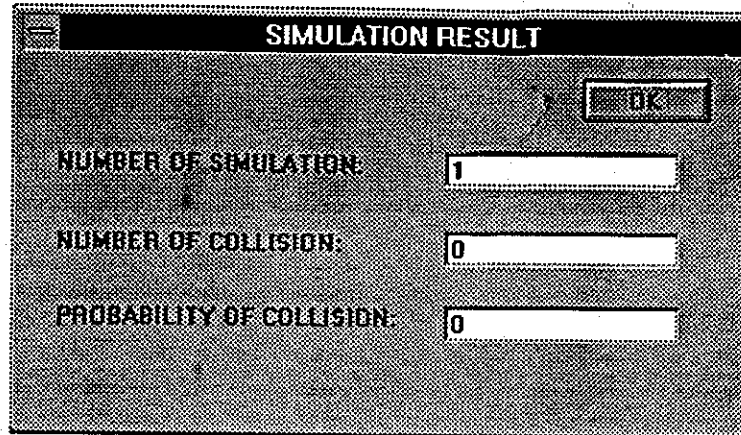
Shear (kip):	Yield Moment (kip-ft):
<input type="text" value="5"/>	<input type="text" value="200000"/>
STD:	STD:
<input type="text" value="6"/>	<input type="text" value="200000"/>

Figure A2.18 Input Jackup Capacity Information

A3. Output

The output of MODUSIM can be in numerical and graphical format.

Click **RESULT** command for simulation result.

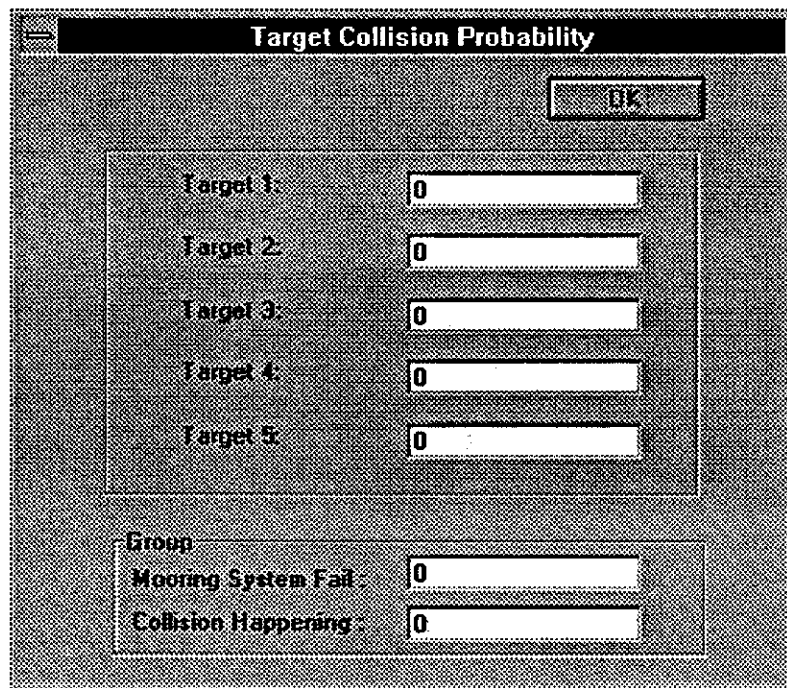


The image shows a dialog box titled "SIMULATION RESULT". It contains three input fields with labels to their left: "NUMBER OF SIMULATION:" with a value of "1", "NUMBER OF COLLISION:" with a value of "0", and "PROBABILITY OF COLLISION:" with a value of "0". An "OK" button is located in the top right corner of the dialog box.

Label	Value
NUMBER OF SIMULATION:	1
NUMBER OF COLLISION:	0
PROBABILITY OF COLLISION:	0

Figure A2.19 Simulation Result

Click **RESUTAR** for output of special target collision probability.



A screenshot of a software dialog box titled "Target Collision Probability". The dialog has a standard Windows-style title bar with a close button. In the top right corner, there is an "OK" button. The main area of the dialog contains two groups of input fields. The first group, labeled "Target 1:" through "Target 5:", each has a text input field containing the number "0". The second group, labeled "Group", contains two items: "Mooring System Fail:" and "Collision Happening:", each followed by a text input field containing the number "0".

Target	Value
Target 1:	0
Target 2:	0
Target 3:	0
Target 4:	0
Target 5:	0


Group	Value
Mooring System Fail:	0
Collision Happening:	0

Figure A2.20 Simulation Result for Target Circles

Click **Summary** command for the simulation result from Strategy function.

Click **Env.Result** to get the result from the simulation of the environmental conditions.

Environmental Simulation Result

 The Probability of Exceeding Critical Env. Data

	Wind Speed(kt)	Wave Height(ft)	Current Velocity(kt)
	50	40	2
6 Hour	0.1192	0.015	0.2077
12 Hour	0.54	0.2963	0.6308
18 Hour	0.3874	0.1482	0.4971
24 Hour	0.0884	0.0112	0.157

Given Risk, The Env. Data are:

	Wind Speed(kt)	Wave Height(ft)	Current Velocity(kt)
6 Hour	51.31	31.97	2.25
12 Hour	86.13	53.66	3.78
18 Hour	69.43	43.26	3.04
24 Hour	49.09	30.58	2.15

Figure A2.21 Environmental Condition Simulation Result

Click **Histogram** command to get the histograms of environmental condition. The following 'Type of Histogram' dialogue box will pop up. Select different forecast time and different forecast type of hurricanes.

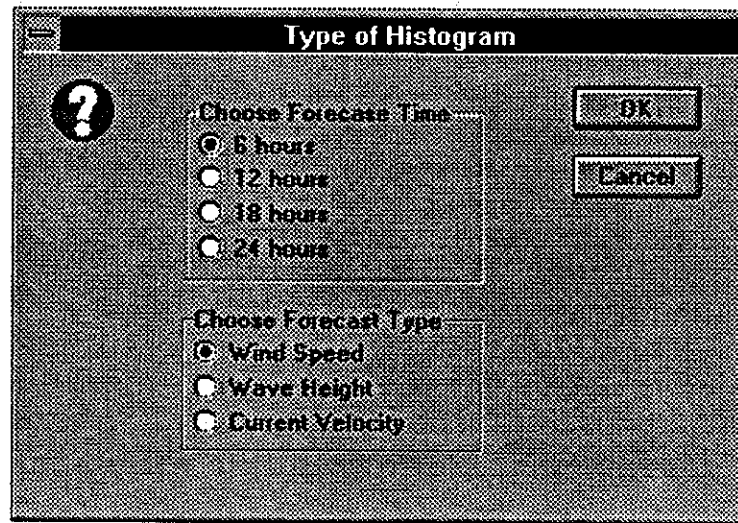


Figure A2.22 Type of Histogram

Click **Return** command to return to the welcome screen.

In case of simulation the MODU's movement during a given hurricane, click **ROUTE** command to get the MODU's moving route during hurricanes.

During the simulation of a given track, a dialogue box 'COLLISION HAPPENING' will pop up whenever a collision happens. Click **STOP HERE** to stop the simulation. Click **NO REPORT** to skip the 'COLLISION HAPPENING!' dialogue box after the following collision. Click **HOLDING** and input **HOLDING TIME** to make the MODU stop at the collision place for a while.

If **Update Screen** is clicked, the MODU route and hurricane track will not be updated each step on the screen. This will make the simulation faster.

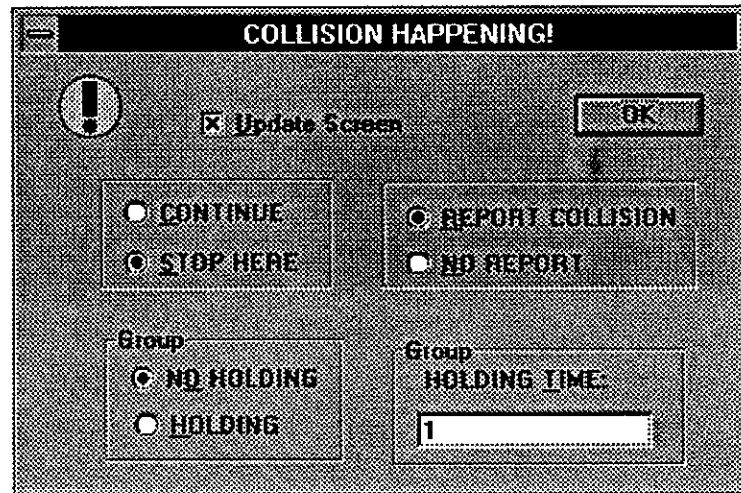


Figure A2.23 Collision Happening Dialogue Box

APPENDIX B

EVACSIM

MODU Evacuation Procedure Simulation Program

User Manual

EVACSIM

MODU Evacuation Procedure Simulation Program

Copyright 1996

This software is provided "as is" by the Marine Technology and Management Group (MTMG) at University of California at Berkeley to sponsors of the research project *Securing Procedures for Mobile Drilling Units in the Gulf of Mexico Subject to Hurricanes*. Any express or implied warranties of merchantability and fitness for a particular purpose are disclaimed. In no event shall the MTMG be liable for any direct, indirect, incidental, special, exemplary, or consequential damages (including, but not limited to, procurement of substitute goods or services; loss of use, data, or profits; or business interruption) however caused on any theory of liability, whether in contract, strict liability, or tort (including negligence or otherwise) arising in any way out of this software, even if advised of possibility of such damage.

B1. Introduction

B1.1 Introduction

EVACSIM 1.0 is a computer simulation program developed for simulating the MODU's evacuation procedures in hurricanes. It is based on offshore evacuation simulation models and associated weather-related downtime techniques developed for the extension research of joint industry - government sponsored research project titled "*Securing Procedures for Mobile Drilling Units in the Gulf of Mexico Subject to Hurricanes*".

This research has been performed at the University of California at Berkeley, Department of Naval Architecture and Offshore Engineering by Research Assistant Jun Ying under supervision of Professor Robert Bea. The theoretical background of EVACSIM is documented in previous chapters of this report.

B1.2 Application Range of EVACSIM 1.0

EVACSIM 1.0 can be applied to typical offshore platform evacuation procedure simulations with project duration up to 3 days. With upgrade version, it can be used to simulate more complex long-term weather sensitive offshore projects. The upgrade version will be available upon request.

B1.3 Program Structure

The program is developed using Microsoft Project 4.0 and Excel 4.0 Software. The following files are bounded together under the directory EVACSIM:

- evacsim.mpp
- merge.mpx
- prtemp.mpx
- ptemp1.mpx
- temp.xlw
- input.xlw
- sinput.xlw
- sdata.txt
- pdata.txt
- input.txt
- temp.txt

B1.4 Installation

B1.4.1 Backup Disk

Before any installation begins, it is always a good practice to backup the program diskette in the back of the report. We assume you are already familiar with DOS commands or Windows operation. For example, in DOS you will need the DISKCOPY command to make backup copies of your program disk.

B1.4.2 System Requirements

To run EVACSIM 1.0, you must have a 486 or higher based PC with 8MB RAM at least, MS DOS 5.0 or higher, Windows 3.1 or higher, Microsoft Project 4.0, EXCEL 4.0 and @Risk for Excel 3.1.

B1.4.3 Installation

To install EVACSIM 1.0, first copy all the files in the attached disk to your hard drive under the directory "c:\evacsim". Then you can expand the zip file by type: pkunzip evacsim.zip.

B2. Input Data

B2.1 Introduction

To run EVACSIM 1.0, you must start MS Project 4.0 and Excel 4.0 at the same time. The program will transfer data between MS Project and Excel automatically. Then, in MS Project, open the file evacsim.mpp under the directory c:\evacsim.

The evacsim.mpp has a evacuation procedure model which is performed on Zane Barnes. The user may modify the model by adding or dropping some tasks or resources, changing task duration or changing task relationship, etc., or even building another new evacuation procedure model. All this operations may be done through tools in MS Project. Please refer to MS Project user menu for detail operation procedures.

B2.2 Input Hurricane Forecasting Data Information

The hurricane forecast data input file is *pdata.txt*. The example input file is as follows:

Evacuation Simulation Input Card

Forecast Data Begin Time:

11/03/95 00:00 AM

Forecast Data at (16.0,114.5):

6,25,4.0

12,26,4.5

18,28,4.5

24,29,5.0

30,30,5.5

36,30,5.5

42,35,6.0

48,52,8.0

54,62,9.7

60,43,7.1

66,32,5.6

72,28,4.7

The file includes the forecast data beginning time: *11/03/95 00:00 AM*; forecast data point location: *(16.0,114.5)*; and every 6 hour forecast data for wind speed and wave height at forecast location up to 72 hours after the forecast beginning time. The forecast data is formatted as: hours to the forecast beginning time, wind speed and wave height. The units can be chosen by the user, but should the same unit system with that used in the input file, *input.txt*.

B2.3 Input Resource Environmental and Operational Down-Time Criteria

To edit resource environmental and operational down-time criteria, click the command **Edit Resource** under the **Option Menu**. The program will shift to MS Excel 4.0 and open the file *input.txt*. The format of *input.txt* is as follows:

Evacuation Simulation Input Card					
Restricted Resource Number:					
5					
Name	ID	Wind.Sp	Wave.Hi	Duration	All(0)/Half(1)Day
Worker.a	1	100	100	1	0
Worker.b	2	100	100	1	0
Tool.a	3	50	8	4	0
Trans.boat	4	36	6	1	1
Ship	5	70	10	2	0
# of Sim	DT of Sim.				
36	6				
Number of Task to be Check:					
1					
Task ID	Res.ID	Allow.Dur			
13	4	3			

User can edit parameters directly in Excel worksheet. **Restricted Resource Number** is the number of the resources which have environmental or operational restrictions on them. Here, five resources are listed. **ID** is the id which is assigned to each resource in the MS Project. They may be found in project view of resource sheet. Wind speed and wave height are the two environmental criteria used here. The units should be the same as that in *pdata.txt*. **Duration** is the minimum continuous operational duration for each resource. In **All(0)/Half(1) Day** input, 0 means the resource can work day & night and 1 means

only day time. # of Sim is the latest evacuation start time of simulations in terms of hours from forecast beginning time. And DT of Sim. is the interval in hours of different evacuation start time. The last inputs, Number of Task to Be Checked, Task ID, Res.ID and Allow.Dur, are the number of un-separable tasks, task id, associated resources id and the maximum allowable operating duration in hours.

After edit the resource parameters, click **Return to Project** command under the **Project** menu to return to MS Project.

B3. Simulation Procedure

The simulation procedure includes deterministic and probabilistic simulations.

B3.1 Deterministic Simulation

Click command **Run Evac** under the **Option** menu to perform the deterministic simulation at a given evacuation start time. The program will pop a window for input of the start time. The simulation result will give the whole project information, includes duration of whole project and of each task, the critical path of the project, etc..

Click command **Run Detsimu** under the **Option** menu to perform the deterministic simulation with the start time changed from 6 hours after the forecast beginning time to the latest simulation evacuation start time which is inputted by the user, with DT hours

interval. The program will shift to Excel to present the result. The result will be in chart format as in Figure 5.6 and 5.7. Also, user can click command **Forecast Data** under **Project** Menu to show a chart of forecast data as in Figure 5.5. Click **Return to Project** to back to MS Project.

B3.2 Probabilistic Simulation

To perform simulation in probabilistic region, first step is to generate the random environmental simulation data based on the forecast data. In the @Risk for Excel 4.0, open the file *sinput.xlw*, and follow the instructions to generate the data, then back to project. Click command **Run Probsimu** under **Option** menu to begin the simulation in probabilistic region. The simulation will take almost 30 minutes for a typical 486-66 PC.

The program will present the simulation results in Excel chart format as in Figure 5.8. The chart shows the probabilities of evacuation failure in different evacuation start time vs. evacuation start time. Click command **Forecast Data** to see forecast information and click **Back to Project** to return to MS Project.

APPENDIX C

DISTRIBUTION FITTING AND GOODNESS-OF-FIT TEST

C.1 Estimating

The goal of Distribution Fitting is to find the parameters of the distribution that best fits the input data from a group of parametric distribution families. The distribution families used in this research are: Beta, Exponential, Lognormal, Normal, Rayleigh, Triangular, Uniform and Weibull. These distributions are used because they are popular in engineering applications. The fitting performed in the research finds a distribution from the distribution families that best fits the input data.

Distribution fitting goes through the following steps to find the best fit for the input data:

- For each distribution type, a first guess of parameters is made using **maximum-likelihood estimators**;
- The Chi-square is minimized using the **Levenberg-Marquardt method**;
- The fits of the best-fitting parametric distributions are compared;
- The parameters of the overall best-fitting parametric model are reported as the parameters of the best fit distribution.

In principle, one should adjust the Chi-square using the number of fitted parameters in model selection. That adjustment is not important here because the number of parameters is about the same for all models (2-4), and the number of data is large ($10^2 - 10^3$).

C.2 Maximum Likelihood Estimators

To fit a distribution to the data set, nonlinear iterative procedures such as the Levenberg-Marquardt algorithm need an initial set of parameters. The maximum likelihood estimators are derived for each distribution function. The MLE of a set of parameters are those values that maximize the likelihood function given a set of observation data. For any density function $f(x)$ with a parameter vector α , and a corresponding set of independent observational data X_i , an expression called the likelihood may be defined:

$$L = \prod_{i=1}^n f(X_i, \alpha) \quad (C.1)$$

To find the MLE, one maximizes L with respect to α by finding a stationary point

$$\frac{dL}{d\alpha} = 0 \quad (C.2)$$

and solving for α .

C.3 The Levenberg-Marquardt Method

The maximum likelihood estimator need not fit the data best in a Chi-square. The Levenberg-Marquardt Method is a nonlinear least-square solver which we can use to improve the Chi-square fit beyond maximum likelihood, using MLE as an initial guess of the parameters.

The Levenberg-Marquardt method does not find the absolute minimum for chi-square, rather, it finds a local minimal. The performance of this method depends on the initial

parameters used. Therefore, a good first guess will produce a good result, while a poor first guess might not provide a useful result.

The following steps outline the Levenberg-Marquardt method:

1. Calculate the “first guess” of all parameters;
2. Find the goodness-of-fit of the input data to the function using these parameters;
3. Vary the parameters by an amount proportional to a factor m ;
4. Measure the goodness-of-fit with the modified parameters;
5. If the modified parameters produce a better fit, update the parameters with these values and decrease the value of m by an order of magnitude;
6. If the modified values produce a worse fit, do not update the parameters; increase the value of m by an order of magnitude;
7. Return to step 3.

These steps are repeated until it finds that varying the parameters has little effect on the goodness-of-fit (measured as the percentage change in the chi-square value). This point is a local minimum of the goodness-of-fit statistic, the sum of squared residuals.

C.4 Goodness-of-Fit Test

The process of calculating MLEs and minimizing the sum of squared residuals gives a “best guess” for each distribution. Then we measure whether each fit is probabilistically adequate using goodness-of-fit statistics.

We can characterize the goodness of fit by the probability that the data would be obtained if the fitted model were correct. This probability is called the P-value. If the P-value is small, the data cast doubt on the validity of the model. If the P-value is large, the data are compatible with the model.

There are a lot of goodness-of-fit tests, e.g., chi-square, Kolmogorov-Smirnov and Anderson-Darling. The Chi-Square is the most common.

Chi-Square Test:

The Chi-Square test is the most common goodness-of-fit test. It can be used with any type of data and any type of distribution function. A weakness of the Chi-Square test is that there are no clear guidelines for selecting intervals (number of classes). In some situations, one can reach different conclusions from the same data depending on how the intervals are chosen.

The Chi-Square statistic is defined as:

$$\chi^2 = \sum_{i=1}^n \frac{(P_i - p_i)^2}{p_i} \quad (C.3)$$

where

P_i = the observed probability of the data in the i th histogram bin

p_i = the theoretical probability that a value will fall within the X range of the i th histogram bin

Kolmogorov-Smirnov Test:

The Kolmogorov-Smirnov Test does not depend on the number of intervals. A weakness of the Kolmogorov-Smirnov Test is that it does not detect tail discrepancies very well.

The Kolmogorov-Smirnov statistic is defined as:

$$D_n = \sup \left| F_n(x) - \hat{F}(x) \right| \quad (C.4)$$

where

n = total number of data points

$\hat{F}(x)$ = the hypothesized distribution

$$F_n(x) = \frac{N_x}{n}$$

N_x = the number of X_i 's less than x .

Anderson Darling Test:

The Anderson Darling Test is very similar to the Kolmogorov-Smirnov Test, but it places more emphasis on tail values. It does not rely on the number of classes.

The Anderson-Darling Statistic is:

$$A_n^2 = n \int_{-\infty}^{\infty} \left[F_n(x) - \hat{F}(x) \right]^2 \Psi(x) \hat{f}(x) dx \quad (C.5)$$

where

$$\Psi^2 = \frac{1}{\hat{F}(x)[1 - \hat{F}(x)]}$$

$\hat{f}(x)$ = the hypothesized density function

$\hat{F}(x)$ = the hypothesized distribution function

$$F_*(x) = \frac{N_*}{n}$$

N_* = the number of X_i 's less than x .

C.5 Confidence Levels and Critical Values

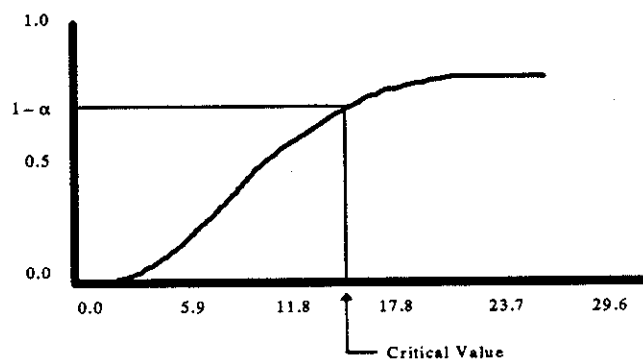
The goodness-of-fit statistic tells how probable it is that a given distribution function produced the data set. But how good is good enough? A critical value is the value in a test that separates the rejection region from the acceptance region. For the goodness of fit tests, this value determines whether or not one should reject a fitted distribution. Statistical hypothesis testing provides a structured analytical method to make a decision regarding fit test results. This method allows one to control or measure the uncertainty involved in the decision.

In the case of research work here, the decision we need to make is whether the input data were generated from the distribution function reported as the estimate. The critical value involved is a goodness-of-fit measurement that is compared to the goodness-of-fit of the best fitting distribution.

The significance level, α , is the probability of rejecting the null hypothesis (in this case, that the estimated distribution is correct) when it is true. In other words, a small value of

α decreases the probability of incorrectly rejecting the null hypothesis that a given set of parameters produce the input data.

For the chi-square test, the critical value is the $1 - \alpha$ percentile of a chi-square distribution with $N-1$ degrees of freedom (N is the number of classes).



A Chi-Square Distribution with 10 degrees of freedom

When the calculated Chi-Square statistic is larger than the critical value, the null hypothesis should be rejected (the distribution is not a good fit). Equivalently, one should reject the null hypothesis when the P-value is less than the significance level.

Critical values for the Anderson-Darling and Kolmogorov-Smirnov goodness-of-fit statistics have been found by Monte-Carlo studies, detail can be found in References.

